EXPERIMENTAL & THEORETICAL ASPECTS OF THE ELECTROWEAK SECTOR

by

Kevin T. Grizzard

A dissertation submitted to The Johns Hopkins University in conformity with the requirements for the degree of Doctor of Philosophy.

Baltimore, Maryland

June, 2015

Abstract

The electroweak sector of the Standard Model (SM) has been extremely successful in predicting and matching observations. The basic form of it was sketched out some fifty years ago with the elucidation of the Higgs mechanism in a non-Abelian Yang-Mills gauge theory, yet the existence of a central player in the story, the (or a) Higgs boson, was confirmed only in 2012. In the intervening years, a great deal of experimental research was done to measure parameters of the model and confirm other predictions. In this sense, it has been an extremely fruitful theory in addition to being robust.

But questions regarding the origin of the values of certain parameters in the theory, and especially regarding obvious but unexplained hierarchies between them, beg to be answered. The question of the technical naturalness of the Higgs mass has been one of the most significant motivating factors behind theories of beyond-the-Standard-Model (BSM) physics, though other striking features (for instance, the large discrepancy between quark masses) have also motivated theories (for instance, 2-Higgs-doublet models and models with Yukawa unification). Thus the electroweak sector has also

proven fruitful for BSM theorists.

The present paper may be divided into two parts: a description and characterization of the electroweak sector as it exists in the Standard Model on the one hand (a SM part), and an exploration of what may lie beyond it on the other (a BSM part).

In the SM part, we first review the conceptual development of the electroweak model of Glashow, Weinberg, and Salam (touching on Yang-Mills theory and the Higgs mechanism), then present the key phenomenology of the electroweak theory. This leads into a presentation of this author's work in studying final-state radiation (FSR) uncertainties in a measurement of $\sin^2\theta_W$, with θ_W being the weak mixing angle, done by the Compact Muon Solenoid (CMS) group at the Large Hadron Collider (LHC) in 2011. The framework necessary to understand the analysis is laid out in the text but this author played only the small role described in the section on FSR. The full analysis was presented in the papers by N. Tran and the CMS Collaboration, referenced in the text.

The BSM part begins with an interlude that includes a review one of the most-discussed puzzles of the SM and a discussion of "naturalness." We then present some of the basics of supersymmetry, including its history, the SUSY algebra, and the MSSM. SUSY is probably the leading contender for an explanation of seemingly "unnatural" parameters. In the next chapter, we present a supersymmetric model in which a new generation of "vector-like" quarks (as opposed to chiral) mixes with the third generation. Such a mixing raises the value of the top Yukawa y_t necessary to

give a top quark of the observed mass, $m_t = 173$ GeV. Since the one-loop quantum corrections to the Higgs mass scale as y_t^4, even a minor increase in y_t can have a large effect. With current experimental bounds, y_t may increase by as much as $\sim 6\%$, which implies the top's contribution to the Higgs mass increases by up to 26%. The model preserves gauge unification and gives a Higgs mass $m_h \approx 125.5$ GeV without requiring soft supersymmetry-breaking masses above 1 TeV while satisfying all experimental constraints and predicting new quarks around the TeV scale, discoverable at the LHC. We conclude with a summary of the model and remarks on future prospects.

Acknowledgments

I am grateful for advice, discussion, and collaboration to Cyrus Faroughy, Andrei Gritsan, Arpit Gupta, Matt Walters, Chris Brust, David Kaplan, Surjeet Rajendran, and Marc Kamionkowski. Thank you all. I thank David Cohen, Marc Sher, Pat Burchat, Jim Beall, Dylan Casey, Michael Blaustein, Anita Kronsberg, and all my professors at St. John's for the challenges and opportunities they provided me; I would not be the same without them. I am also grateful for the support, encouragement, and friendship of my family, friends, supporters, and colleagues, including Jon Beardsley, Michael Adams, Ken Sachs, Jack Pannell, Joel Silverman, Barry Herndon, Stephen McMaster, Jason Malcan, Clay Blancett, Eric Waters, Vitaly Lorman, Logan Maingi, Sean Cantrell, Jake Mokris, and BCMG. I also Sarah Hemminger, Tong Zhang, Joel Pally, Billy Scola, Varun Patel, Richard Dismel, Jameel Young, and Malcome Miller.

Dedication

To my father, with gratitude for his support and his example.

In the words of Brian Wilson:

"God only knows what I'd be without you."

Contents

List of Tables

List of Figures

Chapter 1

Preliminaries

1.1 Early Theory of Weak Interactions

In 1933, Fermi proposed a theory of weak interactions to explain the observation of beta decay (e.g., a neutron decaying to proton and emitting an electron and antineutrino: $n \to p + e^- + \bar{\nu_e}$). In that theory, the interaction occurred via a four-fermion vertex, which corresponds to a term in the Lagrangian like

$$\mathcal{L}_F = \frac{G_F}{\sqrt{2}} \bar{\psi} \gamma^\mu \chi \bar{\chi} \gamma_\mu \psi, \tag{1.1}$$

where ψ, χ are fermion fields [1]. Here the coupling constant G_F is dimensionful, with a value that must be determined empirically. It is found to be [2]

$$G_F = 1.1663788(7) \times 10^{-5}\,\mathrm{GeV}^{-2}. \tag{1.2}$$

In modern language, the dimensions of this coupling constant indicate that this is a (superficially) nonrenormalizable theory. In even more modern language, they indicate that we have an effective theory.

Effective field theories, or EFTs, are key to the modern understanding of quantum field theory. EFT hinges on the fact that we do not need to know the entire theory - that is, the theory at all energies - to describe the low-energy physics of a system. It is intimately connected with the renormalization group (or RG, really a semigroup), which describes how the values of coupling constants in a theory depend on the energy scale at which an interaction takes place. Stueckelberg & Petermann [3], Gell-Mann & Low [4], and Kadanoff [5] made early inroads on the subject, while Symanzik [6], Callan [7], Wilson [8,9], and Weinberg [10] developed it to maturity, and in so doing, clarified why quantum field theory works.

The basic idea is that if one begins by writing down all possible polynomials in the fields of the theory, each multiplied by coupling coefficients of the dimension necessary to make the action dimensionless (that is, of the same dimensions as Planck's constant, h, which we take to be 1), then examines how these couplings evolve as the energy (or equivalently, length) scale is changed, one finds that all but a few of them decrease with decreasing energy scale. Indeed, the expressions multiplying the respective couplings are classified as *relevant, irrelevant*, and *marginal* operators based on how they scale with energy. The RG evolution of a coupling is tied directly to the dimension of the operator, as follows [5, 6, 8, 11]. Suppose we consider

a theory in d spacetime dimensions. Then if one scales the momentum as $k \to k/b$, the Fourier-transformed action of a theory will have a kinetic term that behaves as $\int d^d k\, k^2 \phi^2(k) \to \int d^d k b^{-d} (\frac{k}{b})^2 \phi^2(k/b)$. If we then require these to be equal, we find $\phi \to \phi b^{1+\frac{d}{2}}$. With this information, we can find how any generic term like $c\phi^i$ behaves under scaling. In particular, we find that c has (naively at least) no scaling-dependence if $i = \frac{2d}{d-2}$. If i is greater or less than this critical value then c decreases or increases, respectively, as momentum is scaled down. The key point is that most operators are irrelevant, meaning they become unimportant at low energy. That is why our limited and incomplete theories have nonetheless been so successful.

In the case of Fermi's weak interaction, the amplitude for a process to occur grows with the energy, $\mathcal{M} \sim E^2 G_F$. When $E^2/G_F \sim 1$, perturbation theory breaks down and predictions are no longer valid. This does not mean the theory is worthless. In fact, the Fermi interaction is quite good as an effective theory at energies much below the electroweak scale, $\sim$ 100 GeV, but breaks down near 300 GeV [12]. At the cutoff (the upper limit of the theory's validity), when a theory begins to break down, it is because new physics becomes important at that scale. In the case of the weak interaction, the 4-fermion vertex is seen as an effective vertex arising from the exchange of electroweak bosons, as shown in Fig. 1.1.

The exchange of such a boson introduces a term called the propagator into the calculation for this process, which can be written in the form $g^{\mu\nu}/(k^2 - m^2)$, where $g^{\mu\nu}$ is the metric, m is the mass of the boson and k^μ is its 4-momentum. The value of

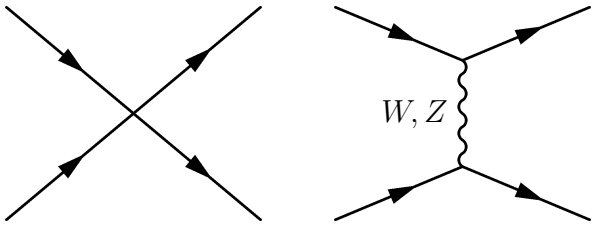

Figure 1.1: Left: the effective 4-fermion vertex. Right: a diagram that contributes to the effective vertex.

k^μ is constrained by conservation of 4-momentum at the vertices, and in particular, if k^2 is much smaller than m^2 then this propagator is approximately just $g^{\mu\nu}/(-m^2)$, i.e., a constant. The mass of the electroweak bosons are [13]

$$m_W = 80.385 \pm 0.015\,\text{GeV} \tag{1.3}$$

$$m_Z = 91.1876 \pm 0.0021\,\text{GeV}. \tag{1.4}$$

This is the reason why the Fermi theory works for energies much less than $\sim$ 100 GeV and breaks down above it. Intuitively, one can interpret this as: near 100 GeV, there is sufficient energy to create W and Z bosons; more precisely, the bosons can be nearly on-shell. Furthermore, the large masses of the bosons cause them to decay quickly, and so the interactions they mediate may easily be mistaken for occuring at a single point.

The fact that the Fermi theory is nonrenormalizable and is invalid above the electroweak scale was not the only motivation for augmenting or replacing it. In 1956, Yang and Lee pointed out that the widely-held assumption of parity invariance had not actually been adequately tested in the weak interactions, and the following year, Wu's team confirmed its violation in the decay of cobalt atoms [14, 15]. This

required that the weak interactions have the form $V - A$, that is, vector minus axial vector [16], to have a "handedness." This led to the proposal by Feynman & Gell-Mann [17], and separately Sudarshan & Marshak [18], that the interaction could be mediated by charged vector bosons $W^{\pm}$. This suggestion was also appealing because it explained why weak processes involving entirely different particles should contain the same coupling factors, particularly when put in the framework of a non-Abelian gauge theory (discussed shortly). This also suggested the weak interaction could be unified with the gauge theory of electromagnetism.

1.2 Yang-Mills Theory

The dynamics of a quantum field theory follow from the action. The action for quantum electrodynamics - the first successful quantum field theory - has a certain symmetry, which Yang-Mills theory generalizes [19]. That action is

$$S[\psi, A_\mu] = \int d^4x \mathcal{L} \tag{1.5}$$

$$= \int d^4x \bar{\psi} \left(\partial_\mu \gamma^\mu - m\right) \psi - \frac{1}{4} F_{\mu\nu} F^{\mu\nu} + ie\bar{\psi} A_\mu \gamma^\mu \psi, \tag{1.6}$$

where ψ is the electron field, γ^μ are the Dirac gamma matrices, $F^{\mu\nu}$ is the electromagnetic field-strength tensor, A_μ is the electromagnetic four-potential, and e is the (absolute value of the) charge of the electron [11]. $\mathcal{L}$ is the Lagrangian density (often

called simply the Lagrangian). This action is invariant under the transformation

$$\psi \to \psi' = e^{i\alpha(x)}\psi \tag{1.7}$$

$$A_\mu \to A'_\mu = A_\mu + \partial_\mu \alpha(x). \tag{1.8}$$

That is,

$$S[\psi, A_\mu] = S[\psi', A'_\mu]. \tag{1.9}$$

The symmetry in electromagnetism corresponds to the group $U(1)$. Yang-Mills theory generalizes this idea to non-Abelian symmetry groups. We then have as many gauge fields A^a_μ as there are generators T^a of the group, and the symmetry transformation is [11]

$$\psi \to \psi' = \exp\left[iT^a\alpha_a(x)\right]\psi \tag{1.10}$$

$$A^a_\mu \to A^{a\prime}_\mu = A^a_\mu + \partial_\mu \alpha^a(x), \tag{1.11}$$

where we employ the Einstein convention (repeated indices are summed over).

Since it is acted on by the generators, ψ must live in a representation of the group. It is natural to expect them to live in the fundamental representation, so for a symmetry group $SU(N)$ or $SO(N)$, ψ is now an N-component vector (this is above and beyond the spinor indices it had before; in other words, each component field ψ^i, with $i = 1, 2, ...N$, may be a four-component Dirac spinor or two-component Weyl spinor). This means that the transformations rotate one kind of field into another. In the foundational 1954 paper of Yang and Mills [19], the symmetry group

is $SU(2)$ and the fields that rotate into one another are the proton and neutron fields (inspired by Heisenberg's model [20] of "isospin," that is, isotopic or isobaric spin, based on the fact that the neutron and proton have nearly the same mass and interact the same way under the strong force, suggesting they may be two states of the same particle). Though we know longer think of protons and neutrons as fundamental particles and the strong force is described by quantum chromodynamics (QCD), their formalism proved to be enormously successful, providing the framework for the modern description of both the electroweak and strong forces, as well as proposed Grand Unified Theories [21].

However, the violation of parity in the weak interactions but respect of the symmetry in the electromagnetic interaction posed a puzzle as to how they could be part of the same force. In 1961 Glashow solved this part of the puzzle by enlarging the proposed gauge group from $SU(2)$ to $SU(2) \times U(1)$ [22]. But another obstacle in describing the weak force by a gauge theory remained: it was widely believed at the time that gauge bosons must be massless, like the photon. Yet as we saw above, the weak bosons were required to have extremely large masses in order to reproduce the successes of Fermi's theory at low energy.

1.3 The Higgs Mechanism

The fact that the W and Z bosons are massive is unusual. The photon (which was the first gauge boson we encountered) and the gluons (of the strong force, quantum chromodynamics) are massless. In a sense, it is not the natural state of affairs in a gauge theory. This is because an explicit mass term for the gauge boson violates gauge symmetry. Recall that the gauge field transforms as

$$A_\mu \to A'_\mu = A_\mu + \partial_\mu \alpha(x). \tag{1.12}$$

Then (omitting the explicit x-dependence) a mass term behaves like

$$\frac{m}{2} A_\mu A^\mu \to \frac{m}{2} A'_\mu A'^\mu = \frac{m}{2}(A_\mu + \partial_\mu \alpha)(A^\mu + \partial^\mu \alpha) \tag{1.13}$$

$$= \frac{m}{2}\left[A_\mu A^\mu + 2(\partial_\mu \alpha) A'^\mu + (\partial_\mu \alpha)^2\right] \tag{1.14}$$

$$\neq \frac{m}{2} A_\mu A^\mu. \tag{1.15}$$

However, we can achieve a mass for a gauge boson through the (Anderson-Englert-Brout-Guralnik-Kibble-)Higgs mechanism [23–27].

The Higgs mechanism relies on the phenomenon of spontaneous symmetry breaking. Before we see how the Higgs gives mass to gauge bosons, we demonstrate how it spontaneously breaks symmetry by acquiring a vacuum expectation value (vev).

1.3.1 Breaking a Discrete Symmetry

The key ingredients for the phenomenon are rather simple. We consider a theory with a real scalar field, ϕ, which has a mass-like term and a self-interaction term:

$$\mathcal{L}_{SB} = \frac{1}{2}(\partial_\mu \phi)^2 - \frac{1}{2}m^2\phi^2 - \frac{1}{4}\lambda\phi^4. \tag{1.16}$$

Now if $m^2 > 0$ then the theory just describes a field with particles of mass m that can interact with itself at a quartic vertex. However, if $m^2 < 0$ then we get new behavior. Let us define $\mu^2 = -m^2$. Then

$$\mathcal{L}_{SB} = \frac{1}{2}(\partial_\mu \phi)^2 + \frac{1}{2}\mu^2\phi^2 - \frac{1}{4}\lambda\phi^4. \tag{1.17}$$

The vacuum prefers the lowest energy state, so we minimize this with respect to ϕ:

$$\frac{\partial}{\partial\phi}\mathcal{L}_{SB}\mid_{\phi=\phi_0} = 0 = \frac{\partial}{\partial\phi}\left[\frac{1}{2}\mu^2\phi^2 - \frac{1}{4}\lambda\phi^4\right]_{\phi=\phi_0} \tag{1.18}$$

$$= \mu^2\phi_0 - \lambda\phi_0^3 \tag{1.19}$$

$$\Rightarrow \phi_0 = \pm\mu/\sqrt{\lambda}. \tag{1.20}$$

So in this theory the lowest-energy state is not the one with all fields equal to zero; instead, in the vacuum ϕ will fluctuate around a constant nonzero value (quantum corrections will in general shift this value slightly but it remains a good approximation). The two solutions we found are indicative of the Z_2 symmetry of the original Lagrangian under which $\phi \to -\phi$. However, that symmetry does not remain once one of these ϕ values is chosen by the vacuum. If we do perturbation theory around the vacuum (as we should), it is convenient to define $\phi = \phi_0 + \Phi$, so that Φ represents the

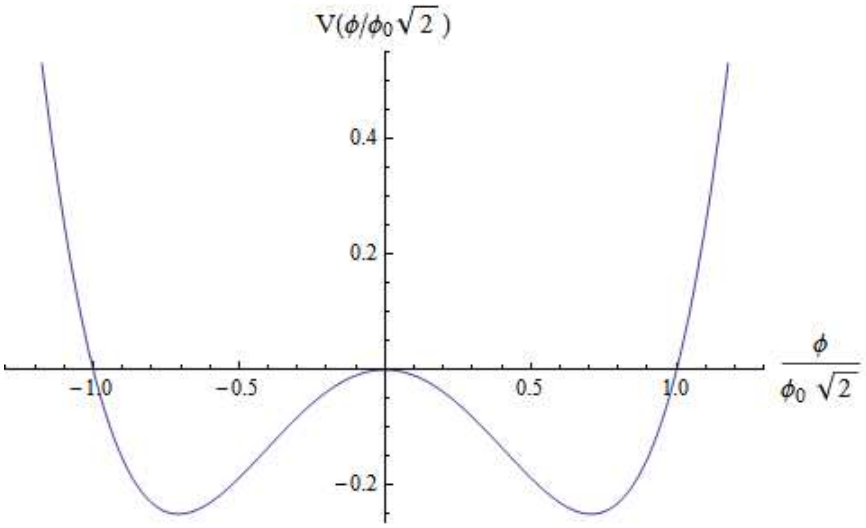

Figure 1.2: The potential for the simple real scalar field example.

fluctuations around the vev. Then the Lagrangian is not symmetric under $\Phi \to -\Phi$. We have

$$\mathcal{L}_H = \frac{1}{2}\partial_\mu(\phi_0+\Phi)\partial^\mu(\phi_0+\Phi) + \frac{1}{2}\mu^2(\phi_0+\Phi)^2 - \frac{1}{4}\lambda(\phi_0+\Phi)^4, \tag{1.21}$$

which (after using $\phi_0 = \mu/\sqrt{\lambda}$) reduces to

$$\begin{aligned}\mathcal{L}_H = &\frac{1}{2}(\partial_\mu\Phi)^2 - \mu^2\Phi^2 - \frac{1}{4}\lambda\Phi^4 - \lambda\phi_0\Phi^3 \\ &+ \frac{1}{2}\mu^2\phi_0^2 - \frac{1}{4}\lambda\phi_0^4.\end{aligned} \tag{1.22}$$

The last two terms are constants and can be ignored. The dynamics are that of a theory with one massive field, Φ, with mass $\sqrt{2}\mu$, and interacting with itself at 3- and 4-point vertices. It is evident that the Z_2 symmetry is broken in the vacuum.

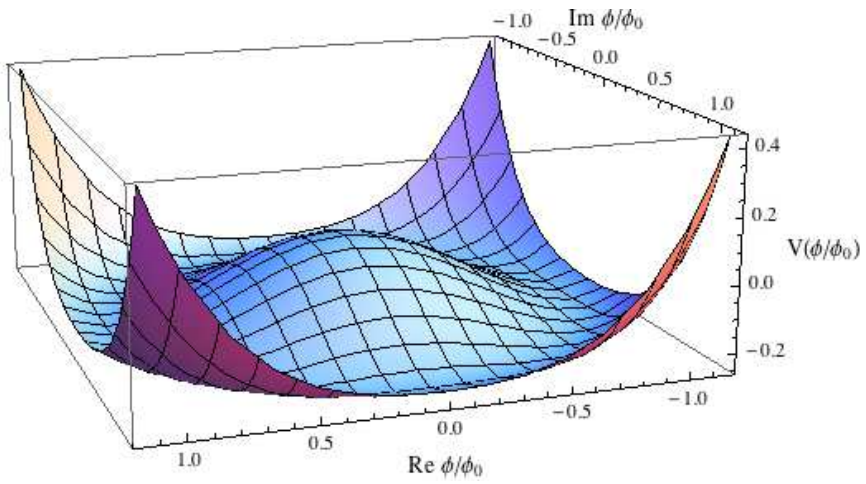

Figure 1.3: The Mexican hat potential.

1.3.2 Breaking a Continous Symmetry

The next simplest example is a theory with a single complex scalar field:

$$\mathcal{L}_{SB2} = \partial_\mu \phi^* \partial^\mu \phi + \mu^2 \phi^* \phi - \lambda(\phi^* \phi)^2. \tag{1.23}$$

In this case, there are not just two possible vacua but a continuum, corresponding to the global $U(1)$ phase symmetry in which $\phi \to e^{i\alpha}\phi$. This is the (in)famous "Mexican hat" potential, with minima anywhere that

$$|\phi| = \mu/\sqrt{\lambda}. \tag{1.24}$$

If we write $\phi = \frac{1}{\sqrt{2}}(\phi_r + i\phi_i)$ then our Lagrangian becomes

$$\mathcal{L}_{SB2} = \frac{1}{2}(\partial_\mu \phi_r)^2 + \frac{1}{2}(\partial_\mu \phi_i)^2 + \frac{1}{2}\mu^2(\phi_r^2 + \phi_i^2) - \frac{1}{4}\lambda(\phi_r^2 + \phi_i^2)^2. \tag{1.25}$$

and if we take the vacuum state to be positive and real ($\phi_0 = \mu/\sqrt{\lambda}$) and expand

around that (so $\phi_r = \phi_0 + \Phi_R$) then we get

$$\begin{aligned}\mathcal{L}_{SB2} = &\frac{1}{2}(\partial_\mu \Phi_R)^2 + \frac{1}{2}(\partial_\mu \phi_i)^2 - \mu^2 \Phi_R^2 - \frac{1}{4}\lambda\left(\phi_i^4 + \Phi_R^4\right) \\ &- \frac{1}{2}\lambda \Phi_R^2 \phi_i^2 - \mu\sqrt{\lambda}\Phi_R \phi_i^2 - \mu\sqrt{\lambda}\Phi_R^3.\end{aligned} \tag{1.26}$$

This Lagrangian describes a theory with two fields, Φ_R and ϕ_i, with mass $\sqrt{2}\mu$ and zero, respectively. They each interact with themselves at quartic vertices and there are three types of vertices at which the two fields couple. The new feature in this theory is the existence of the massless ϕ_i mode, known as a Goldstone boson [28]. Such a mode appears for each broken *continuous* symmetry.

1.3.3 Breaking a Gauged Symmetry

In the case of a continuous *local* (i.e., gauge) symmetry, the massless Goldstone modes are "eaten" by the gauge bosons [23–27]. This is the Higgs mechanism, and it is what occurs in the Standard Model electroweak theory [22, 29, 30]. We first show it in the simpler Abelian case.

We start with the same Lagrangian as before, except now we promote the derivatives to gauge-covariant derivatives and add the gauge field's kinetic term:

$$\mathcal{L}_{SB3} = D_\mu \phi^* D^\mu \phi + \mu^2 \phi^* \phi - \lambda(\phi^* \phi)^2 - \frac{1}{4} F_{\mu\nu} F^{\mu\nu}. \tag{1.27}$$

As before, we have a minimum at ϕ_0 and so we set $\phi = \phi_0 + \Phi_R + i\phi_i$. The terms we

are interested in here are the scalars' kinetic terms, including their gauge interactions:

$$\begin{aligned} D_\mu\phi^* D^\mu\phi =& \left[(\partial_\mu - ieA_\mu)(\phi_0 + \Phi_R + i\phi_i)\right]^* \left[(\partial^\mu - ieA^\mu)(\phi_0 + \Phi_R + i\phi_i)\right] \\ =& (\partial_\mu\Phi_R)^2 + (\partial_\mu\phi_i)^2 + 2eA_\mu(\phi_i\partial^\mu\Phi_R - \phi_0\partial^\mu\phi_i - \Phi_R\partial^\mu\phi_i) \\ &+ e^2A_\mu A^\mu(\phi_0^2 + \Phi_R^2 + \phi_i^2 + 2\phi_0\Phi_R). \end{aligned} \tag{1.28}$$

The key terms here are

$$(\partial_\mu\phi_i)^2 - 2eA_\mu\phi_0\partial^\mu\phi_i + e^2A_\mu A^\mu\phi_0^2. \tag{1.29}$$

Recalling our freedom to choose a gauge, we take what is known as the unitary gauge,

$$A_\mu \to A'_\mu = A_\mu - \frac{1}{e\phi_0}(\partial_\mu\phi_i). \tag{1.30}$$

Then

$$\begin{aligned} (\partial_\mu\phi_i)^2 - 2eA_\mu\phi_0\partial^\mu\phi_i + e^2A_\mu A^\mu\phi_0^2 &= e^2\phi_0^2\left(A_\mu - \frac{1}{e\phi_0}(\partial_\mu\phi_i)\right)^2 \\ &= e^2\phi_0^2(A'_\mu)^2. \end{aligned} \tag{1.31}$$

In fact, the massless Goldstone mode disappears entirely, swallowed up by the gauge choice, while A_μ has picked up a mass proportional to ϕ_0. We say more about this in the context of the SM in the next chapter.

Chapter 2

The SM Electroweak Sector

2.1 The Higgs Mechanism in the SM

Since we do not want to explicitly break any symmetries, any scalar field we add to accomplish the spontaneous symmetry breaking must be in a representation of all of the gauge groups, though possibly just the singlet (trivial) representation. Since we only want to break electroweak symmetry, the simplest thing to add is a field that is in the fundamental representation of the $SU(2)_L$ symmetry and charged under the $U(1)_Y$ (hypercharge) symmetry but is a singlet under the $SU(3)_C$ of QCD. Therefore we add the complex scalar doublet

$$\phi = \begin{pmatrix} \phi^+ \\ \phi^0 \end{pmatrix} = \frac{1}{\sqrt{2}} \begin{pmatrix} \phi_1 + i\phi_2 \\ \phi_3 + i\phi_4 \end{pmatrix}. \tag{2.1}$$

We use a symmetry-breaking potential for the scalar doublet of the same form as in section 1.3, and to retain gauge invariance in the Lagrangian, we promote the derivatives to the gauge-covariant derivatives for $SU(2)_L \times U(1)_Y$ [11]:

$$\mathcal{L}_H = (D_\mu \phi)^\dagger (D^\mu \phi) + \mu^2 \phi^\dagger \phi - \lambda (\phi^\dagger \phi)^2 \tag{2.2}$$

$$D_\mu = \partial_\mu + i\frac{g}{2}\vec{\tau} \cdot \vec{W}_\mu + i\frac{g'}{2} Y B_\mu. \tag{2.3}$$

Here $\vec{W}_\mu = (W^1_\mu, W^2_\mu, W^3_\mu)$ are the three gauge bosons associated to the $SU(2)$ symmetry, while the $\vec{\tau}$ are the associated generators and are equal to one-half the Pauli spin matrices (i.e., $\tau^i = \frac{1}{2}\sigma^i$). B_μ is the single gauge boson associated to the $U(1)$ symmetry and Y is its associated charge operator. We take ϕ to have $Y = 1$, a choice which we justify shortly.

Just as in section 1.3.2, there are now an infinite number of degenerate vacua. We choose to define our component fields such that the vacuum expectation values are

$$\langle \phi \rangle = \begin{pmatrix} 0 \\ \\ v \end{pmatrix}, \tag{2.4}$$

with v real, or in other words,

$$\langle \phi_3 \rangle = v, \tag{2.5}$$

$$\langle \phi_i \rangle = 0 \quad \text{for} \quad i \neq 3, \tag{2.6}$$

and we write the fluctations in ϕ_3 around its vev as

$$h = \phi_3 - v. \tag{2.7}$$

Now

$$D_\mu\phi = \begin{pmatrix} \left[\partial + i\frac{g}{2}W^3 + i\frac{g'}{2}B\right]_\mu \phi^+ + \left[i\frac{g}{2}\left(W^1 - iW^2\right)\right]_\mu \phi^0 \\ \left[i\frac{g}{2}\left(W^1 + iW^2\right)\right]_\mu \phi^+ + \left[\partial - i\frac{g}{2}W^3 + i\frac{g'}{2}B\right]_\mu \phi^0 \end{pmatrix}, \tag{2.8}$$

so, defining $W^\pm = \frac{1}{\sqrt{2}}(W^1 \mp iW^2)$,

$$\begin{aligned} \left(D_\mu\phi\right)^\dagger \left(D^\mu\phi\right) = &\left|\left(\partial_\mu + i\frac{g}{2}W^3_\mu + i\frac{g'}{2}B_\mu\right)\phi^+\right|^2 + \left|i\frac{g}{2}W^-_\mu\phi^0\right|^2 \\ &+ \left[-i\frac{g}{2}W^+_\mu\phi^{0*}\left(\partial^\mu + i\frac{g}{2}W^{3\mu} + i\frac{g'}{2}B^\mu\right)\phi^+ + \text{c.c.}\right] \\ &+ \left|i\frac{g}{2}W^{+\mu}\phi^+\right|^2 + \left|\left(\partial_\mu - i\frac{g}{2}W^3_\mu - i\frac{g'}{2}B_\mu\right)\phi^0\right|^2 \\ &+ \left[i\frac{g}{2}\left(\partial_\mu + i\frac{g}{2}W^3_\mu - i\frac{g'}{2}B_\mu\right)\phi^{0*}W^{+\mu}\phi^+ + \text{c.c.}\right]. \end{aligned} \tag{2.9}$$

From this expression we can see where the mass terms for our gauge bosons will come from. In particular, when we use $\phi^0 = v + h + i\phi_4$, terms that are quadratic in ϕ_0 and have two powers of other fields will become mass terms for those other fields.

2.2 The Weak Mixing Angle

Although we began with massless gauge bosons, their couplings to the scalar field generate the following terms involving the vev from eq. 2.9:

$$\mathcal{L}_{GM} = -\frac{v^2}{8}\left(g'^2 B_\mu B^\mu - gg' W^3_\mu B^\mu + g^2 W^3_\mu W^{3\mu} + g^2 W^{-2}_\mu + g^2 W^{+\mu 2}\right). \tag{2.10}$$

Any term quadratic in the fields acts like (is) a mass term, so we have spontaneously generated masses for the bosons proportional to v. Not only that, but we have a mass term coupling W^3 to B, which will produce mixing. To find the mass eigenstates, we

first note the $W^{\pm}$ mass can be read off as

$$m^2_{W^{\pm}} = -\frac{\partial^2 \mathcal{L}_{GM}}{\partial^2 W^{\pm}} = \frac{1}{4} g^2 v^2. \tag{2.11}$$

For the W^3 and B, we diagonalize the mass matrix:

$$m^2_{ij} = -\frac{\partial^2 \mathcal{L}_{GM}}{\partial A_i \partial A_j} = \frac{v^2}{4} \begin{pmatrix} g^2 & -gg' \\ -gg' & g'^2 \end{pmatrix}. \tag{2.12}$$

The eigenvalues of this matrix are

$$m^2_A = 0 \tag{2.13}$$

$$m^2_Z = \frac{1}{4} v^2 \left(g^2 + g'^2\right), \tag{2.14}$$

with eigenvectors

$$v_A = \begin{pmatrix} \frac{g}{\sqrt{g^2+g'^2}} \\ -\frac{g'}{\sqrt{g^2+g'^2}} \end{pmatrix}, \qquad v_Z = \begin{pmatrix} \frac{g'}{\sqrt{g^2+g'^2}} \\ \frac{g}{\sqrt{g^2+g'^2}} \end{pmatrix} \tag{2.15}$$

and so we define the massless photon,

$$A_\mu \equiv \frac{g}{\sqrt{g^2+g'^2}} B_\mu - \frac{g'}{\sqrt{g^2+g'^2}} W^3_\mu \tag{2.16}$$

and the massive Z boson,

$$Z_\mu \equiv \frac{g'}{\sqrt{g^2+g'^2}} B_\mu + \frac{g}{\sqrt{g^2+g'^2}} W^3_\mu. \tag{2.17}$$

It is standard to define the weak mixing angle θ_W such that $\tan\theta_W = g'/g$ and

$$\begin{pmatrix} A \\ Z \end{pmatrix} = \begin{pmatrix} \cos\theta_W & \sin\theta_W \\ -\sin\theta_W & \cos\theta_W \end{pmatrix} \begin{pmatrix} B \\ W^3 \end{pmatrix}. \tag{2.18}$$

Writing the inverse matrix equation,

$$\begin{pmatrix} B \\ W_3 \end{pmatrix} = \begin{pmatrix} \cos\theta_W & -\sin\theta_W \\ \sin\theta_W & \cos\theta_W \end{pmatrix} \begin{pmatrix} A \\ Z \end{pmatrix}, \tag{2.19}$$

gives the old fields in terms of the new fields, so that the neutral part of the covariant derivative becomes

$$D_\mu^{(\mathrm{nt})} = \partial_\mu + iA_\mu \frac{gg'}{\sqrt{g'^2+g^2}} \left(T^3 + \frac{Y}{2}\right) + iZ_\mu \left(g^2 T^3 - g'^2 \frac{Y}{2}\right). \tag{2.20}$$

Here T^3 is the third component of weak isospin. Then we identify the new coupling e and charge Q as

$$e = g\sin\theta_W = g'\cos\theta_W \tag{2.21}$$

$$Q = T^3 + \frac{Y}{2}. \tag{2.22}$$

The fact that there is a linear combination of the gauge fields that remains massless and does not interact with the Higgs directly (i.e., the photon) suggests that there is a corresponding linear combination of symmetry generators that remains unbroken, which is of course just the electric charge operator Q we just defined. We can verify this is follows. Given a symmetry transformation generated by $e^{i\alpha_a T^a}$, an infinitesimal transformation is $1+\alpha_a T^a$. If $(1+\alpha_a T^a)\phi = \phi$ then the symmetry must be present. In other words, the symmetry generator should annihilate the vacuum: $T^a\phi = 0$. In

this case,

$$Q\phi = (T^3 + \frac{Y}{2}) \begin{pmatrix} 0 \\ v \end{pmatrix} \tag{2.23}$$

$$= \frac{1}{2} \begin{pmatrix} 1 + \frac{Y_\phi}{2} & 0 \\ 0 & 1 - \frac{Y_\phi}{2} \end{pmatrix} \begin{pmatrix} 0 \\ v \end{pmatrix}, \tag{2.24}$$

which is zero if $Y_\phi = 1$. Thus, with our choice of hypercharge for the Higgs doublet, the symmetry generated by Q is indeed unbroken, as desired.

Chapter 3

Measuring the Weak Mixing Angle

The majority of the work described in this chapter was done by A. Gritsan and N. Tran and appears in the latter's Ph.D. thesis [31] as well as in the CMS publication [32]. The present author's work was limited to the final-state radiation uncertainties study presented in the final section of this chapter.

3.1 Introduction & Background

The Large Hadron Collider (LHC) makes possible measurements never before made, as well as to obtain unprecedented precision and robustness in measurements of known quantities [33]. One way in which robustness is improved is by measuring some known quantity using a novel process. The weak mixing angle is one of the most important and fundamental quantities in the Standard Model (and in constraining

BSM physics) [13]. It must be determined empirically but then the fermions' relative couplings to the photon and Z are determined. As such, it has been studied rather extensively [13, 34–42]. However, prior to 2011 only the D0 and CDF collaborations had utilized the Drell-Yan (DY) process, in which a quark-antiquark pair (in that case from a proton and an antiproton) annihilate into oppositely-charged leptons [43–46].

In [32] and [31] this measurement was performed for the first time using proton-proton collision data, studying events observed at the LHC with the Compact Muon Solenoid (CMS) detector. The symmetric nature of these collisions as opposed to the earlier proton-antiproton studies introduced a new difficulty compared to previous studies, but one which allowed for the development and deployment of a novel technique of broad applicability.

The present author contributed to the measurement in [32] primarily through some statistical analysis, particularly involving the systematic uncertainties associated with final-state radiation. We will review some background on the process and the analytic model used in the measurement before expounding these statistical considerations and their incorporation into the measurement, and we conclude the chapter by quoting the measured result. Additional technical details will be given in the appendices.

3.1.1 Running of "Constants"

We have seen in chapter 2 how the angle θ_W emerges in the SM. At its most basic level, it is the angle which rotates the pre-symmetry breaking gauge bosons W^3_μ, B_μ

into the new mass eigenstates A_μ, Z_μ. As we saw in section 2.2, at least naively we have

$$\cos\theta_W = \frac{g}{\sqrt{g'^2 + g^2}} \tag{3.1}$$

$$\sin\theta_W = \frac{g'}{\sqrt{g'^2 + g^2}}. \tag{3.2}$$

Furthermore, we have [13]

$$e = g\sin\theta_W = g'\cos\theta_W \tag{3.3}$$

$$\frac{M_W^2}{M_Z^2} = \frac{g^2}{g^2 + g'^2} = \cos^2\theta_W, \tag{3.4}$$

involving the positron's charge and the gauge boson masses.

Of course, these relationships are only all constant and exact at the classical level. The coupling constants g, g' depend on the energy scale, and their running is not identical. Indeed, while the SM does not predict values for these couplings, one of the key tests of it is their evolution, and therefore the evolution of the relations above.

In a gauge field theory, the coupling h runs (at one loop) according to [47, 48]

$$\beta_h \equiv \frac{dh^2}{\ln\mu} \tag{3.5}$$

$$= -\frac{h^4}{8\pi^2}\left(\frac{11}{3}T(\mathrm{Ad}) - \frac{2}{3}T(F) - \frac{1}{3}T(S)\right) \equiv -\frac{h^4}{8\pi^2}b_h, \tag{3.6}$$

where the index $T(R)$ (which is ½ the Dynkin index) for a representation R is defined by

$$\mathrm{Tr}(T_R^a T_R^b) = T(R)\delta^{ab} \tag{3.7}$$

and the representations here are the adjoint (the gauge fields), the fermions, and the scalars. Both of the latter come in multiplets, living in the fundamental and antifundamental (or conjugate) representations, that must be summed over. The standard normalizations for the fundamental ($R = \square$) and adjoint representations in a $SU(N)$ theory are

$$T(\square) = 1/2, \quad T(\mathrm{Ad}) = N. \tag{3.8}$$

For the $SU(2)_L$ of the SM, then, we have

$$\beta_g = -\frac{g^4}{8\pi^2} \cdot \frac{19}{6}. \tag{3.9}$$

But for an abelian gauge theory such as $U(1)_Y$, the first term in b is absent and $T(\square) = Y$, leaving

$$\beta_{g'} = \frac{g'^4}{8\pi^2} \cdot \frac{41}{6}. \tag{3.10}$$

These equations yield distinctive predictions for the (energy-dependence of the) physical observables mentioned above.

Note that we have not defined a scaled coupling $g_1 \equiv \sqrt{\frac{5}{3}}g'$ here as is common (motivated by $SU(5)$-based unification).

3.1.2 Previous Measurements

Because electroweak observables are sensitive to new physics while also being susceptible to high-precision measurements due to good control of backgrounds, a huge amount of experimental and phenomenological work has been done in the electroweak

sector over the past 50+ years [13, 34–42, 49–53], especially since Yang and Lee's unexpected 1956 suggestion [49] that symmetry under parity reversal could be violated in weak interaction and the observation of the effect the following year [15], followed not long after by the even more surprising discovery that charge-parity (CP), or equivalently, time reversal, was violated [50].

There are many ways to slice and dice the electroweak data, trading one set of observables for another and leveraging specific capabilities or techniques; see, e.g., [13, 34–36]. Of course $\alpha \approx \frac{1}{137}$ and the boson masses are heavily studied, as are the left-right asymmetry A_{LR}, forward-backward asymmetry A_{FB}, the vector and axial-vector couplings, and the Peskin-Takeuchi parameters, among others [13, 54]. The A_{FB} has previously been the primary way to get a measurement for $\sin^2\theta_W$ [32]. The Peskin-Takeuchi parameters are a convenient formalism for evaluating the effects of new theoretical proposals on electroweak precision physics (see chapter 6). The quantity $\sin^2\theta_W$ is one of the most studied. Previous measurements are shown in Table 3.1.

Authors	**Reported** $\sin^2\theta_W$	**Process Studied**
[37]	0.2324 ± 0.0083	Muon-neutrino - electron scattering
[42]	0.212 ± 0.014	Leptonic final states
[42]	0.236 ± 0.015	Hadronic final states
[42]	$0.223 \pm 0.011 \pm 0.007$	Combined
[38]	$0.2236 \pm 0.0028\,(\text{expt.}) \pm 0.0030\,(\text{model})$	Neutrino - nucleon scattering
[41]	0.22647 ± 0.00311	Neutrino - nucleon scattering
[53]	$0.2346 \pm 0.0105(\pm 0.0079)$	Deep inelastic scattering
[55]	$0.2379 \pm 0.0016\,(\text{stat.}) \pm 0.0013(\text{syst.})$	Møller scattering

Table 3.1: Previous measurements of $\sin^2\theta_W$.

3.2 Description of the CMS Analysis

This section describes enough of the analysis performed by CMS [32], and especially by Gritsan and Tran [31], to provide a context for the study of final-state radiation uncertainties described in the next section. Further details of the analysis may be found in the appendix.

3.2.1 The Drell-Yan Process

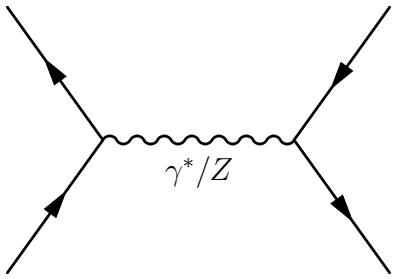

Figure 3.1: The Drell-Yan process at the parton level.

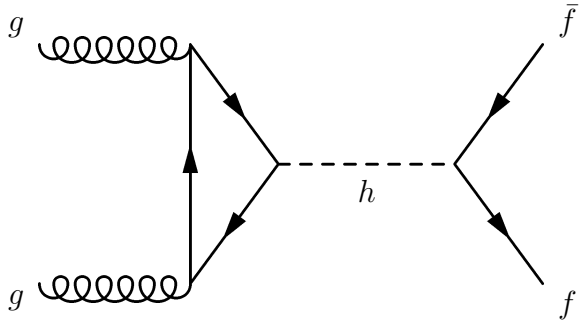

Figure 3.2: Gluon fusion to a Higgs that decays to a fermion-antifermion pair.

As previously mentioned, the Drell-Yan (DY) process (shown at the parton level in Fig. 3.1) is one in which a quark and antiquark annihilate to produce an off-shell photon or Z boson, which then decays to a lepton-antilepton pair. If there are new heavy neutral gauge bosons, they can also contribute to the amplitude [32, 56, 57]. More generally, the process has the potential to expose unexpected deviations in one or more particle's effective couplings to the SM gauge bosons. It is also possible that an excess of final-state lepton pairs could be observed as a result of some new, heavy resonance around the TeV-scale, similar to Higgs production by gluon fusion and

subsequent decay via a fermion pair [32, 58, 59].

The measurement of the weak mixing angle has been performed to a precision of $\sim 0.1\%$ in the clean processes at LEP and SLC [36]. It is not realistic to beat this precision with the data available to CMS as of Run I. However, measurements of $\sin^2\theta_W$ that use processes with different initial and final pairs explore the universality of the coupling constants, and in particular, in a process like that of Fig. 3.1, the measurement tests the universality between leptons and hadrons, an interesting check on the SM [13, 32]. The Tevatron experiments D0 and CDF obtained a precision of $\sim 1\%$ using the DY process, which sets a benchmark for the current study.

3.2.2 Problems Presented by a pp Collider

The benchmark established by the Tevatron collaborations is nontrivial, especially since at the LHC there is no way of knowing which proton carried the quark and which the antiquark. This is significant because interference between vector and axial-vector couplings leads to an asymmetry in the kinematics of the outgoing lepton (the so-called "forward-backward asymmetry" or A_{FB}), with a spatial variation dependent on the direction of the incoming quark, yet we can only match a quark with one proton or the other on a statistical basis [32, 57, 60]. This deduction is based essentially on the parton distribution functions (PDFs) that characterize the probability for a given species of parton to carry a given fraction of a hadron's momentum. For a proton, a valence quark statistically carries much more momentum than any antiquark [61].

	ρ_V	ρ_A
$\gamma \to e^-e^+, \mu^-\mu^+, \tau^-\tau^+$	-1	0
$\gamma \to u\bar{u}, c\bar{c}, t\bar{t}$	$+2/3$	0
$\gamma \to d\bar{d}, s\bar{s}, b\bar{b}$	$-1/3$	0
$Z \to e^-e^+, \mu^-\mu^+, \tau^-\tau^+$	$\frac{-3+12\sin^2\theta_W}{6\sin(2\theta_W)}$	$\frac{-1}{2\sin(2\theta_W)}$
$Z \to u\bar{u}, c\bar{c}, t\bar{t}$	$\frac{+3-8\sin^2\theta_W}{6\sin(2\theta_W)}$	$\frac{+1}{2\sin(2\theta_W)}$
$Z \to d\bar{d}, s\bar{s}, b\bar{b}$	$\frac{-3+4\sin^2\theta_W}{6\sin(2\theta_W)}$	$\frac{-1}{2\sin(2\theta_W)}$

Table 3.2: Vector and axial-vector couplings of the SM charged fermion fields to the neutral electroweak gauge bosons.

The boost direction of the lepton pair indicates the total momentum in the event, and based on it's projection towards one end of the detector or the other, we make our identification. Since the PDFs are not trivial, we will be wrong sometimes. So it is important to study how great a source of error this introduces and how the precision of the measurement suffers. It is found to be within tolerable limits [32, 62].

3.2.3 The Model

The starting point for the analysis [31,32] is an analytic expression obtained from the matrix element for the The parton-level cross section for the process $q\bar{q} \to Z/\gamma^* \to$

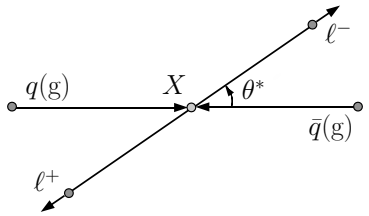

Figure 3.3: The angle θ^*, defined in the dilepton rest frame.

$\ell^-\ell^+$. This is

$$\begin{aligned}\hat{\sigma}_{q\bar{q}}(\hat{s},\cos\theta^*;\theta_W) \propto & \frac{3\left(\rho_V^{q\bar{q}\to\gamma}\right)^2\left(\rho_V^{\gamma\to\ell\ell}\right)^2}{2\,\hat{s}}\times(1+\cos^2\theta^*)\\ &+\frac{3}{2}\frac{\hat{s}}{(\hat{s}-m_Z^2)^2+m_Z^2\Gamma_Z^2}\times\Bigg[\left(\left(\rho_V^{q\bar{q}\to Z}\right)^2+\left(\rho_A^{q\bar{q}\to Z}\right)^2\right)\left(\left(\rho_V^{Z\to\ell\ell}\right)^2+\left(\rho_A^{Z\to\ell\ell}\right)^2\right)\\ &\times\left(1+\cos^2\theta^*\right)+8\,\rho_V^{q\bar{q}\to Z}\rho_A^{q\bar{q}\to Z}\rho_V^{Z\to\ell\ell}\rho_A^{Z\to\ell\ell}\cos\theta^*\Bigg]\\ &+\frac{3(\hat{s}-m_Z^2)\rho_V^{q\bar{q}\to\gamma}\rho_V^{\gamma\to\ell\ell}}{(\hat{s}-m_Z^2)^2+m_Z^2\Gamma_Z^2}\times\left[\rho_V^{q\bar{q}\to Z}\rho_V^{Z\to\ell\ell}\left(1+\cos^2\theta^*\right)+2\,\rho_A^{q\bar{q}\to Z}\rho_A^{Z\to\ell\ell}\cos\theta^*\right].\end{aligned} \tag{3.11}$$

Here$\hat{s}$ is the energy-squared involved in the parton process, while θ^* is defined in the lepton pair's center-of-momentum frame as the angle between the direction of an incoming proton and the outgoing lepton, as shown in 3.3. To reduce the effects of transverse momentum carried by the quark pair, the Collins-Soper frame is used, in which θ^* is the angle between the lepton and an axis which bisects the acute angle between one incoming proton and the extension of the the direction traveled by the other proton [63]. The odd powers of $\cos\theta^*$ are the source of the distinctive asymmetry [31, 32] .

Now the PDFs $f_a(x_i,\hat{s})$ describe the probability for a quark of type a to carry x_i

of the proton momentum $\sqrt{s}/2$ [61]. In fact these values are probability densities, so that the probability to find quark type a carrying a fraction of the momentum in an infinitesimal neighborhood of x_i is $f_a(x_i, \hat{s})\, dx_i$. Also, the $\hat{\sigma}_{q\bar{q}}$ above depends on $\cos\theta^*$ but of course to get a total cross-section for the process we must integrate over this variable. So the product $\hat{\sigma}_{q\bar{q}}$ must be a differential cross-section [31, 32].

$$\begin{aligned}\frac{d\sigma_{pp}(px_1, px_2, \cos\theta^*; \theta_W)}{dx_1\, dx_2\, d\cos\theta^*} \propto \sum_{q=\mathrm{u,d,s,c,b}} &[\hat{\sigma}_{q\bar{q}}(\hat{s}, \mathrm{sgn}(x_1 - x_2)\cos\theta^*; \theta_W)\, f_q(x_1, \hat{s}) f_{\bar{q}}(x_2, \hat{s}) \\ &+ \hat{\sigma}_{q\bar{q}}(\hat{s}, \mathrm{sgn}(x_2 - x_1)\cos\theta^*; \theta_W)\, f_q(x_2, \hat{s}) f_{\bar{q}}(x_1, \hat{s})].\end{aligned} \tag{3.12}$$

Here $\mathrm{sgn}(x_1 - x_2) = \Theta(x_1 - x_2) - \Theta(x_2 - x_1)$. This is the manifestation of the assumption that the quark direction coincides with the boost of the dilepton pair. This assumption introduces a dilution in the odd-power terms in $\cos\theta^*$ because there will be times when what we call θ^* should actually be $\pi - \theta^*$ but the even-power terms are insensitive to whether we feed them $\cos\theta^*$ or $-\cos\theta^*$.

The dilepton rapidity Y and squared invariant mass $\hat{s}$ are put in terms of x_1, x_2 as

$$Y = \frac{1}{2}\ln\left(\frac{x_1}{x_2}\right) = \frac{1}{2}\ln\left(\frac{\hat{E} + \hat{p}_z}{\hat{E} - \hat{p}_z}\right) \tag{3.13}$$

$$\hat{s} = x_1 x_2 s = \hat{E}^2 - \hat{p}^2, \tag{3.14}$$

where $\hat{E}$ is the dilepton energy and $\hat{p}$ is its momentum. To leading order in QCD,

$\hat{p} = \hat{p}_z$ [32]. With these variables the differential cross-section becomes [31, 32]

$$\frac{d\sigma_{pp}(Y, \hat{s}, \cos\theta^*; \theta_W)}{dY\, d\hat{s}\, d\cos\theta^*} \propto \sum_{q=\mathrm{u,d,s,c,b}} F_{q\bar{q}}(\hat{s}, Y) \times [\hat{\sigma}^+_{q\bar{q}}(\hat{s}, \cos^2\theta^*; \theta_W) + D_{q\bar{q}}(\hat{s}, Y) \times \hat{\sigma}^-_{q\bar{q}}(\hat{s}, \cos\theta^*; \theta_W)]. \tag{3.15}$$

The explicit forms of the functions $F, D, \hat{\sigma}^{\pm}$ may be found in the appendix. The $\hat{\sigma}^+$ and $\hat{\sigma}^-$ contain the parts even and odd in $\cos\theta^*$, respectively. The function D is a dilution factor that affects only the odd part, while F contains overall effects from the PDFs in terms of the new variables; because the dilution factor is dependent on how good an approximation the assumption about quark direction is, both functions depend on the PDFs [31, 32]. The leading order approximation in CTEQ6 [64] was extracted numerically and then parametrized, yielding the distributions seen in Fig. 3.4.

The accuracy of the analytical models used in eq. 3.15 and the functions D and F was tested by comparison with output from PYTHIA [65]. The results are shown in Figs. 3.5 and 3.6 [31, 32].

So far the analysis had only dealt with the physical process itself, not the actual detection of the events. The imperfections in detection and uncertainties from various sources are considered next. The major considerations are the acceptance of the detector (and how it varies with different kinematics of the events), the resolution of the detector (including effects from misalignment), and final-state radiation (FSR), as well as contamination from background processes [31, 32]. Formally describing the resolution and FSR effects by a function $\mathcal{R}(x)$, where x is the change in dilepton

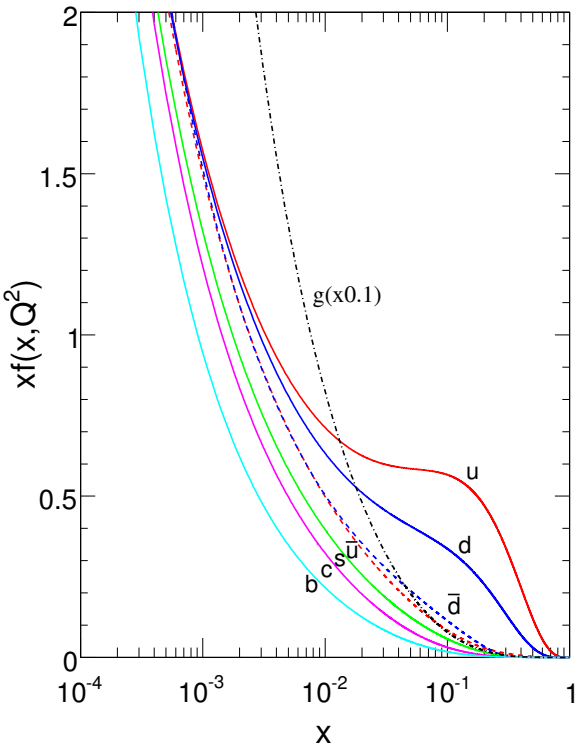

Figure 3.4: Parametrization obtained from CTEQ6 PDFs. The gluon contribution is scaled by a factor of 0.1. Originally appeared in [31, 32].

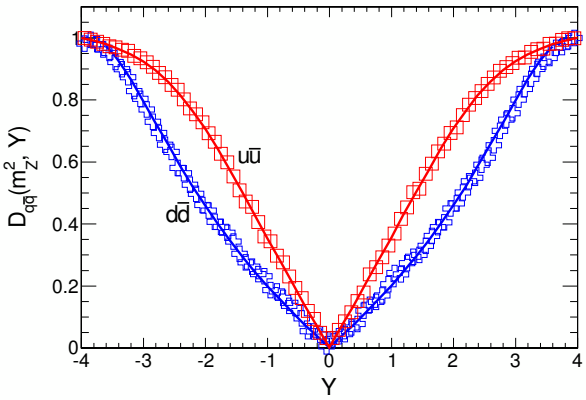

Figure 3.5: Comparison of dilution factor $D_{q\bar{q}}(\hat{s} = m_Z^2, Y)$ for up-type (red) and down-type (blue) quark-antiquark pairs. The boxes and crosses, respectively, show the output from PYTHIA, while the solid lines depict the analytical model. Good agreement is seen across the range of rapidity. Originally appeared in [31, 32].

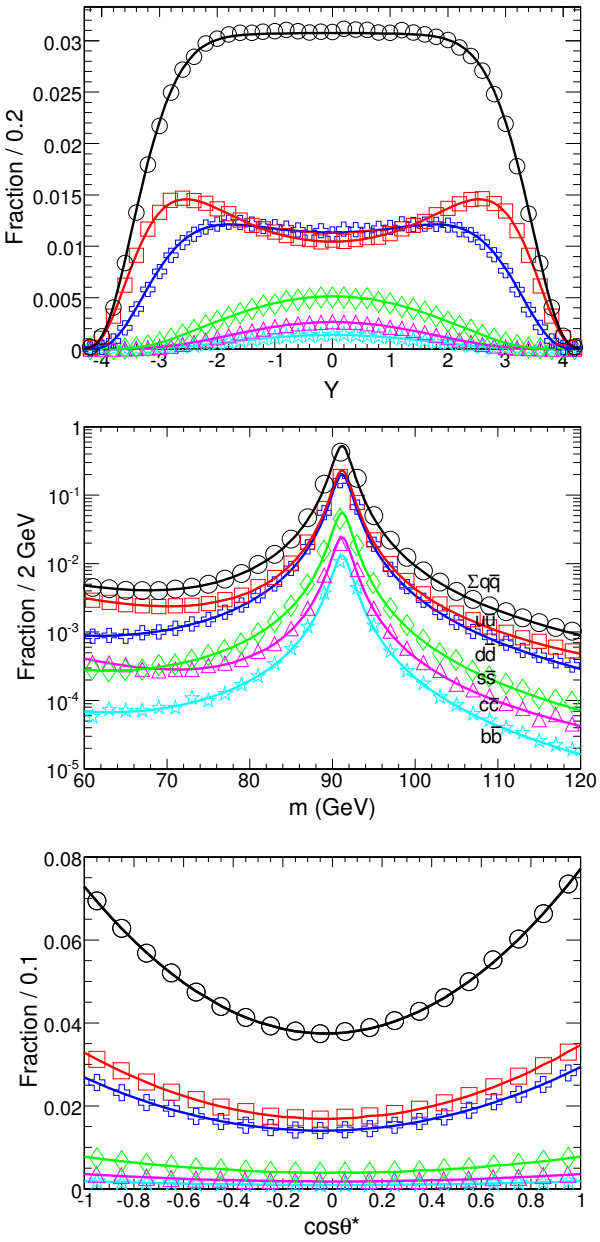

Figure 3.6: Comparison between analytic model and PYTHIA output for normalized distributions of rapidity (top), invariant mass (middle), and $\cos\theta^*$ (bottom), for the five quark flavors up (red), down (blue), strange (green), charm (magenta), and bottom (cyan), as well as for the sum of all five (black). In each case the solid lines are the prediction of the analytic model while the discrete points represent the output from PYTHIA simulation. Originally appeared in [31, 32].

invariant mass squared, and other detector effects (acceptance) by $\mathcal{G}(Y, \hat{s}, \cos\theta^*)$, a signal probability density function is defined,

$$\mathcal{P}_{\rm sig}(Y, \hat{s}, \cos\theta^*; \theta_{\rm eff}) = \mathcal{G}(Y, \hat{s}, \cos\theta^*) \times \int_{-\infty}^{\infty} dx\, \mathcal{R}(x) \mathcal{P}_{\rm ideal}(Y, \hat{s} - x, \cos\theta^*; \theta_{\rm eff}), \quad (3.16)$$

where $\mathcal{P}_{\rm ideal}$ is the differential cross-section defined in eq. 3.15. With this, we further define a likelihood function,

$$\mathcal{L} = \exp(-n_{\rm sig} - n_{\rm bkg}) \prod_i^N \left(n_{\rm sig} \times \mathcal{P}_{\rm sig}(\vec{x}_i; \theta_{\rm eff}; \vec{\zeta}) + n_{\rm bkg} \times \mathcal{P}_{\rm bkg}(\vec{x}_i; \vec{\zeta}) \right), \quad (3.17)$$

where $\vec{x}_i = \{Y_i, \hat{s}_i, \cos\theta_i^*\}$ are the observables for each candidate event, $\vec{\zeta}$ are the parameters of these functions (such as those that describe $\mathcal{G}$ and $\mathcal{R}$), $n_{\rm sig}$ is the number of signal events, $n_{\rm bkg}$ is the number of background events, and $\mathcal{P}_{\rm bkg}$ is the probability density function for background processes [31, 32]. The effects of $\mathcal{G}$ and $\mathcal{R}$ are reproduced in 3.7.

Equations 3.16 and 3.17 essentially complete the formalism necessary to understand the analysis. The background is modeled by Monte Carlo simulation and checked with data, but the total expected background is only about 0.05% of the signal, and therefore not much of a concern [31,32]. The final fit for $\sin^2\theta_W$ in [31,32] was performed by maximizing the likelihood function as defined above. After accounting for systematic bias and uncertainty as well as statistical uncertainty (see the following section and Table 3.3), the result of the analysis, including all uncertainties and corrections [31, 32]

$$\sin^2\theta_{\rm eff} = 0.2287 \pm 0.0020\ (\text{stat.}) \pm 0.0025\ (\text{syst.})\,. \quad (3.18)$$

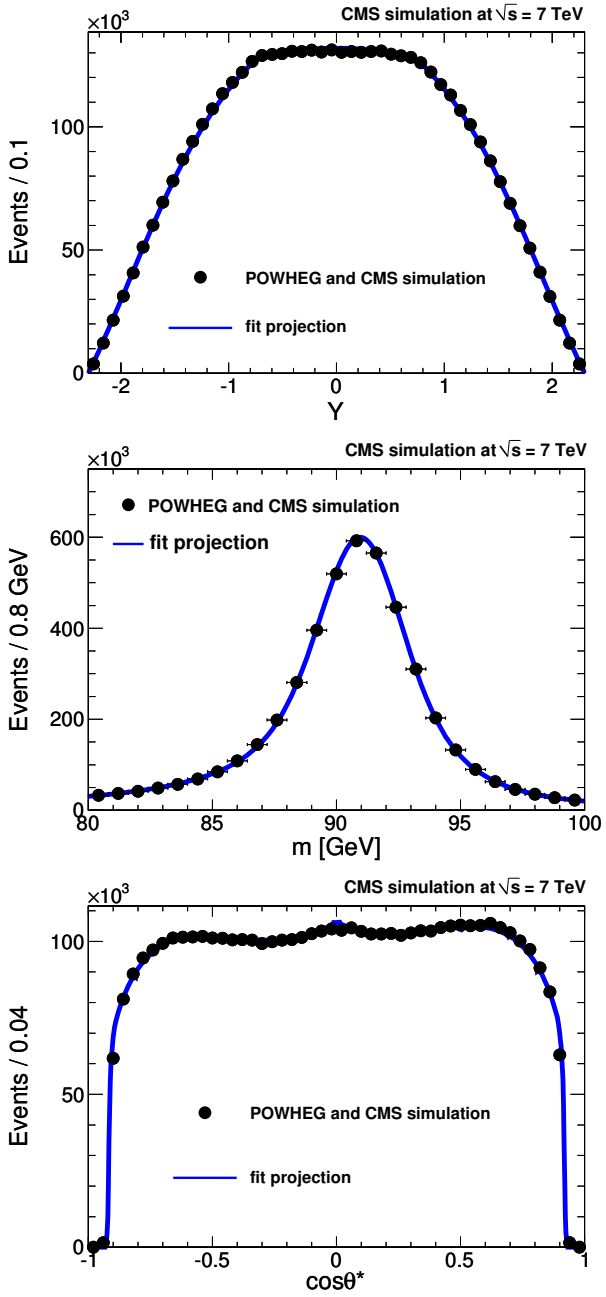

Figure 3.7: Normalized distributions of rapidity (top), invariant mass (middle), and $\cos\theta^*$ (bottom), from PYTHIA simulation (points) and its analytical parameterization (smooth curve). The total distributions of Fig. 3.6 appear in red, while distributions after acceptance and resolution effects, including FSR, appear in blue. The dominant effects in Y and $\cos\theta^*$ come from detector effects, while the dominant effects in m are from FSR and resolution. Originally appeared in [31, 32].

3.3 FSR and Uncertainty

We have sketched the method used by [31, 32] for performing a fit to extract $\sin^2\theta_W$. Uncertainties in the fit are introduced from purely statistical uncertainty stemming from the finite number of events in the data sample, uncertainties in the PDFs, uncertainties in relevant parameters for predictions of the backgrounds, as well as the finite order in perturbation theory at which they are calculated, uncertainties in modeling final state radiation, such as the emission of photons, and the finite resolution and imperfectly-known detector effects [32]. The present author's contribution was primarily in determining the systematic uncertainty from FSR modeling. For a detailed discussion of the origin and determination of other uncertainties, see [31,32]. The final values for each are presented here in Table 3.3.

After the primary Drell-Yan process has occurred, either or both of the leptons can emit some form of radiation. This will affect the measured kinematics of the lepton pair when detected. The primary effect is on the reconstructed invariant mass since such FSR will always reduce the energy while the effects on Y and $\cos\theta^*$ have less bias for any one direction. The effect of this radiation (as well as "smearing" of the observables due to finite detector resolution and possible tracker misalignment) was modeled with the resolution function $\mathcal{R}(x)$ mentioned above. This which was chosen to be a sum of four Gaussians, which provided satisfactory power and flexibility in describing all of the relevant effects while allowing for analytic convolution as shown in eq. 3.16, and the parameters of these four Gaussians were determined by a fit

to simulated data [31, 32]. Thus the precision of the final results depends upon the quality of the simulation used for the fit.

The FSR was modeled with PYTHIA for the actual parameterization of the resolution function $\mathcal{R}(x)$ used in the final fit for $\sin^2\theta_W$. We used four alternative FSR models, with a simplified detector simulation, and examined the change in our final results to estimate the uncertainty originating from the theoretical modeling of FSR: PYTHIA, PHOTOS [66], and two different modes in HORACE [67]. All three generator programs perform $O(\alpha)$ calculations of FSR and provide similar results, while the HORACE generator also allows the exact $O(\alpha)$ calculation and multiple-photon radiation from all charged states. Cross-fits of the four generated samples using the four corresponding resolution functions $\mathcal{R}(x)$ were perfomed by taking a single initial simulation data set, running it through all four FSR modes, extracting $\mathcal{R}$ for each, and then fitting the output of all four modes with each $\mathcal{R}$. The PYTHIA sample was typically the outlier from the other generators. Although a larger effect on the analysis occurred if a wide range of values for the invariant mass m was allowed, with cuts applied to restrict $80 < m < 100$ GeV the effects were small. Differences in the fitted $\sin^2\theta_{\rm eff}$ values were found to be at most 0.0011, and a systematic uncertainty of ± 0.0011 was assigned to cover these deviations.

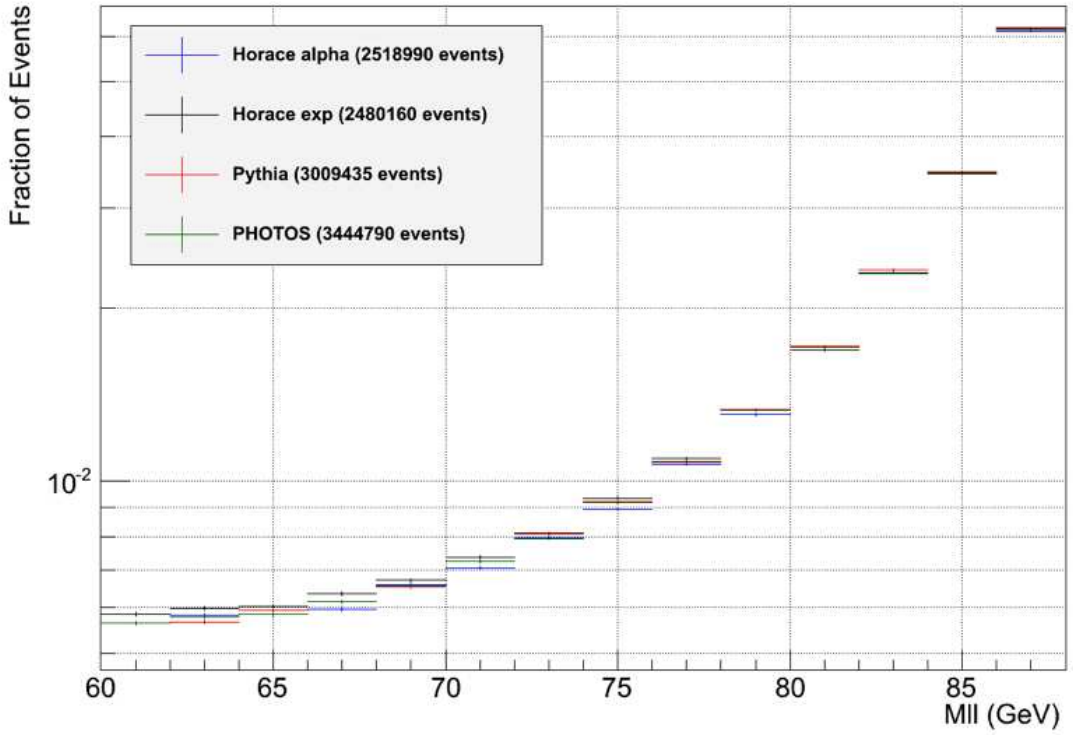

Figure 3.8: A plot of the low end of the dimuon invariant mass m after FSR as modeled by the four simulations: PYTHIA, PHOTOS, and two HORACE modes. Relative discrepancies become more significant at the high and low ends of the mass range.

Table 3.3: Corrections and systematic uncertainties in the measurement of $\sin^2\theta_{\text{eff}}$.

source	correction	uncertainty
PDF	–	±0.0013
FSR	–	±0.0011
LO model (EWK)	–	±0.0002
LO model (QCD)	+0.0012	±0.0012
resolution and alignment	+0.0007	±0.0013
efficiency and acceptance	–	±0.0003
background	–	±0.0001
total	+0.0019	±0.0025

Chapter 4

Interlude: Naturalness and Supersymmetry

We have seen how the electroweak theory was constructed and how it works. We now turn to one of its most puzzling features, at least according to many theorists, along with an introduction to supersymmetry, one of the leading contenders to help solve this puzzle. That puzzling feature is widely referred to as its "unnaturalness" [68–70]. There are a few variations on what exactly the concept of naturalness should mean but these all share a kindred spirit. In [68], two different kinds of unnaturalness are identified in the SM. One is the enormous ratio between Newton's constant and Fermi's constant ($G_F/G_N \sim 10^{33}$), and the other is the existence of high sensitivity of low scale physics to small changes in the high-energy bare parameters, as is found in the SM Higgs mass. These are obviously related but solving one does

not necessarily solve the other. In [71], naturalness is defined according to the rule that a number much different than unity is natural only if setting it to zero increases the symmetry of the theory, in other words, if it is protected by a symmetry. Susskind and Farhi referred to the naturalness problem of the Higgs mass's sensitivity to corrections in proposing technicolor [72], and cited a work by Wilson [73] that referred to the unique status of elementary scalars as prone to corrections from arbitrarily high energy physics. According to [69], as late as 1979 there was little attention paid to the problem (if it was even regarded as one). However, in a 1980 article Veltman emphasized the issue [74] and soon after Witten published an enormously influential paper on dynamical supersymmetry breaking, in which it was pointed out that such a scenario solved the naturalness problem [75]. With these papers, and the 1981 construction by Georgi & Dimopolous [76] of a realistic supersymmetric GUT, SUSY and the question of naturalness had captured the attention of particle theorists.

Supersymmetry has long been associated with the electroweak scale [77–82]. Along with gauge coupling unification [83, 84], provision of a dark matter candidate [85–87], and the Haag–Lopuszanski–Sohnius theorem [88], supersymmetry's clean resolution of the problem of the electroweak scale's naturalness has been one of the major factors fueling research in the subject [68, 70, 89]. When calculating the one-loop quantum corrections to the Higgs mass in the SM, one finds a quadratic dependence on the cutoff Λ:

$$(m_h^{obs})^2 = (m_h^0)^2 + \frac{\lambda}{16\pi^2}\Lambda^2 + ... \tag{4.1}$$

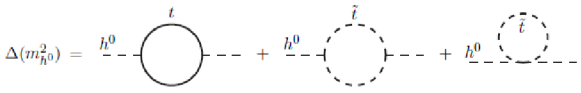

Figure 4.1: Diagrams contributing to Higgs quantum corrections.

The beauty of SUSY in this arena is that it automatically cancels these divergences because of the opposite sign with which the boson and fermion loops contribute [47, 48]. Because particles and superpartners are part of a multiplet and thus have their couplings related, in unbroken SUSY they will contribute exactly opposite terms. When SUSY is broken (as it must be to describe our world), then contributions on the order of the soft masses for the bosons will tend to spoil the cancellation.

This is why explorations of the TeV scale at the LHC have been rather suspenseful for proponents of supersymmetry: it could always be found at higher energies, but one of the strongest reasons for believing in it will be deeply eroded if not found soon. Searches at the LHC have eaten into much of the simplest and most appealing parameter space [90, 91].

Simultaneously, the parameter space has been squeezed by the observation of a Higgs boson with mass $m_h \approx 125.5$ GeV at the LHC [92, 93]. In the Minimal Supersymmetric Standard Model (MSSM), the Higgs's tree-level mass is bounded by m_Z:

$$m_h^0 \leq m_Z |\cos 2\beta| \leq 91.2 \text{ GeV}, \tag{4.2}$$

where $\tan\beta = v_1/v_2$ is the ratio of two Higgs fields' vacuum expectation values (two

are required in the MSSM, one for the up-type particle flavors and one for the down, both to cancel anomalies and for the more technical reason of holomorphicity of the superpotential) [47,86]. This is because unlike in the SM, in supersymmetry the only quartic Higgs term comes from the so-called D-terms, which are tied to the gauge couplings [47,77,86]:

$$D^a = -g^a(\phi^* T^a \phi), \tag{4.3}$$

where a indexes the gauge group generators. The quartic terms appear in the scalar potential as

$$V(\phi, \phi^*) \supset \frac{1}{2}\sum_a D^a D^a = \frac{1}{8}(g^2 + g'^2)(|H_u^0|^2 - |H_d^0|^2)^2. \tag{4.4}$$

The requirement that electroweak symmetry be broken by a nonzero Higgs vacuum expectation value, combined with the above, leads to the quoted tree-level mass bound [47,77,86]. Since supersymmetry is broken, quantum corrections can raise the physical Higgs mass from this value; however, it is not easy to achieve the observed mass without introducing such large SUSY–breaking masses that naturalness of the theory is threatened. In the following chapters, a model is described that manages to obtain the observed Higgs mass without introducing a high degree of fine-tuning between energy scales. But first we give an extremely brief introduction to SUSY.

Chapter 5

Introducing SUSY

When constructing quantum field theories, one of the most fundamental guiding principles is the following rule: *Given some field content, write down every term in the Lagrangian allowed by the symmetries one wishes the theory to have.* For this reason, as well as the existence of associated conserved quantities, the symmetries of a theory go a long way towards characterizing the theory. Thus the determination of the symmetries that should or could exist in a theory (or not) is a natural point of interest.

It was highly significant, then, when Coleman and Mandula showed that in any four-dimensional quantum field theory with a mass gap, the symmetry Lie algebra of the S-matrix could only be a direct product of the Poincare algebra and some internal symmetry's algebra (e.g., a gauge symmetry); spacetime symmetries and internal symmetries could never be combined in a nontrivial way – at least not those symme-

tries corresponding to Lie algebras [94]. This helped bound the space of theories we might consider realistic.

To make this explicit, recall that the Poincare algebra is

$$[P_\mu, P_\nu] = 0 \tag{5.1}$$

$$\frac{1}{i}[M_{\mu\nu}, P_\rho] = \eta_{\mu\rho}P_\nu - \eta_{\nu\rho}P_\mu \tag{5.2}$$

$$\frac{1}{i}[M_{\mu\nu}, M_{\rho\sigma}] = \eta_{\mu\rho}M_{\nu\sigma} - \eta_{\mu\sigma}M_{\nu\rho} - \eta_{\nu\rho}M_{\mu\sigma} + \eta_{\nu\sigma}M_{\mu\rho}, \tag{5.3}$$

where P_μ is the generator of translations and $M_{\mu\nu}$ is the generator of (homogeneous) Lorentz transformations. Then if T^a is a generator of an internal symmetry (e.g., the $SU(3)$ of QCD), we must have

$$[T^a, P_\mu] = [T^a, M_{\mu\nu}] = 0. \tag{5.4}$$

However, building on work of Neveu, Schwarz, and Ramond [95], in 1971 and 1972 three independent groups (Gervais & Sakita [96]; Volkov & Akulov [97]; Golfand & Lihktman [98]) recognized that allowing Lie superalgebras (Lie algebras with both commuting and anticommuting generators) in a quantum field theory yielded a loophole to Coleman-Mandula. In 1975 Haag, Lopuszanski, and Sohnius systematically explored all the extensions of the algebra of this type [88]. One obtains in this way the super-Poincare algebra, which presents the only possible non-trivial combination of an internal symmetry and spacetime symmetry. In addition to the usual Poincare

algebra, one has

$$\left\{Q_\alpha, \bar{Q}_{\dot{\beta}}\right\} = 2(\sigma^\mu)_{\alpha\dot{\beta}} P_\mu \tag{5.5}$$

$$[M_{\mu\nu}, Q_\alpha] = \frac{1}{2}(\sigma^{\mu\nu})^\beta_\alpha Q_\beta \tag{5.6}$$

$$[P_\mu, Q_\alpha] = 0 \tag{5.7}$$

$$\{Q_\alpha, Q_\beta\} = \left\{\bar{Q}_\alpha, \bar{Q}_\beta\right\} = 0, \tag{5.8}$$

with analagous commutation relations for $\bar{Q}$ with M and P and $\alpha, \beta = 1, 2$. The $Q, \bar{Q}$ are fermionic (spin $\frac{1}{2}$) generators with the property of turning bosons into fermions and vice versa. Roughly speaking, the $Q, \bar{Q}$ act like raising and lowering operators, similar to the familiar $a, a^\dagger$ of quantum mechanics. Similar to the case of isospin, we can define a set of "angular momentum" operators that indexes multiplets and the members within multiplets. Then if $|j, m\rangle$ is a one-particle state with spin m and is part of a supermultiplet with maximum spin j then

$$J_3 Q_1 |j, m\rangle = \left(m - \frac{1}{2}\right) Q_1 |j, m\rangle \tag{5.9}$$

$$J_3 Q_2 |j, m\rangle = \left(m + \frac{1}{2}\right) Q_2 |j, m\rangle \tag{5.10}$$

$$J_3 \bar{Q}_1 |j, m\rangle = \left(m + \frac{1}{2}\right) \bar{Q}_1 |j, m\rangle \tag{5.11}$$

$$J_3 \bar{Q}_2 |j, m\rangle = \left(m - \frac{1}{2}\right) \bar{Q}_2 |j, m\rangle \,. \tag{5.12}$$

Since P commutes with $Q, \bar{Q}$, so too does P^2, and therefore states related by supersymmetry transformations have the same mass – that is, as long as supersymmetry is unbroken. Clearly this does not describe our world, so supersymmetry must

be dynamically broken. Several methods of accomplishing this have been devised, notably gauge-mediated, gravity-mediated, and anomaly-mediated supersymmetry breaking [47, 48, 86, 99]. We will not go into detail here but a useful fact to note is that since $Q_\alpha \bar{Q}_{\dot{\beta}} + \bar{Q}_{\dot{\beta}} Q_\alpha = 2\sigma^0_{\alpha\dot{\beta}} P_0$, it follows that $P_0 = H \geq 0$. If the vacuum is supersymmetric then $Q_\alpha |0\rangle = \bar{Q}_{\dot{\beta}} |0\rangle = 0$ and $H = 0$, while if it is not, one of the SUSY generators does not annihilate the vacuum and $H > 0$. Thus a requirement for broken SUSY is a positive vacuum energy. This makes for a useful test.

The baseline for a realistic supersymmetric model is the Minimal Supersymmetric Standard Model, or MSSM. It consists of chiral superfields for each of the Standard Model fermions (each of which is a supermultiplet containing the fermion and two scalars), two chiral Higgs superfields (containing Higgs scalars playing the role of the SM Higgs as well as additional scalars and superpartner fermions), and vector superfields for each of the SM gauge bosons (containing the gauge boson and a superpartner fermion) [47, 48, 86]. The scalar superpartners of fermions are commonly denoted by prefixing an "s" to the fermion name (e.g., selectron, squark) while the fermion superpartners of bosons are commonly referred to by appending "-ino" to the end of the boson's name (e.g., Higgsino, gluino). Much of a supersymmetric Lagrangian can be obtained from the superpotential, denoted W, which is a holomorphic function of chiral superfields. In the expansion of the superfields, there are actually additional components but these can be eliminated in favor of new terms involving the stated components; the F-terms and D-terms commonly referenced in SUSY literature refer

to such terms.

There is vast literature on the subject of SUSY and many good introductory texts; we have only hoped to give the unfamiliar reader sufficient background to follow the modifications, goals, and problems encountered in the next chapter.

Chapter 6

Top mixing, Supersymmetry, and the Higgs Mass

This chapter was born out of work done with C. Faroughy and published in [100].

6.1 Introduction

Dynamically broken supersymmetry offers an elegant way of cutting off leading divergences of quantum corrections to the Higgs mass parameter in the standard model. Unless parameters in the model are finely tuned, one expects that the mass of supersymmetric particles are of the same order as the Z and W masses. In particular, quantum corrections to the Higgs mass parameter are dominated by the contributions from the top quark, because of the large Yukawa coupling. To preserve naturalness,

this leads to the expectation that the top squark should be relatively light.

However, results from the Large Hadron Collider (LHC) indicate that the Higgs mass is ~ 125 GeV [92, 93]. In the MSSM, a mass so much higher than the tree-level upper bound of m_Z can be accommodated only with extremely heavy top squarks, or moderately heavy top squarks and large top squark mixing. The quadratic divergence contributed by such a heavy top squark then needs to be cancelled at the level of $\sim 10^{-4}$, leading to a significantly fine-tuned theory. This tuning is significantly worse than the tuning implied by direct constraints on superpartners at the LHC. In fact, in the case of only moderate mixing, the top squark mass implied by this Higgs mass is higher than the direct collider limit ~ 3 TeV that can ever be set by the LHC.

Unlike many other experimental constraints on the MSSM, this "Little Hierarchy" problem [101, 102] is directly associated with the low energy spectrum of the theory. Consequently, it cannot be solved through ultraviolet mechanisms that are often invoked to address indirect constraints (such as flavor or CP violation, see [103] for an overview) or alteration of the collider signatures of supersymmetry to avoid direct constraints on the theory [104–109]. Several attempts have been made to modify the MSSM spectrum through the addition of matter fields to raise the Higgs mass [110–143]. These mechanisms were originally proposed to accommodate the Higgs mass bound $\gtrapprox 114$ GeV imposed by LEP, and though more recent work has demonstrated the ability for such a mechanism to yield a Higgs mass ~ 125 GeV (e.g., [144]), in general the higher mass needs significantly larger couplings than considered

in the earlier models, leading to the rapid appearance of Landau poles marginally above the weak scale. While such a possibility cannot be logically excluded, it destroys the success of perturbative grand unification in supersymmetric models, an aesthetic success of the MSSM.

In [100], we proposed a new strategy to address the Little Hierarchy problem. The largest loop contribution to the effective potential of the Higgs comes from the top supermultiplet and the magnitude of this contribution is governed by the top Yukawa. The Yukawa coupling used in current estimates of the top quark contribution to the Higgs mass is directly extracted from measurements of the top mass. However, the naive relation between the physical mass of the top quark and the Yukawa coupling, extracted from the tree level Lagrangian, is modified when the top supermultiplet is mixed with other heavier states. When diagonalizing the mass matrix, the new mixing terms will contribute negatively to the naive estimate $y_t v \sin\beta$, thus requiring a larger Yukawa coupling to obtain the measured value of the top, $m_t \sim 173$ GeV. Since the Higgs effective potential depends upon the fourth power of this coupling, even a moderate increase can lead to a significant enhancement of the Higgs mass.

We demonstrate this mechanism through a simple extension of the models [136, 137, 144] where a vector-like fourth generation with Yukawa couplings to the Higgs was introduced. In these models, the additional contributions from the vector-like generation was sufficient to push the Higgs mass above the LEP bound of ~ 114 GeV. This goal could be accommodated with perturbative gauge coupling unification with

relative ease using only the Yukawa couplings of the fourth generation with itself. Consequently, mixing between the fourth generation and the standard model was not explored. But the mixing between the top quark and the fourth generation is experimentally fairly unconstrained. Indeed, recently there has been more interest shown in exploring this possibility, with [145] in particular seeking to constrain the possible dominant mixing angle for any (single) vector-like heavy multiplet. However, it has not been noted that such a mixing can contribute significantly to the mechanism for raising m_h so far above m_Z. When this mixing is $\mathcal{O}(1)$, we show that the Yukawa couplings necessary to obtain the physical top quark mass are large enough to substantially increase the Higgs mass.

This chapter is structured as follows. We describe the model in section 6.2. In section 6.3, we discuss the effects of large mixing on the top Yukawa. We compute the weak-scale mixing Yukawa couplings necessary to achieve a Higgs mass of ~ 125 GeV and the induced top Yukawa Landau pole. In section 6.4 we study the experimental constraints and briefly discuss the LHC phenomenology. Finally, we conclude in section 6.5.

6.2 The Model

In this model, we extend the MSSM by adding a full vector-like fourth generation (i.e., a chiral fourth generation plus its mirror) with Yukawa couplings to the Higgs.

Furthermore, the couplings mixing the fourth generation and the top sector are allowed to take on values close to unity; they have a quasi-fixed point which limits their TeV values to be not much larger than 1 [137]. However, we ignore mixing with the first and second generations since these are constrained by experiment to be small. We consider the simplest model which preserves gauge coupling unification. Therefore, the new vector-like generation contains quark and lepton supermultiplets Q_4, U_4^c and E_4^c, living in the **10** representation of SU(5), plus the corresponding mirror generation $\bar{Q}_4^c$, $\bar{U}_4$, and $\bar{E}_4$ living in the $\bar{\mathbf{10}}$ representation. The $SU(3)_c \times SU(2)_L \times U(1)_Y$ quantum numbers of the additional coloured superfields and the top sector, plus explanation of our conventions and notation are shown in Table 6.1.

The relevant mass-eigenstate Dirac fermions are the top t, bottom b, and the new quarks $t'_{1,2}$ and b' of charge +2/3 and -1/3, respectively. In the scalar sector the relevant particles are the top squarks $\tilde{t}_{1,2}$, bottom squarks $\tilde{b}_{1,2}$, and the corresponding non-MSSM squarks $\tilde{t}'_{1,2,3,4}$, and $\tilde{b}'_{1,2}$. The terms in the superpotential that affect the Higgs mass are:

$$W \subset y_{ij} Q_i H_u U_j^c + \mu_Q \bar{Q}_4^c Q_4 + \mu_U \bar{U}_4 U_4^c + \mu H_u H_d \tag{6.1}$$

where i and j are generation indices than run from 3 to 4, and μ is the usual coefficient of the Higgs bilinear term. Terms such as $\mu_{34} Q_3 \bar{Q}_4^c$ are rotated away without loss of generality. Yukawa couplings of the form $\bar{y}_{44} H_d \bar{Q}_4^c \bar{U}_4$ and Yukawa couplings between the Higgs and the leptons are ignored since their effect in raising the Higgs mass is subdominant in the large $\tan\beta$ limit. In the soft Lagrangian, we assume the same

Supermultiplet	**Scalars**	**Fermions**	$\mathbf{SU(3)_C}$	$\mathbf{SU(2)_L}$	$\mathbf{U(1)_Y}$	$\mathbf{T^3}$	**Q**
Q_3	$(\tilde{u_3}, \tilde{d_3})$	(u_3, d_3)	**3**	**2**	1/6	(1/2,-1/2)	(2/3,-1/3)
U_3^c	$\tilde{u}_3^c$	u_3^c	$\bar{\mathbf{3}}$	**1**	-2/3	0	-2/3
D_3^c	$\tilde{d}_3^c$	d_3^c	$\bar{\mathbf{3}}$	**1**	1/3	0	1/3
Q_4	$(\tilde{u}_4, \tilde{d}_4)$	(u_4, d_4)	**3**	**2**	1/6	(1/2,-1/2)	(2/3,-1/3)
U_4^c	$\tilde{u}_4^c$	u_4^c	$\bar{\mathbf{3}}$	**1**	-2/3	0	-2/3
$\bar{Q}_4^c$	$(\tilde{\bar{d}}_4^c, \tilde{\bar{u}}_4^c)$	$(\bar{d}_4^c, \bar{u}_4^c)$	$\bar{\mathbf{3}}$	**2**	-1/6	(1/2,-1/2)	(1/3,-2/3)
$\bar{U}_4$	$\tilde{\bar{u}}_4$	$\bar{u}_4$	**3**	**1**	2/3	0	2/3

Table 6.1: The third and fourth generation coloured fields and their quantum numbers in the gauge eigenstate basis are listed in the table above. We follow the standard convention that all chiral supermultiplets are defined in terms of 2-component left-handed Weyl spinors, so that charge conjugates of right-handed fields are used. The barred fields denote gauge-eigenstate fields belonging to the $\bar{\mathbf{10}}$ representation of $SU(5)$. 4-component Dirac fermions can be constructed as $q_D = (q_i, q_i^{c\dagger})^T$. The mass basis fermions are the top t, bottom b, and the new quarks $t'_{1,2}$ and b' of charge +2/3 and -1/3, respectively. Their superparters are the top squarks $\tilde{t}_{1,2}$, bottom squarks $\tilde{b}_{1,2}$, and the corresponding non-MSSM squarks $\tilde{t}'_{1,2,3,4}$, and $\tilde{b}'_{1,2}$.

squared mass Δm^2 for all the squarks, $B\mu$ terms corresponding to each vector-like mass (ignoring mixed $B\mu$ terms with the third generation), and A-terms of the form $y_{ij}A$ associated with each Yukawa coupling. Throughout the paper, we set $\tan\beta = 30$. We refer to the appendices for details about the particle spectrum and the interaction Lagrangian.

6.3 The Effects from Mixing

6.3.1 Mixing and the Top Yukawa Coupling

As stated in the introduction, the qualitative difference between this note and earlier work [136, 137, 144] is the emphasis on the mixing terms proportional to y_{34} and y_{43}. In general, we assume a parameter space where y_{34}, y_{43} and y_{44} are allowed to vary from 0 to values $\gtrsim 1$, while the top Yukawa is constrained to give the right top mass. We consider the four following benchmark scenarios for the Yukawas: (1) $y_{34} = -y_{43} \gg y_{44}$, (2) $y_{43} \gg y_{34}, y_{44}$, (3) $y_{34} \gg y_{43}, y_{44}$, and (4) $y_{44} \gg y_{34}, y_{43}$. Case 1 focuses on effects where both mixing Yukawas are significant, whereas cases 2 and 3 focus on mixing from only one term. Case 4 corresponds to earlier work [136,137,144] where the mixing terms y_{34} and y_{43} were ignored, and serves as a useful comparison. As will be shown in section 6.3.2, the parameter space where this model makes sizeable contributions to the Higgs mass is a region where the fourth generation is accessible at the LHC.

When mixing terms are present, and if $y_{44} = 0$, the top Yukawa coupling y_{33} necessary to obtain the measured top mass $m_t = 172.9$ GeV is given by:

$$y_{33} = \frac{m_t}{v \sin\beta} \left(1 + \frac{(y_{43}\, v \sin\beta)^2}{\mu_Q^2 - m_t^2}\right)^{1/2} \left(1 + \frac{(y_{34}\, v \sin\beta)^2}{\mu_U^2 - m_t^2}\right)^{1/2}. \tag{6.2}$$

This formula is exact when $y_{44} = 0$ and is obtained after bi-diagonalizing the up-type fermion mass matrix m_f^u (shown explicitly in appendix B.1), identifying its smallest singular value with the top mass, and solving for y_{33}. If $y_{44} \neq 0$, the above formula still holds to a very good approximation since the coupling y_{44} first makes an appearance at fourth order in the expansion parameter $(v/\mu_{Q,U})$, and therefore has a negligible effect in raising the value of y_{33}.

For simplicity, we take $\mu_Q = \mu_U \equiv \mu_4$. In this case, we can define $\Delta = v/\mu_4$ to quantify the hierarchy between the new vector-like mass scale and the electroweak scale, such that $\Delta = 0$ in the limit $\mu_4 \to \infty$. At large $\tan\beta$, and taking $m_t/v = 1$, equation 6.2 can be approximated as

$$y_{33} \approx 1 + \frac{1}{2}\left(\frac{\Delta^2}{1 - \Delta^2}\right)\left(y_{43}^2 + y_{34}^2\right) + \mathcal{O}(\Delta^4). \tag{6.3}$$

Evidently, $\Delta > 0$ leads to an increase in the top Yukawa. As a result, the soft masses Δm needed to get a 125 GeV Higgs decrease. Taking the value of the mass of the new quarks to be near their experimental limit of $700 - 800$ GeV (see section 6.4.3) leads to the constraint $\Delta \lesssim 1/4$. Then, in the case where the mixing Yukawas are near unity, the effects of mixing between the top sector and the fourth generation

can lead to an increase of y_{33} by about 6%. This can significantly increase the Higgs mass squared since the radiative corrections go as y_{33}^4. Mixing effects on the Higgs mass are studied in detail in section 6.3.2. Lastly, we note that an increase in the top Yukawa also leads to an increase in the Higgs quartic; however, this increase is subdominant compared to the Higgs mass.

6.3.2 Weak-Scale Yukawa Couplings

In this section we compute the weak-scale Yukawa couplings necessary to obtain the required Higgs mass using the one-loop effective potential in the decoupling limit (where $m_A, m_{H^+}, m_{H^-}, m_{H^0} >> m_h$). Contributions to the Higgs effective potential have the following form:

$$\Delta V = \frac{3}{32\pi^2}[\sum_{\{\tilde{m}_a\}} \tilde{m}_a^2 \left(\ln \frac{\tilde{m}_a^2}{Q^2} - \frac{3}{2}\right) - 2\sum_{\{m_a\}} m_a^2 \left(\ln \frac{m_a^2}{Q^2} - \frac{3}{2}\right)] \tag{6.4}$$

where Q is the renormalization scale and m_a ($\tilde{m}_a$) are the quark (squark) masses. The summation runs over the masses of the heavy up-type quarks ($a = t, t_1', t_2'$) and their superpartners ($a = \tilde{t}_{1,2}, \tilde{t}'_{1,2,3,4}$). The resulting physical Higgs mass is then

$$m_h = \sqrt{m_Z^2 \cos^2 2\beta + \frac{1}{2}\left(\frac{\partial^2(\Delta V)}{\partial v_u^2} - \frac{1}{v_u}\frac{\partial(\Delta V)}{\partial v_u}\right)}. \tag{6.5}$$

For numerical efficiency, the algorithm used to solve for the necessary parameters obtains a Higgs mass in the range 125.5 ± 0.5 GeV. For this set of computations

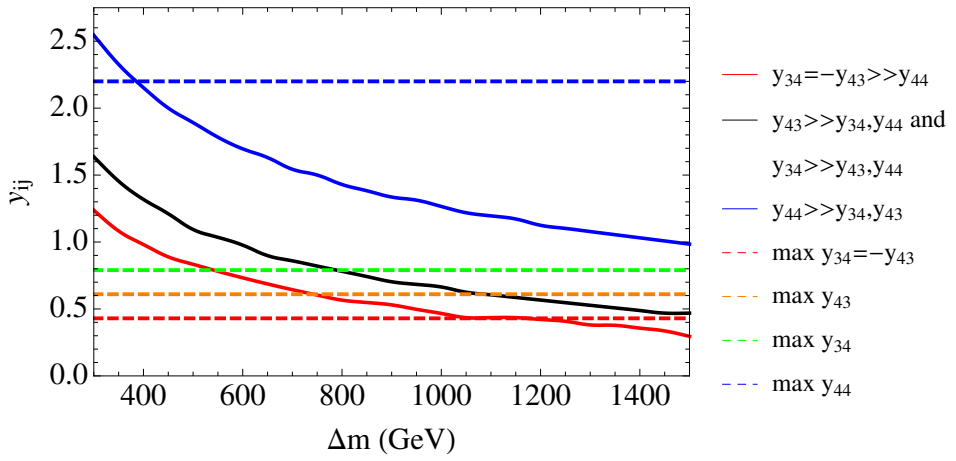

Figure 6.1: We plot the values of the Yukawa couplings at the weak scale necessary to obtain $m_h = 125.5 \pm 0.5$ GeV, as a function of Δm. We take $A = \Delta m$, $\mu_4 = 900$ GeV. When either y_{34} or y_{43} dominates, the same value of the dominant Yukawa is required to get $m_h = 125.5$ GeV so both scenarios are represented by one black line. The dotted lines show the maximum values allowed by EWPM for each mixing scenario (see section 6.4). Since y_{34} and y_{43} contribute to the oblique parameters differently they have different constraints on their maximum values, represented by the green and orange dotted lines, respectively. Above the dotted line requires Yukawas larger than allowed by EWPM and is thus ruled out.

we take the soft terms to be of the form $\Delta m = A$, as might be expected in gravity mediation (or high scale gauge mediation [136]), and choose $\mu_4 = 900$ GeV. The Yukawa values at the weak scale as functions of the soft masses are plotted in Figure 6.1, along with their constraints from electroweak precision measurements. As one would intuitively expect, the mixing Yukawas necessary to achieve a given Higgs mass are smaller when $|y_{34}| \sim |y_{43}|$ than when one of these couplings dominates the other. However, the lowest possible value of Δm consistent with EWPM is $\Delta m \sim 800$ GeV and occurs for the case where $y_{34} \sim 0.8$ and $y_{43} = y_{44} = 0$.

6.3.3 Top Yukawa Landau Pole

The mixing terms y_{34} and y_{43} significantly affect the Higgs mass only when they are $\mathcal{O}(1)$. These $\mathcal{O}(1)$ Yukawas affect the renormalization group evolution of the top Yukawa y_{33} and can cause it to hit a Landau pole. In this section, we estimate the scale at which this Landau pole is attained for various choices of the Yukawas and soft terms necessary to obtain a Higgs mass ~ 125 GeV. The top Yukawa two-loop beta function presented in appendix B.4 is used to calculate the scale Λ where the coupling y_{33} hits a Landau pole. Below, we plot Λ as a function of the soft mass Δm and consider the effects from:

1. Different mixing scenarios.

2. A-terms.

3. The vector-like mass μ_4.

4. The number of extra multiplets in the $\mathbf{5} + \bar{\mathbf{5}}$ of SU(5).

From Figure 6.2, we see that large mixing can push Λ above the GUT scale while retaining soft masses as low as $\sim$ 900 GeV. The three different mixing scenarios give comparable results because these Yukawa couplings reinforce each other in their respective renormalization group evolution. In contrast, to push Λ above $\sim 10^{16}$ in the case with no mixing requires soft masses to be larger than 1.5 TeV.

From Figures 6.3 and 6.4 it is clear that for a given soft mass, the implied Landau

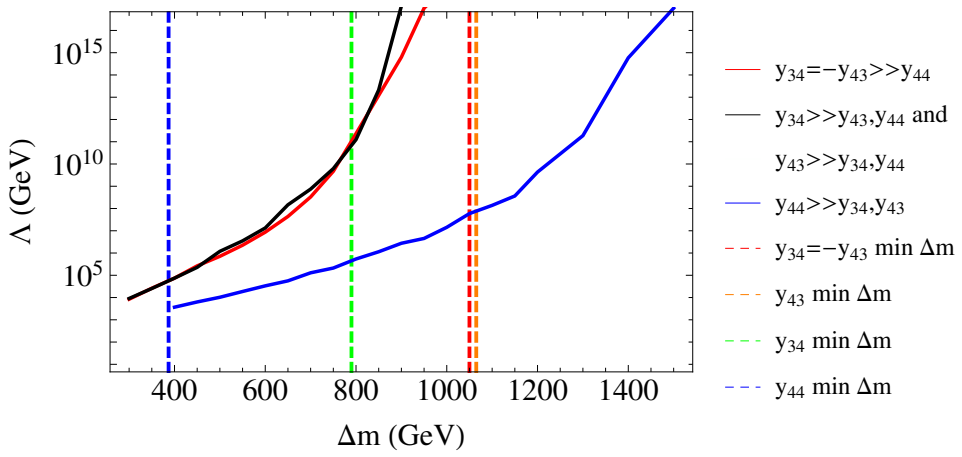

Figure 6.2: We plot the scale Λ where the y_{33} required to get $m_h = 125.5$ GeV hits a Landau pole, as a function of the soft mass Δm. We set $A = \Delta m$, $\mu_4 = 900$ GeV, and $n_5 = 0$. Soft masses to the left of the dotted lines can only yield $m_h = 125.5$ GeV with Yukawa couplings larger than allowed by EWPM and are thus ruled out (see section 6.4). Physically uninteresting values of $\Lambda < 1$ TeV are not plotted. The presence of mixing decreases significantly the value of the soft masses needed. As can be seen from the plot, the scale of the Landau pole in the cases with sizeable mixing are all comparable. The case where either y_{34} or y_{43} dominate (shown in black) yield identical values since each contributes to the top Yukawa beta function in the same way. However, their differing effects on the oblique parameters lead to different minimum values for the soft masses.

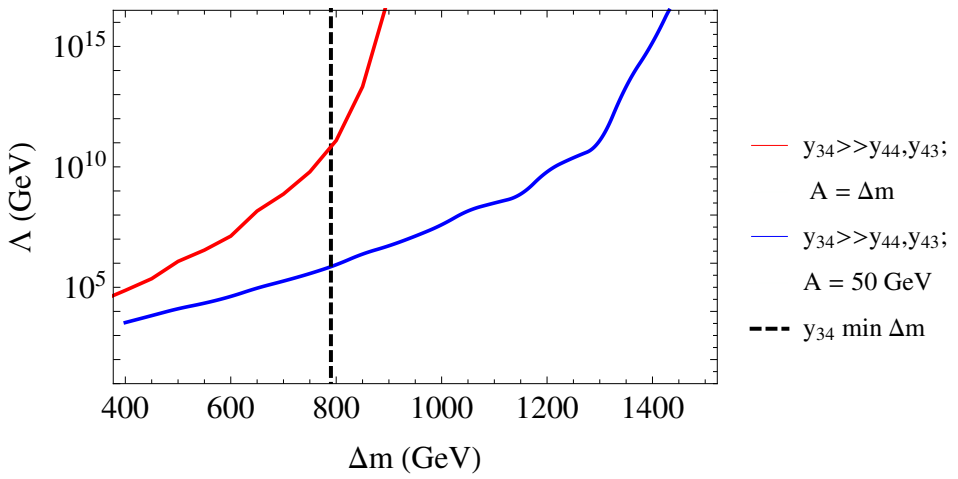

Figure 6.3: We plot the scale Λ where the y_{33} required to get $m_h = 125.5$ GeV hits a Landau pole, as a function of the soft mass Δm. We set $y_{34} \gg y_{44}, y_{43}$, $\mu_4 = 900$ GeV, and $n_5 = 0$. Soft masses to the left of the dotted lines can only yield $m_h = 125.5$ GeV with Yukawa couplings larger than allowed by EWPM and are thus ruled out (see section 6.4). There is only one line here since these limits are independent of the A-terms). For a given soft mass the implied Landau pole gets significantly pushed up by the presence of A-terms.

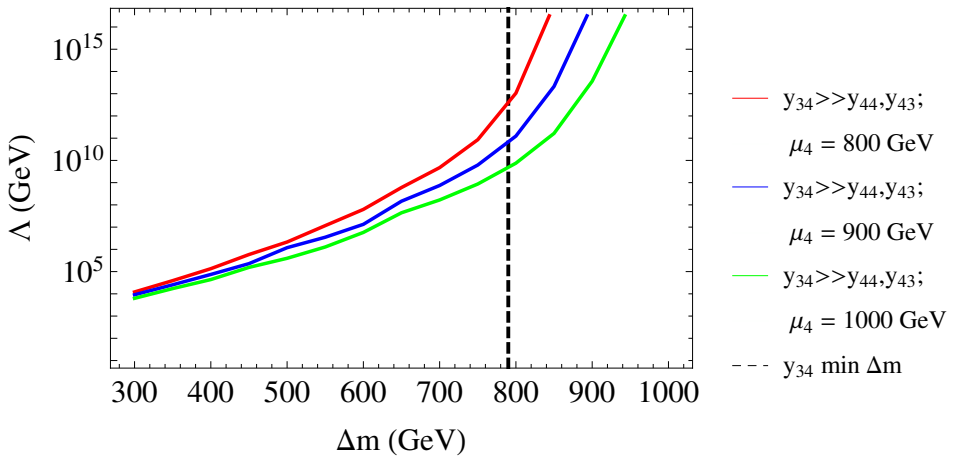

Figure 6.4: We plot the scale Λ where the y_{33} required to get $m_h = 125.5$ GeV hits a Landau pole, as a function of the soft mass Δm. We set $y_{34} \gg y_{44}, y_{43}$, $A = \Delta m$, and $n_5 = 0$. Soft masses to the left of the dotted lines can only yield $m_h = 125.5$ GeV with Yukawa couplings larger than allowed by EWPM and are thus ruled out (see section 6.4). For a given soft mass, the implied Landau pole increases as the vector mass decreases.

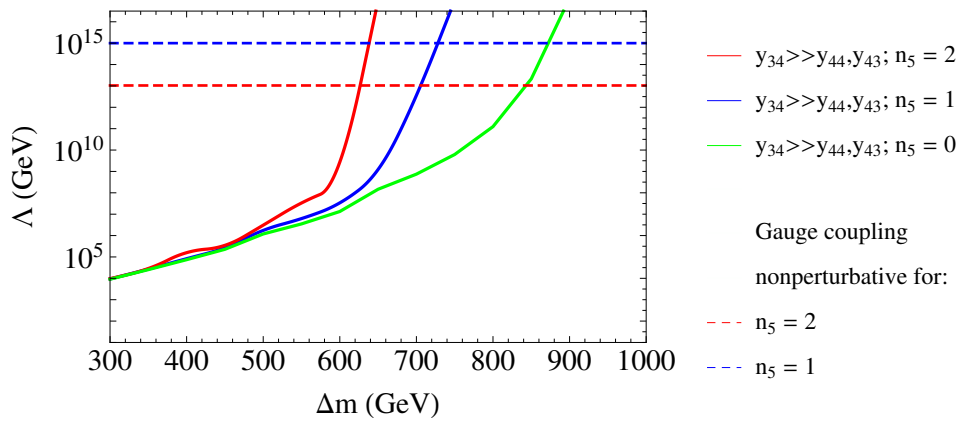

Figure 6.5: We plot the scale Λ where the y_{33} required to get $m_h = 125.5$ GeV hits a Landau pole, as a function of the soft mass Δm. We set $y_{34} \gg y_{44}, y_{43}$, $A = \Delta m$, $\mu_4 = 900$ GeV. Here the dotted lines indicate where the gauge couplings become non-perturbative for $n_5 = 2$ and $n_5 = 1$. They remain perturbative all the way to the GUT scale for $n_5 = 0$.

pole scale can also get pushed up by including larger A-terms or a smaller vector mass. For $A = \Delta m \sim 900$ GeV, Λ can be pushed above the GUT scale. Δm can be as low as 800 GeV, albeit in parts of parameter space with a Landau pole at $\sim 10^{10}$ GeV.

In the last point (4) above, we included one more parameter in our analysis, namely, the number n_5 of multiplets in the $\mathbf{5} + \bar{\mathbf{5}}$ representation of $SU(5)$ that are added to the model. These could correspond, for example in the minimal version of gauge-mediated supersymmetry breaking (GMSB), to messenger fields which don't couple to the Higgs and that communicate SUSY breaking from a hidden sector to the visible sector. This number does not affect the Yukawas necessary to obtain the Higgs mass but it contributes to the running of the gauge couplings, making them stronger in the ultraviolet. And since the gauge couplings contribute negatively to

the renormalization of the Yukawas, a larger ultraviolet gauge coupling slows the growth of the y_{ij}'s, pushing up the Landau pole. However, as we will see, to preserve perturbative gauge coupling unification we cannot add an arbitrary number of n_5 in addition to the vector-like $\mathbf{10} + \bar{\mathbf{10}}$ of SU(5) necessary in our model. To verify perturbativity we used the one-loop beta functions presented in appendix B.4 and required $g_{\text{unif}} \lesssim 3$. From Figure 6.5, we see that the gauge couplings become non-perturbative around 10^{13} GeV for $n_5 = 2$ and 10^{15} GeV for $n_5 = 1$. They remain perturbative all the way to the GUT scale for $n_5 = 0$. Therefore, the Landau pole can still be pushed above the GUT scale if one sacrifices perturbativity at the scale of unification.

6.4 Constraints

In this section, we work out the constraints from Higgs production, measurements of the relevant Cabibbo-Kobayashi-Maskawa matrix element V_{tb}^{CKM}, the most recent mass bounds from direct searches for vector-like quarks at the LHC (with up to 19.5 fb^{-1} of 8 TeV data from CMS [146] and 14.3 fb^{-1} of 8 TeV data from the ATLAS detector) and constraints on the oblique parameters S and T [54] from electroweak precision measurements. We find that the oblique corrections and LHC direct searches place the dominant constraints on the total parameter space but that portions of the remaining parameter space available can still raise the Higgs mass to $\sim$ 125 GeV

while yielding new quarks discoverable at the LHC in the near future.

6.4.1 Higgs Production

The Higgs production rate at the LHC is dominated by the gluon fusion process and recent measurements can be used to put constraints on any model with new particles that get their mass through the Higgs. In the case where a chiral fourth generation is added to the SM, this leads to an increase of the Higgs production rate by gluon fusion by about a factor of nine over the SM rate, in contradiction with experiments. This is a result of the fact that the new quarks get all of their mass via coupling to the Higgs; no decoupling limit exists to ameliorate the situation. However, in the case of a new generation of vector-like quarks the new quarks get their mass only partially through the Higgs, the remaining part coming from the vector-like mass parameter(s), here μ_4. This opens the possibility that the new generation might contribute differently to Higgs production.

One can see the dependence of the relevant amplitude on the parameters of the model as follows. We take the large tanβ limit throughout this discussion, though the procedure can be generalized in an obvious way. Consider an effective vertex coupling two gluons and a Higgs, which can be thought of as arising from a term in an effective Lagrangian with the form

$$\mathcal{L}_0 = g^* G_{\mu\nu} G^{\mu\nu} H, \tag{6.6}$$

where $H \to h+v$ after electroweak symmetry breaking (EWSB) so that $\mathcal{L}_0 \to \mathcal{L}_1+\mathcal{L}_1'$, where

$$\mathcal{L}_1 = g^* G_{\mu\nu} G^{\mu\nu} h \quad , \quad \mathcal{L}_1' = g^* G_{\mu\nu} G^{\mu\nu} v. \tag{6.7}$$

The amplitude associated with the effective ggh vertex is simply the unknown g^*. This is the same amplitude as for the $\mathcal{L}_1'$ "vertex," which can be interpreted as a correction to the gluon self-energy Π^{gg}. In particular, it is that part of the self-energy that comes from the coupling of particles in the loop to the Higgs vacuum expectation value (we consider only the one-loop correction). Rather than directly computing the effective ggh coupling g^* by summing all one-loop $gg \to h$ diagrams, we can use the ggv coupling to obtain g^* from the well-known form of the gluon self-energy in a simple way. For this we need consider all the contributions to the one-loop gluon self-energy, identify all the terms that include a factor of v, and sum the coefficients of v from each term. (Actually, what we need is just the sum, not individual coefficients.) Therefore to extract the information we want out of Π^{gg}, all we have to do is take a partial derivative with respect to v. In equation form, $g^* \sim \frac{\partial}{\partial v}\left[\Pi^{gg}(v)\right]$, where Π^{gg} is thought of as a function of v.

The form of corrections to vector boson propagators is well known. Since the coupling for a non-Abelian gauge theory is universal, all colored fermions in the loop contribute in the same way, i.e., the only difference between their contributions comes from the mass dependence. In particular, for a given quark running in the loop, one

obtains a logarithmic dependence on its squared mass, m_i^2. This implies that

$$\Pi^{gg} \supset c \sum_i \log(m_i^2), \tag{6.8}$$

where c is some constant and the sum is over t, t_1', t_2'. Now in the case under consideration all of the squared masses m_i^2 are the eigenvalues of the matrix $m_f^u m_f^{u\dagger}$ (as given in Appendix B.1). Since $\sum_i \log(m_i^2) = \log(\Pi_i m_i^2) = \log\left[\det\left(m_f^u m_f^{u\dagger}\right)\right]$ and $\det\left(m_f^u m_f^{u\dagger}\right) = \det^2\left(m_f^u\right)$, the relevant terms in Π^{gg} are given by

$$\Pi^{gg} \supset c \sum_i \log\left(m_i^2\right) = c \log\left[\det^2\left(m_f^u\right)\right]. \tag{6.9}$$

Taking the partial derivative,

$$A_{gg\to h} \propto \frac{\partial[\log(\det^2 m_f^u)]}{\partial v} = \frac{1}{\det^2 m_f^u} \frac{\partial \det^2 m_f^u}{\partial v}. \tag{6.10}$$

In the special case $\bar{y}_{44} = 0$, we have $\det(m_f^u) = v(y_{33}\mu_4^2 \sin\beta)$, which (taking $\sin\beta \approx 1$) is the same as in the SM aside from the factor of μ_4^2, which cancels in the amplitude. Thus $A_{gg\to h} \propto 2/v$, with no dependence on the y_{ij}'s or the vector-like mass parameter μ_4, and there is no change from the well-known approximate SM amplitude. We ignore contributions from the scalars, as these are suppressed. We note in passing that this expression has the right mass dimension for the g^* mutiplying the dimension five operator in $\mathcal{L}_0$.

6.4.2 $V_{tb}^{\mathbf{CKM}}$

The addition of the vector-like fourth generation will affect both the weak charged currents (CC) and the weak neutral currents (NC) at tree level. In particular, the

$W^{\pm}$ gauge bosons now couple to both left-handed and right-handed particles. Furthermore, including mixing with the top sector will enrich the flavor structure of the model and induce flavor changing neutral currents (FCNCs) in the mass eigenstate basis. These FCNCs only involve third and fourth generation particles and are therefore fairly unconstrained. In appendix B.2 we derive the triple and quartic gauge boson interaction terms with the quarks and squarks, as well as the interaction terms between the Higgs h_o and quarks.

The rotation from gauge to mass eigenstates leads to generalized CKM matrices between the third generation, fourth generation, and it's mirror generation (which can be viewed as a "fifth" generation), which we denote by K_α^{ab} for quarks, and $\tilde{K}_\alpha^{ab}$ for squarks, with $a, b = u, \bar{u}, d, \bar{d}$ and $\alpha = L, R$. These matrices will be present in every interaction term. Furthermore, they are not square matrices like in the MSSM because there are more up-type quarks than down-type quarks.

The generalized CKM matrix K_L^{ud} is a rectangular (2×3) matrix (see appendix B.2 for more details) in the mass basis (t, t_1', t_2') for the (4-component) up-type quarks and (b, b') for the down-type quarks. This matrix, being rectangular, is not unitary but satisfies the following equation:

$$\begin{aligned} K_L^{ud}(K_L^{ud})^\dagger + K_L^{\bar{u}\bar{u}}(K_L^{\bar{u}\bar{u}})^\dagger &= (V_L^{u\dagger} D_L^{ud} V_L^d)(V_L^{u\dagger} D_L^{ud} V_L^d)^\dagger + (V_L^{u\dagger} S_L^{\bar{u}\bar{u}\dagger} V_L^u)(V_L^{u\dagger} S_L^{\bar{u}\bar{u}\dagger} V_L^u)^\dagger \\ &= V_L^{u\dagger}(D_L^{ud} + S_L^{\bar{u}\bar{u}}) V_L^u \\ &= 1_{3\times 3} \end{aligned}$$

where we have used the unitarity of the mixing matrices V_L^u and V_L^d, and the fact that $D_L^{ud}(D_L^{ud})^\dagger = D_L^{uu}$, $(S_L^{uu})^\dagger S_L^{uu} = S_L^{\bar{u}\bar{u}}$ and $D_L^{uu} + S_L^{\bar{u}\bar{u}} = 1_{3\times3}$ (see appendix B.3 for the explicit form of these matrices).

The $(K_L^{ud})_{11}$ entry predicted by our model should lie within the margin of error of the measured value of $V_{tb}^{\rm CKM}$ (defined as the (3,3) entry of the (3×3) matrix corresponding to the SM CKM matrix V^{CKM}). As usual, we neglect the mixing between the first two generations and the higher generations. When unitary of the SM V^{CKM} is not assumed, $V_{tb}^{\rm CKM}$ was recently measured by CMS [147] to be $|V_{tb}^{\rm CKM}| = 1.14 \pm 0.22$. We therefore require $0.92 < (K_L^{ud})_{11} < 1.36$. After scanning over a large region of our relevant parameter space, we conclude that this restriction is always satisfied. Therefore, the constraints from the measured value of $V_{tb}^{\rm CKM}$ are negligible. This is in agreement with the statements in [144].

6.4.3 Mass Bounds from LHC Direct Searches

LHC direct searches [148–153] are the most obvious source of constraints on the masses of the new vector-like quarks. The branching ratios (BRs) of the new quarks depend on the relative size of the relevant Yukawa, W and Z couplings. Until fairly recently, many searches assumed 100 % BR through one channel, particularly the Wb decay, and therefore had a large degree of model-dependence [154]. However, unlike these searches, ATLAS and CMS now can exclude vector-like quarks in a model independent way by considering general branching ratio scenarios in their data anal-

ysis [146].

At the LHC, the t' (or b') can be either pair produced or singly produced. Typically, the pair produced initial state has a large cross section, however, as shown in [145] it is possible that single production of the heavy quark via the exchange of a t-channel W have a larger cross section than $t't'$. This opens new decay chains such as $t'bj \to htbj \to bbWbbj$. In Table 6.2 and Table 6.3 we list possible event topologies that could arise at the LHC. For the final states, we see that there may be as many as six b jets, or if the Higgs decays via the less common WW^* channel then there may be as many as six W bosons. Finally, we note that $t'bj \to Wbbj$ and $t't' \to WbWb$ present two of the best routes to discovery since m_{Wb} would reconstruct to $m_{t'}$ and the signals are relatively clean.

The most recent search done by CMS is the first search to consider all the three final states, and puts the most stringent constraints to date on the existence of a heavy vector-like top quark. Assuming that the heavy vector-like top quark decays exclusively into bW, tZ, and tH, CMS has set lower limits for its mass between 687 and 782 GeV for all possible branching fractions into these three final states assuming strong production. Their results are summarized in Figure 6.6 (taken from [146]).

For ATLAS, the high multiplicity of jets has recently been used in the search for vector-like quarks, yielding the mass bound on the t' consistent with CMS [155]. Therefore, requiring the vector-like mass parameter $\mu_4 \gtrsim 700$ ensures that the physical masses of the new heavy quarks are above the lower bounds excluded by the

Initial	**Intermediate**	**Final**	**Initial**	**Intermediate**	**Final**
t'	ht	$bbWb$	b'	hb	bbb
t'	Zt	$ffWb$	b'	Zb	ffb
t'	Wb	Wb	b'	Wt	WWb
$t't$	htt	$bbWbWb$	$b'b$	hb	$bbbb$
$t't$	Ztt	$ffWbWb$	$b'b$	Zb	$ffbb$
$t't$	Wbt	$WbWb$	$b'b$	Wtb	$WWbb$
$t'bj$	$htbj$	$bbWbbj$	$b'tj$	$hbWbj$	$bbbWbj$
$t'bj$	$Ztbj$	$ffWbbj$	$b'tj$	$ZbWbj$	$ffbWbj$
$t'bj$	$Wbbj$	$Wbbj$	$b'tj$	$WtWbj$	$WWbWbj$

Table 6.2: Possible event topologies that could arise at the LHC with initial states involving only one single t' or b'. f denotes any fermion, $(f = q, l)$

Initial	**Intermediate**	**Final**	**Initial**	**Intermediate**	**Final**
$t't'$	$htht$	$bbWbbbWb$	$b'b'$	$hbhb$	$bbbbbb$
$t't'$	$htZt$	$bbWbffWb$	$b'b'$	$hbZb$	$bbbffb$
$t't'$	$htWb$	$bbWbWb$	$b'b'$	$hbWt$	$bbWWb$
$t't'$	$ZtZt$	$ffWbffWb$	$b'b'$	$ZbZb$	$ffbffb$
$t't'$	$ZtWb$	$ffWbWb$	$b'b'$	$ZbWt$	$ffbWWb$
$t't'$	$WbWb$	$WbWb$	$b'b'$	$WtWt$	$WWbWWb$

Table 6.3: Possible event topologies that could arise at the LHC with initial states involving pair produced t' or b'. f denotes any fermion, $(f = q, l)$

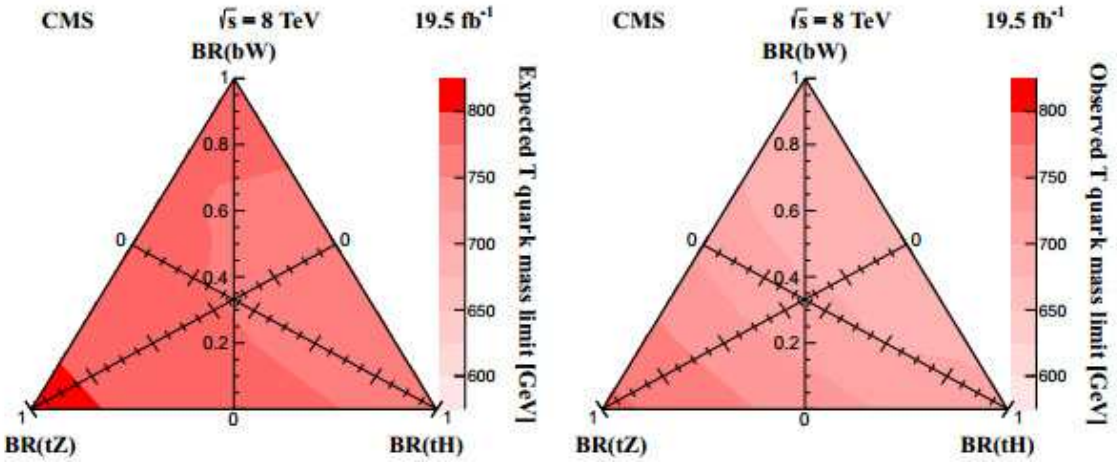

Figure 6.6: Present status of heavy vector-like top searches with 19.5 fb^{-1} of 8 TeV data with the CMS detector (Figure taken from [146]). A Branching-fraction triangle is shown with expected (left) and observed 95% CL limits (right) on the mass. Every point in the triangle corresponds to a specific set of branching-fraction values subject to the constraint that all three add up to 1.

LHC.

6.4.4 Electroweak Precision Observables

We now study the total contribution of the new generation to the electroweak oblique parameters S and T. In appendix B.2, we work out the interaction terms between the new particles and the electroweak gauge bosons in the mass basis Lagrangian, as these are needed to derive the necessary Feynman rules to calculate the self energy loops in the definitions of S and T. The relevant interaction terms are of the form Wff, Zff, Aff and for quarks, and $W\tilde{f}\tilde{f}$, $Z\tilde{f}\tilde{f}$, $A\tilde{f}\tilde{f}$, $WW\tilde{f}\tilde{f}$, $ZZ\tilde{f}\tilde{f}$, $AA\tilde{f}\tilde{f}$ and $ZA\tilde{f}\tilde{f}$ for squarks. In appendix B.5 we calculate the contributions to the oblique parameters from both fermions (T_f, S_f) and scalars (T_s, S_s). We note that

in the full decoupling limit, $\mu_4 \to \infty$ and $y_{ij} \to 0$ we recover SM values.

To get the total contribution of the new sector, we define $T_{new} = T_f + T_s - T_{SM}$ and $S_{new} = S_f + S_s - S_{SM}$. The values $T_{SM} \approx 1.22$ and $S_{SM} \approx -0.08$ were calculated to account for the top sector alone. In general, we find that $T_s << T_f$ and $S_f \approx S_s$.

The μ_4 dependences of S_{new} and T_{new} are shown in Figures 6.7 and 6.8, respectively, for the benchmark scenario $y_{34} = 0.6$ and $y_{44} = y_{43} = 0$ with the Yukawa values kept fixed. As a sanity check, we see that for a large range of μ_4, the values of S and T remain very small.

The dependences of S_{new} and T_{new} on the mixing Yukawa couplings are shown in Figures and 6.9 and 6.10, respectively, for the benchmark scenario $y_{34} >> y_{44}, y_{43}$ with $\mu_4 = 900$ GeV kept fixed and $A = \Delta m = 800$ GeV. As y_{34} increases from 0.5 to 1, S_{new} increases by a negligible amount of the order of 10^{-4}. However, T_{new} increases by ~ 0.25. For $T \gtrsim 0.15$, there is tension with the EWPM fit (as can be seen in Figure 6.11) and therefore the maximum allowed value for y_{34} in this case is ~ 0.8.

To get a more general picture, we scanned over a wide range of the parameter space from the new sector consistent with the mass bounds from the LHC (see section 6.4.3). We varied the relevant y_{ij}'s, μ_4, and Δm but kept the A-terms fixed at 800 GeV. The results are presented in Figure 6.11. We see that $-0.1 \lesssim S_{new} \lesssim 0$, while T_{new} can be positive or negative. The positive contributions of T_{new} can be large enough to be in tension with EWPD. Nevertheless, from Figure 6.11 it is clear that with vector masses $\mu_4 \gtrsim 900$ GeV a large set of our parameter space of interest

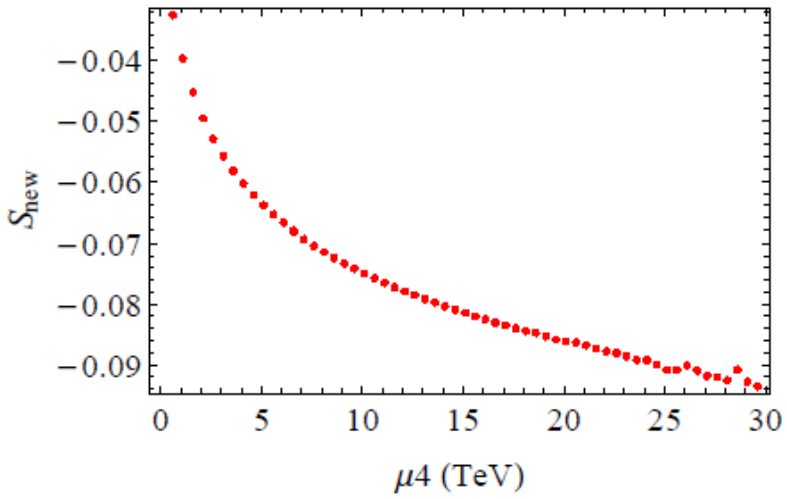

Figure 6.7: S_{new} versus μ_4 for $y_{34} = 0.6$ and $y_{44} = y_{43} = 0$. S_{new} remains small as $\mu_4 \to \infty$.

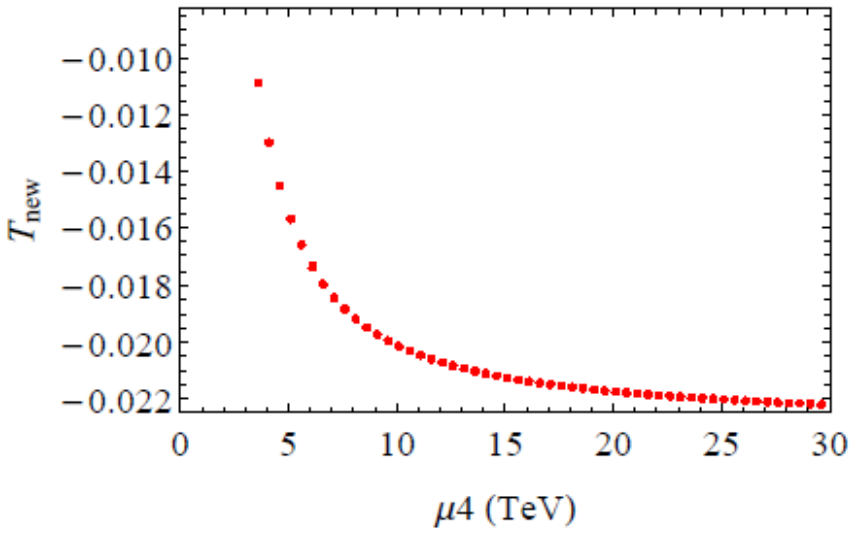

Figure 6.8: T_{new} versus μ_4 for $y_{34} = 0.6$ and $y_{44} = y_{43} = 0$. T_{new} remains small as $\mu_4 \to \infty$.

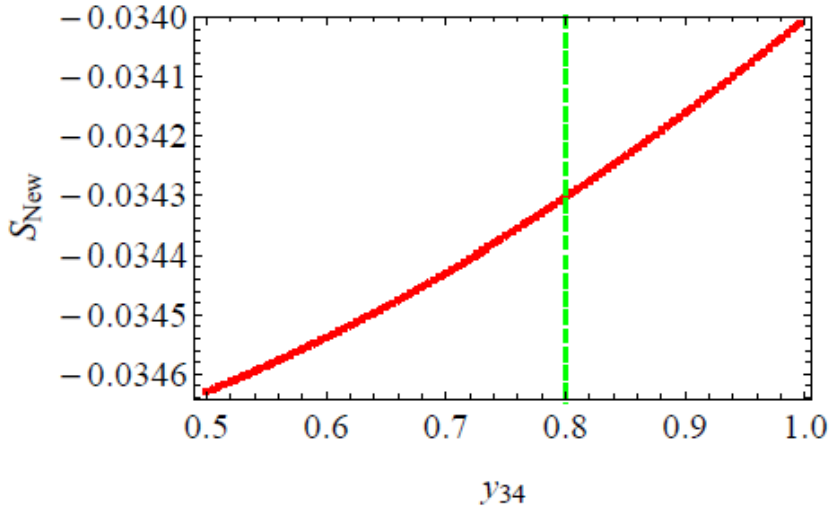

Figure 6.9: S_{new} versus y_{34} for the benchmark scenario $y_{34} >> y_{44}, y_{43}$, $\mu_4 = 900$ GeV, $A = \Delta m = 800$ GeV. S_{new} remains small in this region. As y_{34} increases from 0.5 to 1, S_{new} increases by a negligible amount of the order of 10^{-4}. The region $y_{34} \gtrsim 0.8$ to the right of the dashed line is disfavored by EWPM due to the T parameter (see Figure 6.10).

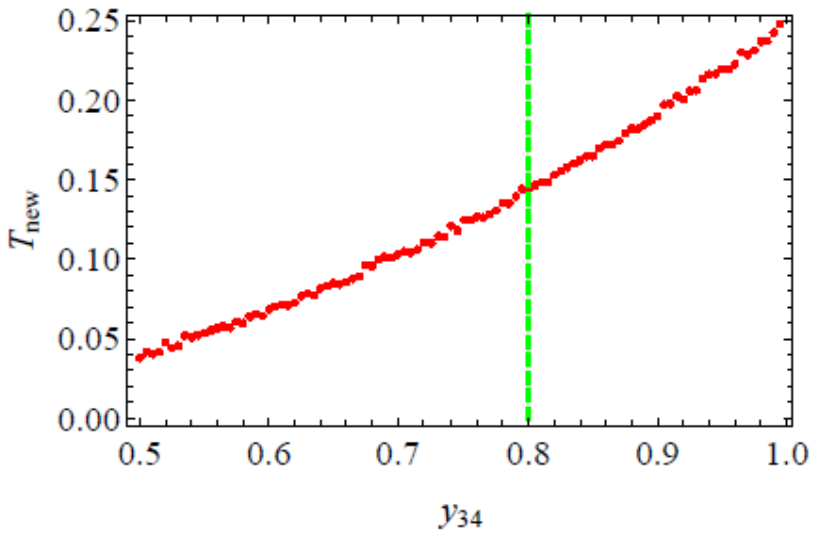

Figure 6.10: T_{new} versus y_{34} for the benchmark scenario $y_{34} >> y_{44}, y_{43}$, $\mu_4 = 900$ GeV, $A = \Delta m = 800$ GeV. As y_{34} increases from 0.5 to 1, T_{new} increases from ~ 0.05 to ~ 0.25. The region $y_{34} \gtrsim 0.8$ to the right of the dashed line is disfavored by EWPM as can be seen in Figure 6.11.

falls within the 95% and 68% confidence limits on the electroweak observables.

Furthermore, while taking $\mu_U/\mu_Q = 1$ is a natural simplification, in general this condition does not hold. Indeed, if the vector masses are taken to be equal at some high SUSY-breaking scale, then differences in the beta functions will result in unequal vector masses at the weak scale. We therefore probed the effect of varying this ratio while keeping the sum of the masses constant. The ratio is less constrained for smaller mixing Yukawas, with $2.3 \gtrsim \mu_U/\mu_Q \gtrsim 0.85$ allowed by EWPM for $y_{34} = -y_{43} = 0.1$ and $\mu_Q + \mu_U = 1800$ GeV, while for large $y_{34} = -y_{43}$ we find $1.2 \gtrsim \mu_U/\mu_Q \gtrsim 0.9$. On the other hand, there are scenarios in which the effects from a non-unity ratio value counteract the effects from large mixing Yukawas. For example, with $\mu_U/\mu_Q = 1.1$ it was found that $y_{34} = -y_{43}$ can be as large as 0.56 and still fall within the 95% confidence limits on EWPD, up from 0.43 for a ratio of one. Since EWPM give the most significant constraints on the y_{ij}'s, we see by referring to Figure 6.1 that soft masses $\lesssim 800$ GeV are then the minimum required for the $y_{34} = -y_{43}$ case, rather than the ~ 1000 GeV it requires when the ratio is one (the y_{ij}'s needed to give the desired Higgs mass have negligible dependence on the value of the ratio). In Figure 6.12 we plot the S_{new}, T_{new} for ratios $\mu_U/\mu_Q = 0.9, 1.0, 1.1$, and Yukawa values $y_{34} = -y_{43}$ ranging from 0.01 to 0.56 in steps of 0.05.

We conclude that in concert with the results of section 6.3.2, precision electroweak observables permit sufficiently large Yukawa mixing to obtain a Higgs mass ~ 125 GeV with soft parameters below a TeV while yielding new quarks discoverable at the

LHC.

6.5 Conclusions and Outlook

In this chapter we studied the effects of sizeable mixing Yukawa terms between the top sector and a vector-like quark generation. We computed the energy scale of the Landau pole induced by the top Yukawa for various scenarios. We also discussed the LHC phenomenology and the consequences of including top mixing effects on final state event topologies.

We found that sizeable mixing Yukawa couplings (y_{34} and y_{43}) in the superpotential require an increase of the value of the top Yukawa coupling by at most $\sim 6\%$ to produce the observed top mass. Since loop corrections to m_h go as y_{top}^4, mixing will increase the predicted value of the physical Higgs mass, a point not previously emphasized in the literature. This high sensitivity to the top Yukawa is in contrast with the weaker logarithmic dependence on top squark masses.

The mixing Yukawas necessary to achieve a given Higgs mass are smaller when $|y_{34}| \sim |y_{43}|$ than when one of these couplings dominates the other, and if one allows $\mu_U/\mu_Q \neq 1$ then the lowest soft masses ($\Delta m \sim 750$ GeV) can be accommodated for this case. However, under the restriction $\mu_U/\mu_Q = 1$, then the lowest possible value of Δm consistent with EWPM is $\Delta m \sim 800$ GeV, which occurs when $y_{34} \sim 0.8$ and $y_{43} = y_{44} = 0$ (see Figure 6.1).

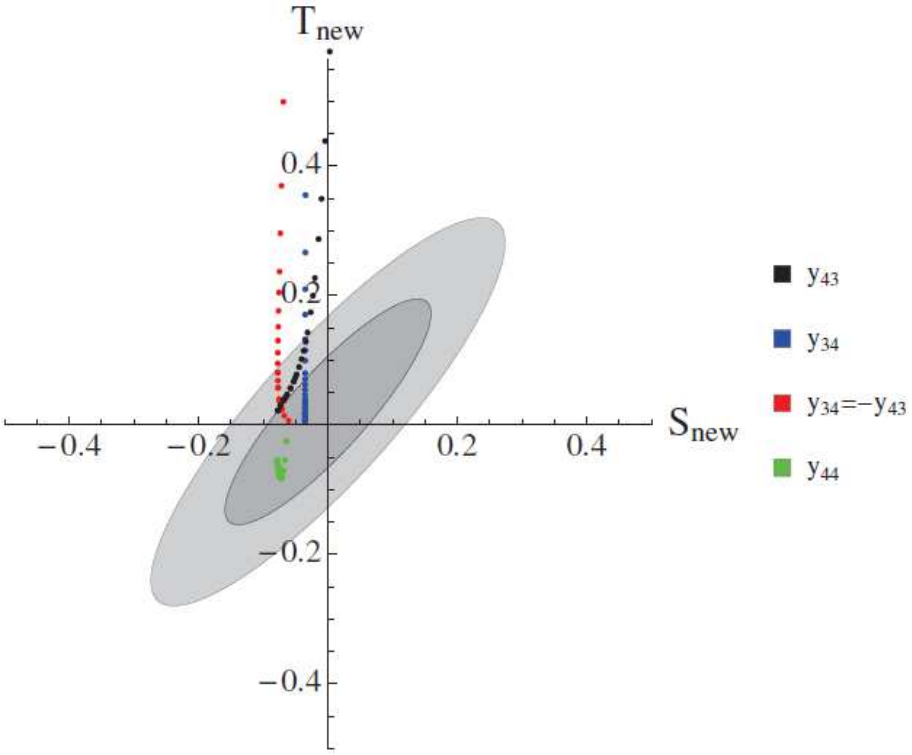

Figure 6.11: We calculate S_{new} and T_{new} for each of the benchmark scenarios: $y_{34} >> y_{43}, y_{44}$; $y_{43} >> y_{34}, y_{44}$; and $y_{34} = -y_{43} >> y_{44}$. Within each scenario $\mu_4 = 900$ GeV, $A = 600$ GeV, and we vary Δm from 300 to 1500 GeV. Each of these points satisfies current mass bounds (see section 6.4.3) and gives a Higgs mass $m_h = 125.5 \pm .5$ GeV while yielding new quarks discoverable at the LHC. The points corresponding to very low Δm and larger Yukawas lie farthest from the best fit, with the agreement improving as Δm grows and the Yukawas decrease. For many of these points the net effect from the new sector falls within the 95% or 68% confidence limits on the electroweak observables. The experimental best fit corresponds to the center of the ellipses, at $(0.00, 0.02)$ [156]. The light (dark) grey ellipse denote the 95% (65%) CL on the EW observables. The origin is defined to be the Standard Model prediction with a 125 GeV Higgs. In concert with the results of section 6.3.2, precision electroweak observables permit sufficiently large Yukawa mixing to obtain a Higgs mass ~ 125 GeV with soft terms below a TeV.

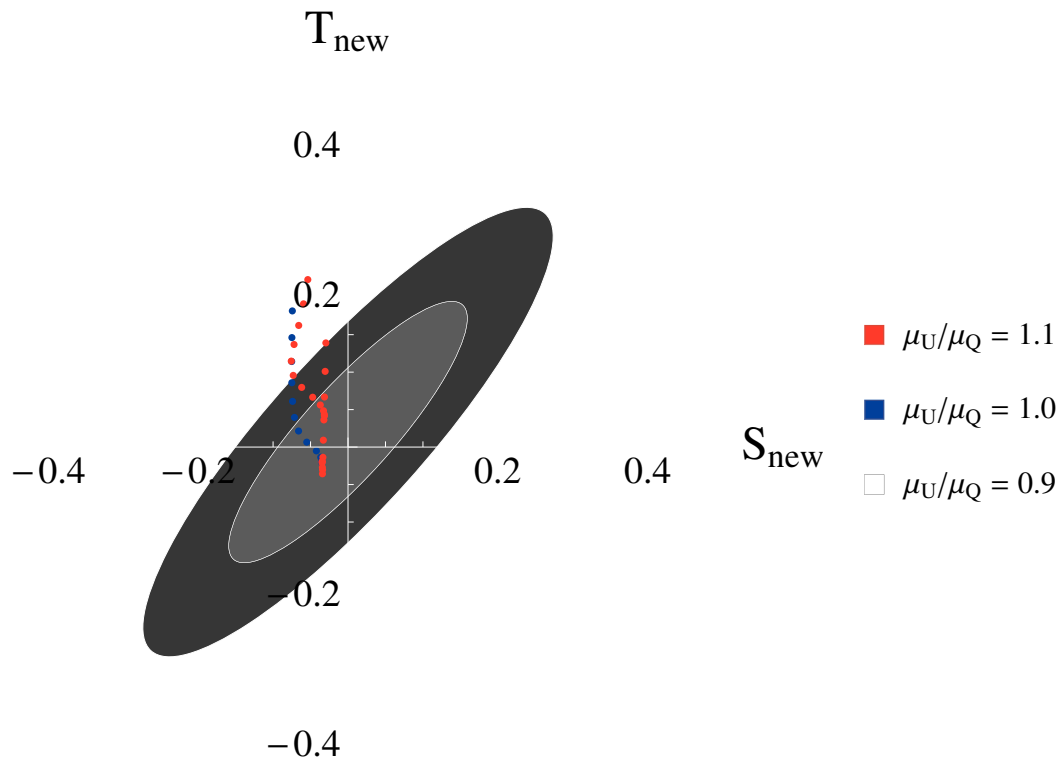

Figure 6.12: We plot the S_{new}, T_{new} for ratios $\mu_U/\mu_Q = 0.9, 1.0, 1.1$, and Yukawa values $y_{34} = -y_{43}$ ranging from 0.01 to 0.56 in steps of 0.05. Each of these points satisfies current mass bounds (see section 6.4.3) and gives a Higgs mass $m_h = 125.5 \pm .5$ GeV while yielding new quarks discoverable at the LHC. The points corresponding to very low Δm and larger Yukawas lie farthest from the best fit, with the agreement improving as Δm grows and the Yukawas decrease. For many of these points the net effect from the new sector falls within the 95% or 68% confidence limits on the electroweak observables. The experimental best fit corresponds to the center of the ellipses, at $(0.00, 0.02)$ [156]. The light (dark) grey ellipse denote the 95% (65%) CL on the EW observables. The origin is defined to be the Standard Model prediction with a 125 GeV Higgs. In concert with the results of section 6.3.2, precision electroweak observables permit sufficiently large Yukawa mixing to obtain a Higgs mass $\sim$ 125 GeV with soft terms below a TeV.

Moreover, mixing can significantly raise the Higgs mass while retaining perturbativity to much higher scales than possible with only the self coupling y_{44} of the fourth generation (see Figure 6.2). For A-terms and soft masses around 900 GeV, the top Yukawa Landau pole can be pushed above the GUT scale. For $\mu_Q = \mu_U$, soft masses can be as low as 800 GeV and still generate a Higgs mass of 125 GeV, albeit in parts of parameter space with a Landau pole at $\sim 10^{10}$ GeV. Smaller supersymmetry-breaking terms suffice if one sacrifices perturbativity at the unification scale by adding fields in a $\mathbf{5}+\bar{\mathbf{5}}$ (see Figure 6.5).

We studied the constraints from electroweak precision measurements, the measurements of V_{tb}^{CKM}, Higgs production, and the most recent mass bounds from direct searches for vector-like quarks at the LHC. We found that the oblique corrections and LHC direct searches give the dominant constraints. With vector masses $\mu_4 \gtrsim 900$ GeV and soft scalar masses $\Delta m \gtrsim 800$ GeV, the net effect from the new sector falls within the 95% confidence limits on the electroweak observables.

We conclude that there is a large parameter space available for a supersymmetric model with a vector-like fourth generation that passes all tests from previous experimental analyses with sufficiently large Yukawa mixing to obtain a Higgs mass ~ 125 GeV, while yielding new quarks discoverable at the LHC. These models have a soft SUSY breaking scale that remains moderate and can therefore address the little hierarchy problem.

We refer the reader to the appendix for details about the particle spectrum, the

derivation of the mass matrices in the model and the calculation of the oblique parameters. In addition, we give the explicit form of all of the matrices needed to write the interaction Lagrangian. These include generalized CKM matrices, couplings matrices and projection matrices. We also list the beta functions used in the study of Landau poles and perturbativity, as well as loop functions used in the calculation of the oblique parameters.

Two interesting avenues to extend this work are apparent. One is to embed the model in an explicit realization of dynamical supersymmetry-breaking and to examine whether constraints from any of the known SUSY-breaking methods makes it incompatible with the model or well-suited for it. The second is to calculate the running of the vector masses μ_Q, μ_U down from the SUSY-breaking scale. We have found that their ratio μ_Q/μ_U must lie within $\sim 1\pm 0.2$, depending on the specifics. It is generically true that equal vector masses at the SUSY-breaking scale will not be equal when evolved down to the weak scale, so this could be an important constraint on not only this model but any model with vector-like quarks. Due to the nonrenormalization of the superpotential, the evolution of such parameters in the superpotential follows simply from wavefunction renormalization, and is given by [47]

$$\frac{d}{dt}\mu^{ij} = \gamma^i_k \mu^{kj} + \gamma^j_k \mu^{ik} \tag{6.11}$$

$$\gamma^i_j = \frac{1}{32\pi^2}\left((f^i_{kl})^* f_{jkl} - 4g^2 \sum_i C_2(\mathcal{R}_i)\delta^i_j \right). \tag{6.12}$$

We intend to perform an analysis of the constraints from this equation in a future work.

Appendix A

Appendix, Part I

A.1 Detection and Selection of Events

The analysis of [31,32] focuses on the muon final state ($\mu^+\mu^-$), which had not been used in a study of $\sin^2\theta_W$. The primary elements of the CMS machine used in these measurements were the silicon tracker and the muon system, which capture muons with pseudorapidity $|\eta| \equiv |\ln\cot\frac{\theta}{2}| < 2.5$ [31,32,157]. The tracker system consists of thousands of silicon pixels and strips, and knowing the relative location of each to a high accuracy is crucial for precise measurements [31, 32, 157]. This issue of tracker alignment and its effect on the measured $\sin^2\theta_W$ was studied thoroughly in [31, 32] as one source of systematic uncertainty. The analysis was performed on (1.07 ± 0.05 fb^{-1}) of $\sqrt{s} = 7$ TeV data from 2010 and 2011. The triggering system required events to have two muons within $|\eta| < 2.4$, with transverse momentum $p_T \geq 8$ and 13 GeV,

but later event selection strengthened the p_T requirement to 8 and 18 GeV [31,32]. It was also required that the muons to have a small (2 mm) impact parameter and that the angle between the two muons be ≥ 2.5 milliradians (in the lab frame) to remove cosmic-ray and background events, while further cuts on variables in the Collins-Soper frame required $|\eta^*| < 2.3$ and $p_T^* > 18$ GeV [31,32]. Requirements were also placed on the dimuon system as a whole. They were identified by two oppositely-charged and isolated muons, with cuts requiring the pair's invariant mass to be between 80 and 100 GeV and transverse momentum < 25 GeV [31, 32]. In terms of $\cos\theta^*$, detector acceptance and event selection led to the requirement $|\cos\theta^*| < \tanh(Y_{\max} - |Y|)$ and $|\cos\theta^*| < \sqrt{1 - 4p_{\min}^2/\hat{s}}$, where $Y_{\max} = 2.3$ and $p_{\min} = 18$ GeV. The number of events passing all requirements was 297,364 [31, 32].

A complete description of the CMS detector can be found in [157]. More details on the kinematic event-selection requirements as well as discussion of the study of systematic uncertainties from sources other than FSR can be found in [31, 32].

A.2 Dilution and Parton Factors

The explicit forms of the functions $F, D, \hat{\sigma}^{\pm}$

detailed discussion of the origin and determination of other uncertainties,

The dilution factor function used in eq. 3.15 is given as [31, 32]

$$D_{q\bar{q}}(\hat{s},Y)=\frac{f_q\left(e^{+|Y|}\sqrt{\hat{s}/s},\,\hat{s}\right)\;f_{\bar{q}}\left(e^{-|Y|}\sqrt{\hat{s}/s},\,\hat{s}\right)-f_q\left(e^{-|Y|}\sqrt{\hat{s}/s},\,\hat{s}\right)\;f_{\bar{q}}\left(e^{+|Y|}\sqrt{\hat{s}/s},\,\hat{s}\right)}{f_q\left(e^{+Y}\sqrt{\hat{s}/s},\,\hat{s}\right)\;f_{\bar{q}}\left(e^{-Y}\sqrt{\hat{s}/s},\,\hat{s}\right)+f_q\left(e^{-Y}\sqrt{\hat{s}/s},\,\hat{s}\right)\;f_{\bar{q}}\left(e^{+Y}\sqrt{\hat{s}/s},\,\hat{s}\right)} \tag{A.1}$$

The parton factor in the same equation is [31, 32]

$$F_{q\bar{q}}(\hat{s},Y)=f_q\left(e^{+Y}\sqrt{\hat{s}/s},\,\hat{s}\right)\;f_{\bar{q}}\left(e^{-Y}\sqrt{\hat{s}/s},\,\hat{s}\right)+f_q\left(e^{-Y}\sqrt{\hat{s}/s},\,\hat{s}\right)\;f_{\bar{q}}\left(e^{+Y}\sqrt{\hat{s}/s},\,\hat{s}\right) \tag{A.2}$$

Appendix B

Appendix, Part II

B.1 The Physical Spectrum and Mass Matrices

After the $SU(2)_L \times U(1)_Y$ gauge symmetry is broken, Yukawa terms in the superpotential (equation 6.1), soft terms, F terms, and D terms lead to the following fermion mass matrices:

$$M_f^u = \begin{pmatrix} 0 & m_f^u \\ m_f^{u\dagger} & 0 \end{pmatrix}, \qquad \text{with} \qquad m_f^u \equiv \begin{pmatrix} y_{33}v_u & y_{34}v_u & 0 \\ y_{43}v_u & y_{44}v_u & \mu_Q \\ 0 & \mu_U & 0 \end{pmatrix},$$

$$M_f^d \equiv \begin{pmatrix} 0 & m_f^d \\ m_f^{d\dagger} & 0 \end{pmatrix}, \qquad \text{with} \qquad m_f^d \equiv \begin{pmatrix} m_{\rm bot} & 0 \\ 0 & \mu_Q \end{pmatrix},$$

and the scalar squared mass matrices:

$$(M_s^u)^2 = (M_f^u)^2 + \begin{pmatrix} Y_{u_3} & 0 & 0 & -y_{33}v_uX_u & -y_{34}v_uX_u & 0 \\ 0 & \mu_Q^2 + Y_{u_4} & 0 & -y_{43}v_uX_u & -y_{44}v_uX_u & B\mu \\ 0 & 0 & \mu_U^2 + Y_{\bar{u}_4} & 0 & B\mu & 0 \\ -y_{33}v_uX_u & -y_{43}v_uX_u & 0 & Y_{u_3^c} & 0 & 0 \\ -y_{34}v_uX_u & -y_{44}v_uX_u & B\mu & 0 & \mu_U^2 + Y_{u_4^c} & 0 \\ 0 & B\mu & 0 & 0 & 0 & \mu_Q^2 + Y_{\bar{u}_4^c} \end{pmatrix},$$

$$(M_s^d)^2 = (M_f^d)^2 + \begin{pmatrix} Y_{d_3} & 0 & -m_{\rm bot}X_d & 0 \\ 0 & \mu_Q^2 + Y_{d_4} & 0 & B\mu \\ -m_{\rm bot}X_d & 0 & Y_{d_3^c} & 0 \\ 0 & B\mu & 0 & \mu_Q^2 + Y_{\bar{d}_4^c} \end{pmatrix}.$$

Here, $v_u = v\sin\beta$, with $v \approx 174$ GeV, and $m_{\rm bot} \approx 4.2$ GeV is the mass of the bottom quark. $X_u = A + \mu\cot\beta$ and $X_d = A + \mu\tan\beta$. Along the diagonal, $Y_q \equiv \Delta m^2 + D_a$, where the D-term contribution is $D_a = (T_a^3 - Q_a\sin^2\theta_w)\cos(2\beta)m_Z^2$ for each quark field a, T^3 is the third component of weak isospin, Q_a is the electric charge, and θ_w is the weak mixing angle. We take all parameters to be real. With

the mass matrices defined as above, the relevant mass Lagrangian (after EWSB) in the gauge eigenstate basis can be written as:

$$-\mathcal{L}_m = (f_L^{uT} m_f^u f_R^u + f_L^{dT} m_f^d f_R^d + \text{h.c}) + \tilde{f}^{u\dagger}(M_s^u)^2 \tilde{f}^u + \tilde{f}^{d\dagger}(M_s^d)^2 \tilde{f}^d \tag{B.1}$$

where the basis is:

$$\begin{aligned} f_L^u &= (u_3, u_4, \bar{u}_4)^T \\ f_R^u &= (u_3^c, u_4^c, \bar{u}_4^c)^T \\ f_L^d &= (d_3, d_4)^T \\ f_R^d &= (d_3^c, \bar{d}_4^c)^T \\ \tilde{f}^u &= (\tilde{u}_3, \tilde{u}_4, \tilde{\bar{u}}_4, \tilde{u}_3^c, \tilde{u}_4^c, \tilde{\bar{u}}_4^c)^T \\ \tilde{f}^d &= (\tilde{d}_3, \tilde{d}_4, \tilde{d}_3^c, \tilde{\bar{d}}_4^c)^T. \end{aligned} \tag{B.2}$$

The physical masses of the fermions are obtained by bi-diagonalizing the fermion mass matrices using the singular value decomposition:

$$\begin{aligned} m_D^u &= V_L^{u\dagger} m_f^u V_R^u \\ m_D^d &= V_L^{d\dagger} m_f^d V_R^d \end{aligned}$$

where $V_L^{u,d}$ and $V_R^{u,d}$ are unitary matrices and the $m_D^{u,d}$ matrices are diagonal. The diagonal entries of m_f^u (m_f^d) correspond to the physical masses of the top (bottom) and the new non-MSSM quarks $t'_{1,2}$ (b'). Similarly, the scalar squared matrices are

diagonalized by the unitary matrices $W^{u,d}$ as:

$$(\tilde{M}_D^u)^2 = W^{u\dagger}(M_s^u)^2 W^u$$

$$(\tilde{M}_D^d)^2 = W^{d\dagger}(M_s^d)^2 W^d,$$

where the $(\tilde{M}_D^{u,d})^2$ matrices are diagonal. The positive square roots of $(\tilde{M}_D^u)^2$ (and $(\tilde{M}_D^d)^2$) correspond to the physical masses of the top squarks (bottom squarks) and the new non-MSSM squarks $\tilde{t}_{1,2}$, $\tilde{t}'_{1,2,3,4}$ ($\tilde{b}_{1,2}$, $\tilde{b}'_{1,2}$). To obtain a Lagrangian in the mass eigenstate basis, we rotate the gauge eigenstates by left-multiplying the vectors $f^{u,d}$ and $\tilde{f}^{u,d}$ in equation B.2 by the corresponding mixing matrices $V_{L,R}^{u,d\dagger}$ and $W^{u,d\dagger}$, respectively. We denote the mass eigenstate basis with a hat, $\hat{f}_{L,R}^{u,d} = V_{L,R}^{u,d\dagger} f_{L,R}^{u,d}$ and $\hat{\tilde{f}}^{u,d} = W^{u,d\dagger}\tilde{f}^{u,d}$. A typical particle spectrum is shown in Table B.1 for $\mu_4 = 900$ GeV.

B.2 The Interaction Lagrangian

The rotation from gauge to mass eigenstates leads to generalized CKM matrices between the third and fourth generation, which we denote by K_α^{ab} for quarks, and $\tilde{K}_\alpha^{ab}$ for squarks, with $a, b = u, \bar{u}, d, \bar{d}$ and $\alpha = L, R$. These matrices will be present in every interaction term. Furthermore, they are not square matrices like in the MSSM because there are more up-type quarks (squarks) than down-type quarks (squarks). Their general form is $K_\alpha^{ab} = V_\alpha^{a\dagger} D_\alpha^{ab} V_\alpha^b$ or $K_\alpha^{ab} = V_\alpha^{a\dagger} S_\alpha^{ab} V_\alpha^b$, and $\tilde{K}_\alpha^{ab} = W^\dagger \tilde{D}_\alpha^{ab} W$ or $\tilde{K}_\alpha^{ab} = W^\dagger \tilde{S}_\alpha^{ab} W$. The projection matrices, D_α^{ab} and $\tilde{D}_\alpha^{ab}$ (S_α^{ab} and $\tilde{S}_\alpha^{ab}$) select

Mass (GeV)	**Scenario 1**	**Scenario 2**	**Scenario 3**
$m_{t'_1}$	909	900	900
$m_{t'_2}$	913	911	900
$m_{b'}$	900	900	900
$\tilde{m}_{\tilde{t}_1}$	814	818	821
$\tilde{m}_{\tilde{t}_2}$	982	991	1000
$\tilde{m}_{\tilde{t}'_1}$	1275	1271	1271
$\tilde{m}_{\tilde{t}'_2}$	1276	1273	1272
$\tilde{m}_{\tilde{t}'_3}$	1287	1275	1273
$\tilde{m}_{\tilde{t}'_4}$	1300	1294	1274
$\tilde{m}_{\tilde{b}_1}$	860	860	860
$\tilde{m}_{\tilde{b}_2}$	940	940	940
$\tilde{m}_{\tilde{b}'_1}$	1271	1271	1271
$\tilde{m}_{\tilde{b}'_2}$	1274	1275	1274

Table B.1: A typical particle spectrum for the three different benchmark scenarios: 1) $y_{34} = -y_{43} = 0.8$ and $y_{44} = 0$; 2) $y_{34} = 0.8$ and $y_{43}, y_{44} = 0$; 3) $y_{44} = 0.8$ and $y_{34}, y_{43} = 0$. The scenario $y_{43} = 0.8$ and $y_{34}, y_{44} = 0$ gives the same masses as scenario 2) and we therefore omit it. We set $A = \Delta m = \mu_4 = 900$ GeV. As we can see, mixing doesn't change drastically the mass spectrum.

the appropriate doublet (singlet) field component of f^a and $\tilde{f}^a$, respectively, before rotating to the mass basis. We note that, in general, $K_\alpha^{aa} = K_\alpha^{ab} K_\alpha^{ab\dagger}$, so we can construct all of the generalized CKM matrices from all the possible products of K_α^{ab} and $K_\alpha^{ab\dagger}$. It is therefore the non-unitarity and off-diagonal entries of K_α^{ab} that leads to FCNC's. K_α^{ab} and $\tilde{K}_\alpha^{ab}$ depend on the flavor and chirality of the particles involved in the interaction, and on the parameters of the model (e.g. μ_4,the y_{ij}'s) which are present in the corresponding mixing matrices V_α^a and W^a.

In Tables B.2 and B.3, we give the form of all these generalized CKM matrices and write down the corresponding interaction term coupling the vector bosons $V_\mu = W_\mu, Z_\mu, A_\mu$ to the quarks or squarks, in the mass basis. The matrices D_α^{ab}, $\tilde{D}_\alpha^{ab}$, S_α^{ab} and $\tilde{S}_\alpha^{ab}$ are listed in appendix B.3, and the mixing matrices V_α^a and W^a were calculated numerically and depend on the parameters of the model.

As an example, let us write down in matrix form the term in the Lagrangian corresponding to the charged current interaction vertex W^+ff. In terms of the gauge eigenstate basis vectors $f_L^{u\dagger}$ (a 3-dimensional row vector in generation space) and $f_L^{d\dagger}$ (a 2-dimensional column vector in generation space), the interaction term needs a 3×2 projection matrix, which we call D_L^{ud}, to couple the L.H fields with $T_3 = 1/2$ (u_3^c and u_4^c) in $f_L^{u\dagger}$ to the left-handed fields with $T_3 = -1/2$ (d_3 and d_4) in f_L^d. This gives a term $\propto W_\mu^+ f_L^{u\dagger} D_L^{ud} \bar{\sigma}^\mu f_L^d$. Similarly, in terms of the gauge eigenstate basis vectors $f_R^{d\dagger}$ (a 2-dimensional row vector in generation space) and f_R^u (a 3-dimensional column vector in generation space), the interaction term needs a 2×3 projection

$\mathbf{V}_\mu \hat{\mathbf{f}}^{\mathbf{a}\dagger}_\alpha \mathbf{K}^{\mathbf{ab}}_\alpha \bar{\sigma}^\mu \hat{\mathbf{f}}^{\mathbf{b}}_\alpha$	$\mathbf{K}^{\mathbf{ab}}_\alpha$
$W^+_\mu \hat{f}^{u\dagger}_L K^{ud}_L \bar{\sigma}^\mu \hat{f}^d_L$	$V^{u\dagger}_L D^{ud}_L V^d_L$
$W^+_\mu \hat{f}^{d\dagger}_R K^{\bar{u}\bar{d}\dagger}_R \bar{\sigma}^\mu \hat{f}^u_R$	$V^{u\dagger}_R D^{\bar{u}\bar{d}}_R V^d_R$
$Z^0_\mu \hat{f}^{u\dagger}_L K^{uu}_L \bar{\sigma}^\mu \hat{f}^u_L$	$V^{u\dagger}_L D^{uu}_L V^u_L$
$Z^0_\mu \hat{f}^{u\dagger}_L K^{\bar{u}\bar{u}}_L \bar{\sigma}^\mu \hat{f}^u_L$	$V^{u\dagger}_L S^{\bar{u}\bar{u}}_L V^u_L$
$Z^0_\mu \hat{f}^{u\dagger}_R K^{\bar{u}\bar{u}}_R \bar{\sigma}^\mu \hat{f}^u_R$	$V^{u\dagger}_R D^{\bar{u}\bar{u}}_R V^u_R$
$Z^0_\mu \hat{f}^{u\dagger}_R K^{uu}_R \bar{\sigma}^\mu \hat{f}^u_R$	$V^{u\dagger}_R S^{uu}_R V^u_R$
$Z^0_\mu \hat{f}^{d\dagger}_L K^{dd}_L \bar{\sigma}^\mu \hat{f}^d_L$	$V^{d\dagger}_L D^{dd}_L V^d_L$
$Z^0_\mu \hat{f}^{d\dagger}_R K^{\bar{d}\bar{d}}_R \bar{\sigma}^\mu \hat{f}^d_R$	$V^{d\dagger}_R D^{\bar{d}\bar{d}}_R V^d_R$
$Z^0_\mu \hat{f}^{d\dagger}_R K^{dd}_R \bar{\sigma}^\mu \hat{f}^d_R$	$V^{d\dagger}_R S^{dd}_R V^d_R$

Table B.2: We give the form of all the generalized CKM matrices K^{ab}_α and their corresponding triple interaction term coupling the vector bosons $V_\mu = W_\mu, Z_\mu, A_\mu$ to the quarks in the mass basis (see equation B.4). Here, $\hat{f}^a_\alpha$ are the quark vectors in equation B.2, and $a, b = u, \bar{u}, d, \bar{d}$ and $\alpha = L, R$. The projection matrices D^{ab}_α and S^{ab}_α are listed in appendix B.3. The mixing matrices V^a_α were calculated numerically and depend on the parameters of the model.

$\mathbf{V}_\mu \hat{\tilde{\mathbf{f}}}^{\mathbf{a}\dagger} \tilde{\mathbf{K}}_\alpha^{\mathbf{ab}} \overleftrightarrow{\partial}^\mu \hat{\tilde{\mathbf{f}}}^{\mathbf{b}}$	$\mathbf{V}_\mu \mathbf{V}^\mu \hat{\tilde{\mathbf{f}}}^{\mathbf{a}\dagger} \tilde{\mathbf{K}}_\alpha^{\mathbf{ab}} \hat{\tilde{\mathbf{f}}}^{\mathbf{b}}$	$\tilde{\mathbf{K}}_\alpha^{\mathbf{ab}}$
$W_\mu^+ \hat{\tilde{f}}^{u\dagger} \tilde{K}_L^{ud} \overleftrightarrow{\partial}^\mu \hat{\tilde{f}}^d$	$W_\mu^+ W^{\mu+} \hat{\tilde{f}}^{u\dagger} \tilde{K}_L^{ud} \hat{\tilde{f}}^d$	$W^{u\dagger} \tilde{D}_L^{ud} W^d$
$W_\mu^+ \hat{\tilde{f}}^{d\dagger} \tilde{K}_R^{\bar{u}\bar{d}\dagger} \overleftrightarrow{\partial}^\mu \hat{\tilde{f}}^u$	$W_\mu^+ W^{\mu+} \hat{\tilde{f}}^{d\dagger} \tilde{K}_R^{\bar{u}\bar{d}\dagger} \hat{\tilde{f}}^u$	$W^{u\dagger} \tilde{D}_R^{\bar{u}\bar{d}} W^d$
$Z_\mu^0 \hat{\tilde{f}}^{u\dagger} \tilde{K}_L^{uu} \overleftrightarrow{\partial}^\mu \hat{\tilde{f}}^u$	$Z_\mu^0 Z^{\mu 0} \hat{\tilde{f}}^{u\dagger} \tilde{K}_L^{uu} \hat{\tilde{f}}^u$	$W^{u\dagger} \tilde{D}_L^{uu} W^u$
$Z_\mu^0 \hat{\tilde{f}}^{u\dagger} \tilde{K}_L^{\bar{u}\bar{u}} \overleftrightarrow{\partial}^\mu \hat{\tilde{f}}^u$	$Z_\mu^0 Z^{\mu 0} \hat{\tilde{f}}^{u\dagger} \tilde{K}_L^{\bar{u}\bar{u}} \hat{\tilde{f}}^u$	$W^{u\dagger} \tilde{S}_L^{\bar{u}\bar{u}} W^u$
$Z_\mu^0 \hat{\tilde{f}}^{u\dagger} \tilde{K}_R^{\bar{u}\bar{u}} \overleftrightarrow{\partial}^\mu \hat{\tilde{f}}^u$	$Z_\mu^0 Z^{\mu 0} \hat{\tilde{f}}^{u\dagger} \tilde{K}_R^{\bar{u}\bar{u}} \hat{\tilde{f}}^u$	$W^{u\dagger} \tilde{D}_R^{\bar{u}\bar{u}} W^u$
$Z_\mu^0 \hat{\tilde{f}}^{u\dagger} \tilde{K}_R^{uu} \overleftrightarrow{\partial}^\mu \hat{\tilde{f}}^u$	$Z_\mu^0 Z^{\mu 0} \hat{\tilde{f}}^{u\dagger} \tilde{K}_R^{uu} \hat{\tilde{f}}^u$	$W^{u\dagger} \tilde{S}_R^{uu} W^u$
$Z_\mu^0 \hat{\tilde{f}}^{d\dagger} \tilde{K}_L^{dd} \overleftrightarrow{\partial}^\mu \hat{\tilde{f}}^d$	$Z_\mu^0 Z^{\mu 0} \hat{\tilde{f}}^{d\dagger} \tilde{K}_L^{dd} \hat{\tilde{f}}^d$	$W^{d\dagger} \tilde{D}_L^{dd} W^d$
$Z_\mu^0 \hat{\tilde{f}}^{d\dagger} \tilde{K}_R^{\bar{d}\bar{d}} \overleftrightarrow{\partial}^\mu \hat{\tilde{f}}^d$	$Z_\mu^0 Z^{\mu 0} \hat{\tilde{f}}^{d\dagger} \tilde{K}_R^{\bar{d}\bar{d}} \hat{\tilde{f}}^d$	$W^{d\dagger} \tilde{D}_R^{\bar{d}\bar{d}} W^d$
$Z_\mu^0 \hat{\tilde{f}}^{d\dagger} \tilde{K}_R^{dd} \overleftrightarrow{\partial}^\mu \hat{\tilde{f}}^d$	$Z_\mu^0 Z^{\mu 0} \hat{\tilde{f}}^{d\dagger} \tilde{K}_R^{dd} \hat{\tilde{f}}^d$	$W^{d\dagger} \tilde{S}_R^{dd} W^d$

Table B.3: We give the form of all the generalized CKM matrices $\tilde{K}_\alpha^{ab}$ and their corresponding triple and quartic interaction term coupling the vector bosons $V_\mu = W_\mu, Z_\mu, A_\mu$ to the squarks in the mass basis (see equation B.5). Here, $\hat{\tilde{f}}^a$ are the squark vectors in equation B.2, and $a, b = u, \bar{u}, d, \bar{d}$ and $\alpha = L, R$. The projection matrices $\tilde{D}_\alpha^{ab}$ and $\tilde{S}_\alpha^{ab}$ are listed in appendix B.3. The mixing matrices W^a were calculated numerically and depend on the parameters of the model.

matrix, $D_R^{\bar{u}\bar{d}}$, to couple the R.H field with $T_3 = 1/2$ ($\bar{d}_4$) in $f_R^{d\dagger}$ to the right-handed field with $T_3 = -1/2$ ($\bar{u}_4^c$) in f_R^u. This gives a new term $\propto W_\mu^+ f_R^{d\dagger} D_R^{\bar{u}\bar{d}\dagger} \bar{\sigma}^\mu f_R^u$ that is not in the MSSM which couples R.H fields to the W boson. After rotating to the mass eigenstate basis and including the couplings, we get

$$-\mathcal{L}_{W^+ff} = \frac{g}{\sqrt{2}} W_\mu^+ \hat{f}_L^{u\dagger} K_L^{ud} \bar{\sigma}^\mu \hat{f}_L^d + \frac{g}{\sqrt{2}} W_\mu^+ \hat{f}_R^{d\dagger} K_R^{\bar{u}\bar{d}\dagger} \bar{\sigma}^\mu \hat{f}_R^u \tag{B.3}$$

from which the coupling matrix $G_{ud}^W = \frac{g}{\sqrt{2}} K_L^{ud}$ and $G_{\bar{u}\bar{d}}^W = -\frac{g}{\sqrt{2}} K_R^{\bar{u}\bar{d}}$ can be extracted. We give the explicit form of the coupling matrices in Table B.4, Table B.5 and Table B.6.

Proceeding similarly to the above example, the interaction Lagrangian for gauge bosons, quarks and the Higgs in the mass eigenstate basis is:

$$\begin{aligned}
-\mathcal{L}_f = {} & W_\mu^+ (\hat{f}_L^{u\dagger} G_{ud}^W \bar{\sigma}^\mu \hat{f}_L^d + \hat{f}_R^{d\dagger} G_{\bar{u}\bar{d}}^{W\dagger} \bar{\sigma}^\mu \hat{f}_R^u) + W_\mu^- (\hat{f}_L^{d\dagger} G_{ud}^{W\dagger} \bar{\sigma}^\mu \hat{f}_L^u + \hat{f}_R^{u\dagger} G_{\bar{u}\bar{d}}^W \bar{\sigma}^\mu \hat{f}_R^d) \\
& + Z_\mu^0 (\hat{f}_L^{u\dagger} G_{u_L}^Z \bar{\sigma}^\mu \hat{f}_L^u + \hat{f}_L^{d\dagger} G_{d_L}^Z \bar{\sigma}^\mu \hat{f}_L^d + \hat{f}_R^{u\dagger} G_{u_R}^Z \bar{\sigma}^\mu \hat{f}_R^u + \hat{f}_R^{d\dagger} G_{d_R}^Z \bar{\sigma}^\mu \hat{f}_R^d) \\
& + A_\mu (\hat{f}_L^{u\dagger} G_{u_L}^A \bar{\sigma}^\mu \hat{f}_L^u + \hat{f}_L^{d\dagger} G_{d_L}^A \bar{\sigma}^\mu \hat{f}_L^d + \hat{f}_R^{u\dagger} G_{u_R}^A \bar{\sigma}^\mu \hat{f}_R^u + \hat{f}_R^{d\dagger} G_{d_R}^A \bar{\sigma}^\mu \hat{f}_R^d) \\
& + (h_o \hat{f}_L^{uT} Y^{u\bar{u}} \hat{f}_R^u + h_o \hat{f}_L^{dT} Y^{d\bar{d}} \hat{f}_R^d + \text{h.c})
\end{aligned} \tag{B.4}$$

where $Y^{u\bar{u}} = V_L^{u\dagger} y^{u\bar{u}} V_R^u$ and $Y^{d\bar{d}} = V_L^{d\dagger} y^{d\bar{d}} V_R^d$, with y^{ab} defined as in appendix B.3, are the matrices coupling the scalar Higgs to the quarks. Similarly, the interaction

Coupling Matrix	**Explicit Form**
G^W_{ud}	$\frac{g}{\sqrt{2}} K^{ud}_L$
$G^Z_{u_L}$	$g^Z_{(\frac{1}{2},\frac{2}{3})} K^{uu}_L + g^Z_{(0,\frac{2}{3})} K^{\bar{u}\bar{u}}_L$
$G^Z_{d_L}$	$g^Z_{(-\frac{1}{2},-\frac{1}{3})} K^{dd}_L$
$G^A_{u_L}$	$g^A_{\frac{2}{3}} [K^{uu}_L + K^{\bar{u}\bar{u}}_L]$
$G^A_{d_L}$	$g^A_{-\frac{1}{3}} K^{dd}_L$
$G^W_{\bar{u}\bar{d}}$	$-\frac{g}{\sqrt{2}} K^{\bar{u}\bar{d}}_R$
$G^Z_{u_R}$	$g^Z_{(0,-\frac{2}{3})} K^{uu}_R + g^Z_{(-\frac{1}{2},-\frac{2}{3})} K^{\bar{u}\bar{u}}_R$
$G^Z_{d_R}$	$g^Z_{(0,\frac{1}{3})} K^{dd}_R + g^Z_{(\frac{1}{2},\frac{1}{3})} K^{\bar{d}\bar{d}}_R$
$G^A_{u_R}$	$g^A_{\frac{2}{3}} [K^{uu}_R + K^{\bar{u}\bar{u}}_R]$
$G^A_{d_R}$	$g^A_{-\frac{1}{3}} K^{dd}_R$

Table B.4: The coupling matrices at the triple vertex between quarks and gauge bosons. We define $g^Z_{(T^3,Q)} = \frac{g}{\cos\theta_W}(T^3 - Q\sin^2\theta_W)$, $g^A_Q = Qe$

Coupling Matrix	**Explicit Form**
$\tilde{G}^W_{ud}$	$\frac{g}{\sqrt{2}} \tilde{K}^{ud}_L$
$\tilde{G}^Z_u$	$g^Z_{(\frac{1}{2},\frac{2}{3})} \tilde{K}^{uu}_L + g^Z_{(0,\frac{2}{3})} \tilde{K}^{\bar{u}\bar{u}}_L + g^Z_{(0,-\frac{2}{3})} \tilde{K}^{uu}_R + g^Z_{(-\frac{1}{2},-\frac{2}{3})} \tilde{K}^{\bar{u}\bar{u}}_R$
$\tilde{G}^A_u$	$g^A_{\frac{2}{3}} \tilde{K}^{uu}_L + g^A_{\frac{2}{3}} \tilde{K}^{\bar{u}\bar{u}}_L + g^A_{\frac{-2}{3}} \tilde{K}^{uu}_R + g^A_{\frac{-2}{3}} \tilde{K}^{\bar{u}\bar{u}}_R$
$\tilde{G}^W_{\bar{u}\bar{d}}$	$-\frac{g}{\sqrt{2}} \tilde{K}^{\bar{u}\bar{d}}_R$
$\tilde{G}^Z_d$	$g^Z_{(-\frac{1}{2},-\frac{1}{3})} \tilde{K}^{dd}_L + g^Z_{(0,\frac{1}{3})} \tilde{K}^{dd}_R + g^Z_{(\frac{1}{2},\frac{1}{3})} \tilde{K}^{\bar{d}\bar{d}}_R$
$\tilde{G}^A_d$	$g^A_{-\frac{1}{3}} \tilde{K}^{dd}_L + g^A_{\frac{1}{3}} \tilde{K}^{dd}_R + g^A_{\frac{1}{3}} \tilde{K}^{\bar{d}\bar{d}}_R$

Table B.5: The coupling matrices at the triple vertex between squarks and gauge bosons. We define $g^Z_{(T^3,Q)} = \frac{g}{\cos\theta_W}(T^3 - Q\sin^2\theta_W)$, $g^A_Q = Qe$

Coupling Matrix	**Explicit Form**
$\tilde{G}_u^{WW}$	$\frac{g^2}{2}[\tilde{K}_L^{uu} + \tilde{K}_R^{\bar{u}\bar{u}}]$
$\tilde{G}_d^{WW}$	$\frac{g^2}{2}[\tilde{K}_L^{dd} + \tilde{K}_R^{\bar{d}\bar{d}}]$
$\tilde{G}_u^{ZZ}$	$(g^Z_{(\frac{1}{2},\frac{2}{3})})^2\tilde{K}_L^{uu} + (g^Z_{(0,\frac{2}{3})})^2\tilde{K}_L^{\bar{u}\bar{u}} + (g^Z_{(0,-\frac{2}{3})})^2\tilde{K}_R^{uu} + (g^Z_{(-\frac{1}{2},-\frac{2}{3})})^2\tilde{K}_R^{\bar{u}\bar{u}}$
$\tilde{G}_d^{ZZ}$	$(g^Z_{(-\frac{1}{2},-\frac{1}{3})})^2\tilde{K}_L^{dd} + (g^Z_{(0,\frac{1}{3})})^2\tilde{K}_R^{dd} + (g^Z_{(\frac{1}{2},\frac{1}{3})})^2\tilde{K}_R^{\bar{d}\bar{d}}$
$\tilde{G}_u^{ZA}$	$2[g^A_{\frac{2}{3}}g^Z_{(\frac{1}{2},\frac{2}{3})}\tilde{K}_L^{uu} + g^A_{-\frac{2}{3}}g^Z_{(0,\frac{2}{3})}\tilde{K}_L^{\bar{u}\bar{u}} + g^A_{\frac{2}{3}}g^Z_{(0,-\frac{2}{3})}\tilde{K}_R^{uu} + g^A_{-\frac{2}{3}}g^Z_{(-\frac{1}{2},-\frac{2}{3})}\tilde{K}_R^{\bar{u}\bar{u}}]$
$\tilde{G}_d^{ZA}$	$2[g^A_{-\frac{1}{3}}g^Z_{(-\frac{1}{2},-\frac{1}{3})}\tilde{K}_L^{dd} + g^A_{-\frac{1}{3}}g^Z_{(0,\frac{1}{3})}\tilde{K}_R^{dd} + g^A_{\frac{1}{3}}g^Z_{(\frac{1}{2},\frac{1}{3})}\tilde{K}_R^{\bar{d}\bar{d}}]$
$\tilde{G}_u^{AA}$	$2(g^A_{\frac{2}{3}})^2[\tilde{K}_L^{uu} + \tilde{K}_L^{\bar{u}\bar{u}} + \tilde{K}_R^{uu} + \tilde{K}_R^{\bar{u}\bar{u}}]$
$\tilde{G}_d^{AA}$	$2(g^A_{\frac{1}{3}})^2[\tilde{K}_L^{dd} + \tilde{K}_R^{dd} + \tilde{K}_R^{\bar{d}\bar{d}}]$

Table B.6: The coupling matrices at the quartic vertex between squarks and gauge bosons. We define $g^Z_{(T^3,Q)} = \frac{g}{\cos\theta_W}(T^3 - Q\sin^2\theta_W)$, $g^A_Q = Qe$

Lagrangian for gauge bosons and squarks in the mass eigenstate basis is:

$$-\mathcal{L}_{\tilde{f}} = W^+_\mu(\hat{\tilde{f}}^{u\dagger}\tilde{G}^W_{ud}\overleftrightarrow{\partial}^\mu\hat{\tilde{f}}^d + \hat{\tilde{f}}^{d\dagger}\tilde{G}^{W\dagger}_{\bar{u}\bar{d}}\overleftrightarrow{\partial}^\mu\hat{\tilde{f}}^u) + W^-_\mu(\hat{\tilde{f}}^{d\dagger}\tilde{G}^{W\dagger}_{ud}\overleftrightarrow{\partial}^\mu\hat{\tilde{f}}^u + \hat{\tilde{f}}^{u\dagger}\tilde{G}^W_{\bar{u}\bar{d}}\overleftrightarrow{\partial}^\mu\hat{\tilde{f}}^d) \tag{B.5}$$

$$+ Z^0_\mu(\hat{\tilde{f}}^{u\dagger}\tilde{G}^Z_u\overleftrightarrow{\partial}^\mu\hat{\tilde{f}}^u + \hat{\tilde{f}}^{d\dagger}\tilde{G}^Z_d\overleftrightarrow{\partial}^\mu\hat{\tilde{f}}^d) + A_\mu(\hat{\tilde{f}}^{u\dagger}\tilde{G}^A_u\overleftrightarrow{\partial}^\mu\hat{\tilde{f}}^u + \hat{\tilde{f}}^{d\dagger}\tilde{G}^A_d\overleftrightarrow{\partial}^\mu\hat{\tilde{f}}^d)$$

$$+ W^+_\mu W^{-\mu}(\hat{\tilde{f}}^{u\dagger}\tilde{G}^{WW}_u\hat{\tilde{f}}^u + \hat{\tilde{f}}^{d\dagger}\tilde{G}^{WW}_d\hat{\tilde{f}}^d) + Z^0_\mu Z^{0\mu}(\hat{\tilde{f}}^{u\dagger}\tilde{G}^{ZZ}_u\hat{\tilde{f}}^u + \hat{\tilde{f}}^{d\dagger}\tilde{G}^{ZZ}_d\hat{\tilde{f}}^d)$$

$$+ Z^0_\mu A^\mu(\hat{\tilde{f}}^{u\dagger}\tilde{G}^{ZA}_u\hat{\tilde{f}}^u + \hat{\tilde{f}}^{d\dagger}\tilde{G}^{ZA}_d\hat{\tilde{f}}^d) + A_\mu A^\mu(\hat{\tilde{f}}^{u\dagger}\tilde{G}^{AA}_u\hat{\tilde{f}}^u + \hat{\tilde{f}}^{d\dagger}\tilde{G}^{AA}_d\hat{\tilde{f}}^d)$$

.

B.3 Projection Matrices

Below, we write down explicitly all of the projection matrices D^{ab}_α, S^{ab}_α, $\tilde{D}^{ab}_\alpha$ and $\tilde{S}^{ab}_\alpha$ used in the construction of the generalized CKM matrices (see appendix B.2). It follows that only D^{ud}_L and $D^{\bar{u}\bar{d}}_R$ (and $\tilde{D}^{ud}_L$ and $\tilde{D}^{\bar{u}\bar{d}}_R$) are independent, since all of the other matrices can be obtained from their products. For example, $D^{ud}_L(D^{ud}_L)^\dagger = D^{uu}_L$, $(S^{uu}_L)^\dagger S^{uu}_L = S^{\bar{u}\bar{u}}_L$, It also follows that $D^{uu}_L + S^{\bar{u}\bar{u}}_L = 1_{3\times3}$. For completeness, we also include the matrices $y^{ab} \subset Y^{ab}$ present in the interaction term coupling the Higgs scalar particle to all third and fourth generation quarks (see B.4).

B.3.0.0.1 Quark Sector:

$$D_L^{ud} = \begin{pmatrix} 1 & 0 \\ 0 & 1 \\ 0 & 0 \end{pmatrix}. \quad \text{Couples } (T_3 = \frac{-1}{2})\ u_3^\dagger, u_4^\dagger \in f_L^{u\dagger} \text{ to } (T_3 = \frac{1}{2})\ d_3, d_4 \in f_L^d.$$

$$D_R^{\bar{u}\bar{d}} = \begin{pmatrix} 0 & 0 \\ 0 & 0 \\ 0 & 1 \end{pmatrix}. \quad \text{Couples } (T_3 = \frac{-1}{2})\ \bar{d}_4^{c\dagger} \in f_R^{d\dagger} \text{ to } (T_3 = \frac{1}{2})\ \bar{u}_4^c \in f_R^u.$$

From the two matrices above, we can construct:

- $D_L^{uu} = \text{Diag}(1,1,0)$. Couples $(T_3 = \frac{-1}{2})\ u_3^\dagger, u_4^\dagger \in f_L^{u\dagger}$ to $(T_3 = \frac{1}{2})\ u_3, u_4 \in f_L^u$.
- $S_L^{\bar{u}\bar{u}} = \text{Diag}(0,0,1)$. Couples $(T_3 = 0)\ \bar{u}_4^c \in f_L^{u\dagger}$ to $(T_3 = 0)\ \bar{u}_4 \in f_L^u$.
- $S_R^{uu} = \text{Diag}(1,1,0)$. Couples $(T_3 = 0)\ u_3^{c\dagger}, u_4^{c\dagger} \in f_R^{u\dagger}$ to $(T_3 = 0)\ u_3^c, u_4^c \in f_R^u$.
- $D_R^{\bar{u}\bar{u}} = \text{Diag}(0,0,1)$. Couples $(T_3 = \frac{1}{2})\ \bar{u}_4^{c\dagger} \in f_R^{u\dagger}$ to $(T_3 = \frac{-1}{2})\ \bar{u}_4^c \in f_R^u$.
- $D_L^{dd} = \text{Diag}(1,1)$. Couples $(T_3 = \frac{1}{2})\ d_3^\dagger, d_4^\dagger \in f_L^{d\dagger}$ to $(T_3 = \frac{-1}{2})\ d_3, d_4 \in f_L^d$.
- $S_R^{dd} = \text{Diag}(1,0)$. Couples $(T_3 = 0)\ d_3^{c\dagger} \in f_R^{d\dagger}$ to $(T_3 = 0)\ d_3^c \in f_R^d$.
- $D_R^{\bar{d}\bar{d}} = \text{Diag}(0,1)$. Couples $(T_3 = \frac{-1}{2})\ \bar{d}_4^{c\dagger} \in f_R^{u\dagger}$ to $(T_3 = \frac{1}{2})\ \bar{d}_4^c \in f_R^d$.

B.3.0.0.2 Squark Sector:

$$\tilde{D}_L^{ud} = \begin{pmatrix} 1 & 0 & 0 & 0 \\ 0 & 1 & 0 & 0 \\ 0 & 0 & 0 & 0 \\ 0 & 0 & 0 & 0 \\ 0 & 0 & 0 & 0 \\ 0 & 0 & 0 & 0 \end{pmatrix}. \qquad \text{Couples } (T_3 = \frac{-1}{2})\ \tilde{u}_3^*, \tilde{u}_4^* \in \tilde{f}^{u\dagger} \text{ to } (T_3 = \frac{1}{2})\ \tilde{d}_3, \tilde{d}_4 \in \tilde{f}^d.$$

$$\tilde{D}_R^{\bar{u}\bar{d}} = \begin{pmatrix} 0 & 0 & 0 & 0 \\ 0 & 0 & 0 & 0 \\ 0 & 0 & 0 & 0 \\ 0 & 0 & 0 & 0 \\ 0 & 0 & 0 & 0 \\ 0 & 0 & 0 & 1 \end{pmatrix}. \qquad \text{Couples } (T_3 = \frac{-1}{2})\ \tilde{\bar{d}}_4^{c*} \in \tilde{f}^{d\dagger} \text{ to } (T_3 = \frac{1}{2})\ \tilde{\bar{u}}_4^c \in \tilde{f}^u.$$

From the two matrices above, we can construct:

- $\tilde{D}_L^{uu} = \text{Diag}(1, 1, 0, 0, 0, 0)$. Couples $(T_3 = \frac{-1}{2})\ \tilde{u}_3^*, \tilde{u}_4^* \in \tilde{f}^{u\dagger}$ to $(T_3 = \frac{1}{2})\ u_3, u_4 \in \tilde{f}^u$.

- $\tilde{S}_L^{\bar{u}\bar{u}} = \text{Diag}(0, 0, 1, 0, 0, 0)$. Couples $(T_3 = 0)\ \tilde{\bar{u}}_4^c \in \tilde{f}^{u\dagger}$ to $(T_3 = 0)\ \bar{u}_4 \in \tilde{f}^u$.

- $\tilde{S}_R^{uu} = \text{Diag}(0,0,0,1,1,0)$. Couples $(T_3 = 0)$ $\tilde{u}_3^{c*}, \tilde{u}_4^{c*} \in \tilde{f}^{u\dagger}$ to $(T_3 = 0)$ $\tilde{u}_3^c, \tilde{u}_4^c \in \tilde{f}^u$.

- $\tilde{D}_R^{\bar{u}\bar{u}} = \text{Diag}(0,0,0,0,0,1)$. Couples $(T_3 = \frac{1}{2})$ $\tilde{\bar{u}}_4^{c*} \in \tilde{f}^{u\dagger}$ to $(T_3 = \frac{-1}{2})$ $\tilde{\bar{u}}_4^c \in \tilde{f}^u$.

- $\tilde{D}_L^{dd} = \text{Diag}(1,1,0,0)$.Couples $(T_3 = \frac{1}{2})$ $\tilde{d}_3^*, \tilde{d}_4^* \in \tilde{f}^{d\dagger}$ to $(T_3 = \frac{-1}{2})$ $\tilde{d}_3, \tilde{d}_4 \in \tilde{f}^d$.

- $\tilde{S}_R^{dd} = \text{Diag}(0,0,1,0)$. Couples $(T_3 = 0)$ $\tilde{d}_3^{c*} \in \tilde{f}^{d\dagger}$ to $(T_3 = 0)$ $\tilde{d}_3^c \in \tilde{f}^d$.

- $\tilde{D}_R^{\bar{d}\bar{d}} = \text{Diag}(0,0,0,1)$. Couples $(T_3 = \frac{-1}{2})$ $\tilde{\bar{d}}_4^{c*} \in \tilde{f}^{u\dagger}$ to $(T_3 = \frac{1}{2})$ $\tilde{\bar{d}}_4^c \in \tilde{f}^d$.

B.3.0.0.3 Higgs Sector:

$$y^{u\bar{u}} = \begin{pmatrix} y_{33} & y_{34} & 0 \\ y_{43} & y_{44} & 0 \\ 0 & 0 & 0 \end{pmatrix} \quad \text{and} \quad y^{d\bar{d}} = \begin{pmatrix} y_{\text{bot}} & 0 \\ 0 & 0 \end{pmatrix}.$$

B.4 Beta Functions

Gauge Couplings:

The beta function for the gauge couplings are:

$$16\pi^2 \frac{dg_i}{dt} = -b_i g_i^3.$$

Here, $t = \ln Q$ where Q is the renormalization scale. The beta function coefficients for an arbitrary number of SU(5) multiplets n_5 and n_{10} are given by:

$$b1 = \frac{3}{5}(11) + n_{10}b_{10} + n_5 b_5$$

$$b2 = 1 + n_{10}b_{10} + n_5 b_5$$

$$b3 = -3 + n_{10}b_{10} + n_5 b_5$$

with $b_{10} = 3$, $b_5 = 1$ denoting group theoretic coefficients.

Top Yukawa Coupling:

Using the general results in [158], we obtain the following top Yukawa two-loop beta function:

$$\beta_{Y_u}(t) = \frac{1}{16\pi^2}\Bigg((3\mathrm{Tr}[Y_u(t).Y_u^\dagger(t)]Y_u(t) + 3Y_u(t)Y_u^\dagger(t)Y_u(t) + Y_u(t)Y_d^\dagger(t)Y_d(t)) - (\frac{16}{3}g_3(t)^2 + 3g_2(t)^2 + \frac{13}{15}g_1(t)^2)Y_u(t)\Bigg).$$

Here, Y_u is the up-type Yukawa coupling matrix containing y_{33}, y_{34}, y_{43} and y_{44}.

B.5 Calculation of Oblique Parameters

Fermion Contribution:

In [159], the authors derived a general formula for computing the values of S and T for any model with vector-like quarks, where the number of up and down quarks

are arbitrary and not necessarily equal. Adapting these general results to our model, we get:

$$
\begin{aligned}
T_f = \frac{3}{16\pi \sin^2\theta_W \cos^2\theta_W}\Bigg\{ & \sum_{\alpha=1}^{3}\sum_{i=2}^{2}\Bigg([(K_L^{ud})^2_{\alpha i} + (K_R^{\bar{u}\bar{d}})^2_{\alpha i}]\theta_+(y_\alpha, y_i) \\
& + 2[(K_L^{ud})_{\alpha i}(K_R^{\bar{u}\bar{d}})_{\alpha i}]\theta_-(y_\alpha, y_i)\Bigg) \\
& - \sum_{\beta<\alpha}\Big([(K_L^{uu})^2_{\alpha\beta} + (K_R^{\bar{u}\bar{u}})^2_{\alpha\beta}]\theta_+(y_\alpha, y_\beta) + 2[(K_L^{uu})_{\alpha\beta}(K_R^{\bar{u}\bar{u}})_{\alpha\beta}]\theta_-(y_\alpha, y_\beta)\Big) \\
& - \sum_{j<i}\Big([(K_L^{dd})^2_{ij} + (K_R^{\bar{d}\bar{d}})^2_{ij}]\theta_+(y_i, y_j) + 2[(K_L^{dd})_{ij}(K_R^{\bar{d}\bar{d}})_{ij}]\theta_-(y_i, y_j)\Big)\Bigg\}, \\
S_f = \frac{3}{2\pi}\Bigg\{ & \sum_{\alpha=1}^{3}\sum_{i=2}^{2}\Big([K_L^{ud})^2_{\alpha i} + (K_R^{\bar{u}\bar{d}})^2_{\alpha i}]\psi_+(y_\alpha, y_i) + 2[(K_L^{ud})_{\alpha i}(K_R^{\bar{u}\bar{d}})_{\alpha i}]\psi_-(y_\alpha, y_i)\Big) \\
& - \sum_{\beta<\alpha}\Big([(K_L^{uu})^2_{\alpha\beta} + (K_R^{\bar{u}\bar{u}})^2_{\alpha\beta}]\chi_+(y_\alpha, y_\beta) + 2[(K_L^{uu})_{\alpha\beta}(K_R^{\bar{u}\bar{u}})_{\alpha\beta}]\chi_-(y_\alpha, y_\beta)\Big) \\
& - \sum_{j<i}\Big([(K_L^{dd})^2_{ij} + (K_R^{\bar{d}\bar{d}})^2_{ij}]\chi_+(y_i, y_j) + 2[(K_L^{dd})_{ij}(K_R^{\bar{d}\bar{d}})_{ij}]\chi_-(y_i, y_j)\Big)\Bigg\}
\end{aligned}
$$

where the K's are the generalized CKM matrices for fermions, derived in appendix B.2. The Greek indices sum over the up-type quark generations (i.e from 1 to 3) and the Latin indices sum over the number of down-type quark generations (i.e from 1 to 2). The functions $\theta_\pm(y_1, y_2)$, $\psi_\pm(y_1, y_2)$ and $\chi_\pm(y_1, y_2)$ are defined in appendix B.6, and $y_i \equiv m_i^2/m_Z^2$.

Scalar Contribution:

The scalar partners also contribute to the oblique corrections.For this calculation, we use the notation and conventions of [160], where the oblique parameters S and T

are defined as

$$S_s = \frac{4\sin^2\theta_W\cos^2\theta_W}{\alpha m_Z^2}\left(\Pi_{ZZ}(m_Z^2) - \Pi_{ZZ}(0) - \frac{\cos^2\theta_W}{\cos\theta_W\sin\theta_W}\Pi_{Z\gamma}(m_Z^2) - \Pi_{\gamma\gamma}(m_Z^2)\right)$$
$$T_s = \frac{1}{\alpha}\left(\frac{\Pi_{WW}(0)}{m_W^2} - \frac{\Pi_{ZZ}(0)}{m_Z^2}\right)$$

where the Π's are the electroweak vector boson self-energies. The contributions to the self-energies of the vector bosons from the additional scalars $\tilde{t}'_{1,2,3,4}$ and $\tilde{b}'_{1,2}$ are [161]:

$$\Delta\Pi_{\gamma\gamma} = \frac{3}{16\pi^2}g^2\sin^2\theta_W\left(\left(\frac{2}{3}\right)^2\sum_{i=3}^{6}F(\tilde{t}'_i,\tilde{t}'_i) + \left(\frac{1}{3}\right)^2\sum_{i=3}^{4}F(\tilde{b}'_i,\tilde{b}'_i)\right)$$
$$\Delta\Pi_{Z\gamma} = \frac{3}{16\pi^2}g\sin\theta_W\left(\frac{2}{3}\sum_{i=3}^{6}(\tilde{G}_u^Z)_{ii}F(\tilde{t}'_i,\tilde{t}'_i) + \frac{1}{3}\sum_{i=3}^{4}(\tilde{G}_d^Z)_{ii}F(\tilde{b}'_i,\tilde{b}'_i)\right)$$
$$\Delta\Pi_{ZZ} = \frac{3}{16\pi^2}\left(\sum_{i,j=3}^{6}|(\tilde{G}_u^Z)_{ij}|^2F(\tilde{t}'_i,\tilde{t}'_j) + \sum_{i,j=3}^{4}|(\tilde{G}_d^Z)_{ij}|^2F(\tilde{b}'_i,\tilde{b}'_j)\right)$$
$$\Delta\Pi_{WW} = \frac{3}{16\pi^2}\sum_{i=3}^{6}\sum_{j=3}^{4}|(\tilde{G}_{ud}^W)_{ij}|^2F(\tilde{b}'_i,\tilde{t}'_j)$$

where the $\tilde{G}$'s are the coupling matrices for scalars derived in appendix B.2 and the function $F(x,y)$ is given in appendix B.6.

B.6 Useful Functions

The expressions for $\theta_\pm(y_i, y_j)$, $\psi_\pm(y_i, y_j)$ and $\chi_\pm(y_i, y_j)$, used in appendix B.5 are [162]:

$$\begin{aligned}
\theta_+(y_i, y_j) &= y_i + y_j - \frac{2y_i y_j}{y_i - y_j} \ln \frac{y_i}{y_j} \\
\theta_-(y_i, y_j) &= 2\sqrt{y_i y_j} \left(\frac{y_i + y_j}{y_i - y_j} \ln \frac{y_i}{y_j} - 2 \right) \\
\psi_+(y_i, y_j) &= \frac{1}{3} - \frac{1}{9} \ln \frac{y_i}{y_j} \\
\psi_-(y_i, y_j) &= -\frac{y_i + y_j}{6\sqrt{y_i y_j}} \\
\chi_+(y_i, y_j) &= \frac{5(y_i^2 + y_j^2) - 22 y_i y_j}{9(y_i + y_j)^2} + \frac{3y_1 y_2 (y_i + y_j) - y_i^3 - y_j^3}{3(y_i - y_j)^3} \ln \frac{y_i}{y_j} \\
\chi_-(y_i, y_j) &= -\sqrt{y_i y_j} \left(\frac{y_i + y_j}{6 y_i y_j} - \frac{y_i + y_j}{(y_i - y_j)^2} + \frac{2y_i y_j}{(y_i + y_j)^3} \ln \frac{y_i}{y_j} \right).
\end{aligned}$$

Here, $y_i = m_i^2/m_Z^2$, $y_i = m_i^2/m_Z^2$ and the limit $\epsilon \to 0$ of Dimensional Regularization is assumed. The expression for $F(x, y)$ in the self-energy functions in appendix B.5 is [161]:

$$\begin{aligned}
F(x, y) &= H(x, y) + (x + y - p^2) B(x, y) \\
H(x, y) &= \left(2p^2 - x - y - (x - y)^2/p^2 \right) B(x, y)/3 \\
&\quad + \left(x \bar{\ln} x + m_y^2 \bar{\ln} y - p^2/3 + (x \bar{\ln} x - x - y \bar{\ln} y + y)(y - x)/(2p^2) \right) 2/3 \\
B(x, y) &= -\int_0^1 dt \bar{\ln} \left(tx + (1 - t)y - t(1 - t)p^2 - i\epsilon \right),
\end{aligned}$$

where now $x = m_x^2$, $y = m_y^2$ and $\bar{\ln} X = \ln(X/m_Z^2)$.

B.7 Haag – Lopuszanski – Sohnius theorem

Prior to 1975, the Coleman-Mandula theorem had shown that under fairly general assumptions, internal symmetries could not be combined with spacetime symmetries (like Lorentz symmetry) in any but a trivial way, that is, as a direct product [94]. The Haag – Lopuszanski - Sohnius theorem weakened one of the assumptions of Coleman and Mandula by allowing symmetries generated not only by Lie algebras but by Lie superalgebras, that is, Z_2 graded Lie algebras, with an even and odd part, and allowing anticommutators as well as commutators [88]. Under these conditions, the unique nontrivial extension of the Poincaré algebra is the supersymmetry algebra. The supersymmetry algebra has fermionic (or odd) internal-symmetry generators Q (and $\bar{Q}$, who live in the conjugate representation) whose anticommutator yields P, the generator of spacetime translations. Furthermore, the Q can be taken to transform nontrivially under some compact Lie group, generated by Lorentz scalars B, which is an internal symmetry group. Due to Coleman and Mandula, we know B must commute with the usual generators of the Poincaré group, P and M. The algebra is

then

$$\begin{aligned}
\{Q^A_\alpha, Q^B_\beta\} &= \epsilon_{\alpha\beta} Z^{AB} \\
\{\bar{Q}^A_{\dot{\alpha}}, \bar{Q}^B_{\dot{\beta}}\} &= \epsilon_{\dot{\alpha}\dot{\beta}} (Z^+)^{AB} \\
\{Q^A_\alpha, \bar{Q}^B_{\dot{\beta}}\} &= 2\delta^{AB} (\sigma^\mu)_{\alpha\dot{\beta}} P_\mu \\
[Q^A_\alpha, P_\mu] &= [\bar{Q}^A_{\dot{\alpha}}, P_\mu] = 0 \\
[Q^A_\alpha, B_i] &= i S_i^{AB} Q^B_\alpha \\
[Q^A_\alpha, M^{\mu\nu}] &= -\frac{1}{4} (\sigma^\mu \bar{\sigma}^\nu - \sigma^\nu \bar{\sigma}^\mu)^\beta_\alpha Q^A_\beta \\
[B_i, B_j] &= i f^k_{ij} B_k \\
[Z^{AB}, B_i] &= 0,
\end{aligned} \tag{B.6}$$

along with the usual Poincaré algebra of P and M [163]. Here A, B go from 1 to $\mathcal{N}$, where $\mathcal{N}$ is the dimension of the representation of B that the Q's live in, and α, β are spinor indices that go from 1 to 2. B_i is the i^{th} generator of an internal symmetry group while S is an $\mathcal{N} \times \mathcal{N}$ representation matrix of the internal symmetry. The $\sigma^\mu = (1, \sigma^i)$ are the identity matrix along with the Pauli matrices, while $\bar{\sigma}^\mu = (1, -\sigma^i)$. Z is known as a central charge and may only be nonzero for $\mathcal{N} > 1$. The most commonly studied case is $\mathcal{N} = 1$; $\mathcal{N} > 1$ is known as extended supersymmetry and is not considered in this work.

Bibliography

[1] E. Fermi. Versuch einer theorie der β-strahlen. i. *Zeitschrift fr Physik*, 88(3-4):161–177, 1934.

[2] D. M. Webber, V. Tishchenko, Q. ˜Peng, S. Battu, R. M. Carey, D. B. Chitwood, J. Crnkovic, P. T. Debevec, S. Dhamija, W. Earle, A. Gafarov, K. Giovanetti, T. P. Gorringe, F. E. Gray, Z. Hartwig, D. W. Hertzog, B. Johnson, P. Kammel, B. Kiburg, S. Kizilgul, J. Kunkle, B. Lauss, I. Logashenko, K. R. Lynch, R. McNabb, J. P. Miller, F. Mulhauser, C. J. G. Onderwater, J. Phillips, S. Rath, B. L. Roberts, P. Winter, and B. Wolfe. Measurement of the Positive Muon Lifetime and Determination of the Fermi Constant to Part-per-Million Precision. *Physical Review Letters*, 106(7), February 2011. arXiv: 1010.0991.

[3] Andreas Petermann and Ernst Carl Gerlach Stueckelberg de Breidenbach. La normalisation des constantes dans la thorie des quanta. 1953. presented 9 May 1952.

[4] M. Gell-Mann and F. E. Low. Quantum electrodynamics at small distances.

Phys. Rev., 95:1300–1312, Sep 1954.

[5] L.P. Kadanoff. Scaling laws for Ising models near T(c). *Physics*, 2:263–272, 1966.

[6] K. Symanzik. Small distance behaviour in field theory and power counting. *Communications in Mathematical Physics*, 18(3):227–246, 1970.

[7] Curtis G. Callan. Broken scale invariance in scalar field theory. *Phys. Rev. D*, 2:1541–1547, Oct 1970.

[8] Kenneth G. Wilson. The renormalization group: Critical phenomena and the kondo problem. *Rev. Mod. Phys.*, 47:773–840, Oct 1975.

[9] Kenneth G. Wilson. The renormalization group and critical phenomena. *Rev. Mod. Phys.*, 55:583–600, Jul 1983.

[10] S. Weinberg. Phenomenological Lagrangians. *Physica A Statistical Mechanics and its Applications*, 96:327–340, April 1979.

[11] Michael E Peskin and Daniel V Schroeder. *An introduction to quantum field theory*. Westview, 1995.

[12] Matthew D Schwartz. *Quantum Field Theory and the Standard Model*. Cambridge University Press, 2013.

[13] K.A. Olive et al. Review of Particle Physics. *Chin.Phys.*, C38:090001, 2014.

[14] T. D. Lee and C. N. Yang. Question of parity conservation in weak interactions. *Phys. Rev.*, 104:254–258, Oct 1956.

[15] C. S. Wu, E. Ambler, R. W. Hayward, D. D. Hoppes, and R. P. Hudson. Experimental test of parity conservation in beta decay. *Phys. Rev.*, 105:1413–1415, Feb 1957.

[16] T. W B Kibble. Englert-Brout-Higgs-Guralnik-Hagen-Kibble mechanism (history). 4(1):8741, 2009. revision 137393.

[17] R. P. Feynman and M. Gell-Mann. Theory of the fermi interaction. *Phys. Rev.*, 109:193–198, Jan 1958.

[18] E. C. G. Sudarshan and R. E. Marshak. Chirality invariance and the universal fermi interaction. *Phys. Rev.*, 109:1860–1862, Mar 1958.

[19] C. N. Yang and R. L. Mills. Conservation of isotopic spin and isotopic gauge invariance. *Phys. Rev.*, 96:191–195, Oct 1954.

[20]

[21] Howard Georgi and S. L. Glashow. Unity of all elementary-particle forces. *Phys. Rev. Lett.*, 32:438–441, Feb 1974.

[22] Sheldon L. Glashow. Partial-symmetries of weak interactions. *Nuclear Physics*, 22(4):579 – 588, 1961.

[23] P. W. Anderson. Plasmons, gauge invariance, and mass. *Phys. Rev.*, 130:439–442, Apr 1963.

[24] F. Englert and R. Brout. Broken Symmetry and the Mass of Gauge Vector Mesons. *Physical Review Letters*, 13:321–323, August 1964.

[25] P.W. Higgs. Broken symmetries, massless particles and gauge fields. *Physics Letters*, 12(2):132 – 133, 1964.

[26] P. W. Higgs. Broken Symmetries and the Masses of Gauge Bosons. *Physical Review Letters*, 13:508–509, October 1964.

[27] G. S. Guralnik, C. R. Hagen, and T. W. B. Kibble. Global conservation laws and massless particles. *Phys. Rev. Lett.*, 13:585–587, Nov 1964.

[28] Jeffrey Goldstone, Abdus Salam, and Steven Weinberg. Broken symmetries. *Phys. Rev.*, 127:965–970, Aug 1962.

[29] Steven Weinberg. A model of leptons. *Phys. Rev. Lett.*, 19:1264–1266, Nov 1967.

[30] A. Salam and J.C. Ward. Electromagnetic and weak interactions. *Physics Letters*, 13(2):168 – 171, 1964.

[31] Nhan V. Tran. *Angles and Daemons: Spin correlations at the LHC*. PhD thesis, Johns Hopkins University, 2011.

[32] Serguei Chatrchyan et al. Measurement of the weak mixing angle with the Drell-Yan process in proton-proton collisions at the LHC. *Phys.Rev.*, D84:112002, 2011.

[33]

[34] W. J. Marciano. Spin and precision electroweak physics. Technical report, 1993.

[35] K.S. Kumar, Sonny Mantry, W.J. Marciano, and P.A. Souder. Low Energy Measurements of the Weak Mixing Angle. *Ann.Rev.Nucl.Part.Sci.*, 63:237–267, 2013.

[36] LEP Electroweak Working Group. Precision Electroweak Measurements and Constraints on the Standard Model. 2010.

[37] P. Vilain et al. Precision measurement of electroweak parameters from the scattering of muon-neutrinos on electrons. *Phys.Lett.*, B335:246–252, 1994.

[38] Kevin Scott McFarland et al. A Precision measurement of electroweak parameters in neutrino - nucleon scattering. *Eur.Phys.J.*, C1:509–513, 1998.

[39] P. L. Anthony, R. G. Arnold, C. Arroyo, K. Bega, J. Biesiada, P. E. Bosted, G. Bower, J. Cahoon, R. Carr, G. D. Cates, J.-P. Chen, E. Chudakov, M. Cooke, P. Decowski, A. Deur, W. Emam, R. Erickson, T. Fieguth, C. Field, J. Gao, M. Gary, K. Gustafsson, R. S. Hicks, R. Holmes, E. W. Hughes, T. B. Humensky, G. M. Jones, L. J. Kaufman, L. Keller, Yu. G. Kolomensky, K. S. Kumar,

P. LaViolette, D. Lhuillier, R. M. Lombard-Nelsen, Z. Marshall, P. Mastromarino, R. D. McKeown, R. Michaels, J. Niedziela, M. Olson, K. D. Paschke, G. A. Peterson, R. Pitthan, D. Relyea, S. E. Rock, O. Saxton, J. Singh, P. A. Souder, Z. M. Szalata, J. Turner, B. Tweedie, A. Vacheret, D. Walz, T. Weber, J. Weisend, M. Woods, and I. Younus. Precision measurement of the weak mixing angle in møller scattering. *Phys. Rev. Lett.*, 95:081601, Aug 2005.

[40] G. P. Zeller, K. S. McFarland, T. Adams, A. Alton, S. Avvakumov, L. de Barbaro, P. de Barbaro, R. H. Bernstein, A. Bodek, T. Bolton, J. Brau, D. Buchholz, H. Budd, L. Bugel, J. Conrad, R. B. Drucker, B. T. Fleming, R. Frey, J. A. Formaggio, J. Goldman, M. Goncharov, D. A. Harris, R. A. Johnson, J. H. Kim, S. Koutsoliotas, M. J. Lamm, W. Marsh, D. Mason, J. McDonald, C. McNulty, D. Naples, P. Nienaber, A. Romosan, W. K. Sakumoto, H. Schellman, M. H. Shaevitz, P. Spentzouris, E. G. Stern, N. Suwonjandee, M. Tzanov, M. Vakili, A. Vaitaitis, U. K. Yang, J. Yu, and E. D. Zimmerman. Precise determination of electroweak parameters in neutrino-nucleon scattering. *Phys. Rev. Lett.*, 88:091802, Feb 2002.

[41] G. P. Zeller, K. S. McFarland, T. Adams, A. Alton, S. Avvakumov, L. de Barbaro, P. de Barbaro, B. H. Bernstein, A. Bodek, T. Bolton, J. Brau, D. Buccholz, H. Budd, L. Bugel, J. Conrad, R. B. Drucker, B. T. Fleming, R. Frey, J. A. Formaggio, J. Goldman, M. Goncharov, D. A. Harris, R. A. Johnson,

J. H. Kim, S. Koutsoliotas, M. J. Lamm, W. Marsh, D. Mason, J. McDonald, C. McNulty, D. Naples, P. Nienaber, A. Romosan, W. K. Sakumoto, H. Schellman, M. H. Shaevitz, P. Spentzouris, E. G. Stern, N. Suwonjandee, M. Tzanov, M. Vakili, A. Vaitaitis, U. K. Yang, J. Yu, and E. D. Zimmerman. Erratum: Precise determination of electroweak parameters in neutrino-nucleon scattering [phys. rev. lett. **88** , 091802 (2002)]. *Phys. Rev. Lett.*, 90:239902, Jun 2003.

[42]

[43] Sidney D. Drell and Tung-Mow Yan. Massive lepton-pair production in hadron-hadron collisions at high energies. *Phys. Rev. Lett.*, 25:316–320, Aug 1970.

[44] D. Acosta et al. Measurement of the forward-backward charge asymmetry of electron positron pairs in $p\bar{p}$ collisions at $\sqrt{s} = 1.96$ TeV. *Phys.Rev.*, D71:052002, 2005.

[45] V.M. Abazov et al. Measurement of the forward-backward charge asymmetry and extraction of sin**2 Theta(W)(eff) in p anti-p —¿ Z/gamma* + X —¿ e+ e- + X events produced at $\sqrt{s} = 1.96$-TeV. *Phys.Rev.Lett.*, 101:191801, 2008.

[46] V.M. Abazov et al. Measurement of $\sin^2\theta^{\ell}_{\text{eff}}$ and Z-light quark couplings using the forward-backward charge asymmetry in $p\bar{p} \to Z/\gamma^* \to e^+e^-$ events with $L = 5.0$ fb^{-1} at $\sqrt{s} = 1.96$ TeV. *Phys.Rev.*, D84:012007, 2011.

[47] Manuel Drees, Probir Roy, and Rohini Godbole. Theory and phenomenology of sparticles. 2004.

[48] John Terning. *Modern supersymmetry: Dynamics and duality*, volume 132. Oxford University Press, 2006.

[49] T. D. Lee, Reinhard Oehme, and C. N. Yang. Remarks on possible noninvariance under time reversal and charge conjugation. *Phys. Rev.*, 106:340–345, Apr 1957.

[50] J. H. Christenson, J. W. Cronin, V. L. Fitch, and R. Turlay. Evidence for the 2π Decay of the K20 Meson. *Physical Review Letters*, 13:138–140, July 1964.

[51] Makoto Kobayashi and Toshihide Maskawa. Cp-violation in the renormalizable theory of weak interaction. *Progress of Theoretical Physics*, 49(2):652–657, 1973.

[52] K. Ackerstaff et al. Measurement of the branching fractions and forward - backward asymmetries of the Z0 into light quarks. *Z.Phys.*, C76:387–400, 1997.

[53] G.L. Fogli and D. Haidt. Structure of the hadronic neutral current and parameters of the standard model from an analysis of the neutrino-induced deep-inelastic scattering. *Zeitschrift fr Physik C Particles and Fields*, 40(3):379–402, 1988.

[54] M. E. Peskin and T. Takeuchi. New constraint on a strongly interacting higgs sector. *Physical Review Letters*, 65(8):964, 1990.

[55] K. Bega. *Measurement of the weak mixing angle in Moller scattering.* PhD thesis, California Institute of Technology, 2004.

[56] David London and Jonathan L. Rosner. Extra gauge bosons in e_6. *Phys. Rev. D*, 34:1530–1546, Sep 1986.

[57] Jonathan L. Rosner. Off-peak lepton asymmetries from new Z 's. *Phys. Rev. D*, 35:2244–2247, Apr 1987.

[58] Laura Reina. TASI 2011: lectures on Higgs-Boson Physics. 2012.

[59] S. Dawson. Introduction to electroweak symmetry breaking. pages 1–83, 1998.

[60] Michael Dittmar. Neutral current interference in the TeV region: The Experimental sensitivity at the LHC. *Phys.Rev.*, D55:161–166, 1997.

[61] A. De Roeck and R.S. Thorne. Structure Functions. *Prog.Part.Nucl.Phys.*, 66:727–781, 2011.

[62] Yanyan Gao, Andrei V. Gritsan, Zijin Guo, Kirill Melnikov, Markus Schulze, et al. Spin determination of single-produced resonances at hadron colliders. *Phys.Rev.*, D81:075022, 2010.

[63] John C. Collins and Davison E. Soper. Angular distribution of dileptons in high-energy hadron collisions. *Phys. Rev. D*, 16:2219–2225, Oct 1977.

[64] S. Kretzer, H.L. Lai, F.I. Olness, and W.K. Tung. Cteq6 parton distributions with heavy quark mass effects. *Phys.Rev.*, D69:114005, 2004.

[65] Torbjorn Sjostrand, Stephen Mrenna, and Peter Z. Skands. PYTHIA 6.4 Physics and Manual. *JHEP*, 0605:026, 2006.

[66] Piotr Golonka and Zbigniew Was. PHOTOS Monte Carlo: A Precision tool for QED corrections in Z and W decays. *Eur.Phys.J.*, C45:97–107, 2006.

[67] C.M. Carloni Calame, G. Montagna, O. Nicrosini, and A. Vicini. Precision electroweak calculation of the production of a high transverse-momentum lepton pair at hadron colliders. *JHEP*, 0710:109, 2007.

[68] Savas Dimopoulos and Stuart Raby. Supercolor. *Nuclear Physics B*, 192(2):353–368, 1981.

[69] Gian Francesco Giudice. Naturally Speaking: The Naturalness Criterion and Physics at the LHC. 2008.

[70] Jonathan L. Feng. Naturalness and the Status of Supersymmetry. *Ann.Rev.Nucl.Part.Sci.*, 63:351–382, 2013.

[71] G.t Hooft. Naturalness, chiral symmetry, and spontaneous chiral symmetry breaking. In G.t Hooft, C. Itzykson, A. Jaffe, H. Lehmann, P.K. Mitter, I.M. Singer, and R. Stora, editors, *Recent Developments in Gauge Theories*, volume 59 of *NATO Advanced Study Institutes Series*, pages 135–157. Springer US, 1980.

[72] Edward Farhi and Leonard Susskind. Technicolour. *Physics Reports*, 74(3):277–321, 1981.

[73] Kenneth G. Wilson. Renormalization group and strong interactions. *Phys. Rev. D*, 3:1818–1846, Apr 1971.

[74] M.J.G. Veltman. The Infrared - Ultraviolet Connection. *Acta Phys.Polon.*, B12:437, 1981.

[75] Edward Witten. Dynamical Breaking of Supersymmetry. *Nucl.Phys.*, B188:513, 1981.

[76] Savas Dimopoulos and Howard Georgi. Softly broken supersymmetry and su (5). *Nuclear Physics B*, 193(1):150–162, 1981.

[77] H. Baer and X. Tata. *Weak Scale Supersymmetry: From Superfields to Scattering Events*. Cambridge University Press, 2006.

[78] A. Brignole, J.A. Casas, J.R. Espinosa, and I. Navarro. Low scale supersymmetry breaking: Effective description, electroweak breaking and phenomenology. *Nucl.Phys.*, B666:105–143, 2003.

[79] Heinz Pagels and Joel R. Primack. Supersymmetry, Cosmology and New TeV Physics. *Phys.Rev.Lett.*, 48:223, 1982.

[80] L.J. Hall and Lisa Randall. Weak scale effective supersymmetry. *Phys.Rev.Lett.*, 65:2939–2942, 1990.

[81] Howard E. Haber and Gordon L. Kane. The Search for Supersymmetry: Probing Physics Beyond the Standard Model. *Phys.Rept.*, 117:75–263, 1985.

[82] Piotr H. Chankowski and Stefan Pokorski. Supersymmetry at the electroweak scale. *Acta Phys.Polon.*, 27:1719–1738, 1996.

[83] S. Dimopoulos, S. Raby, and Frank Wilczek. Supersymmetry and the scale of unification. *Phys. Rev. D*, 24:1681–1683, Sep 1981.

[84] William J. Marciano and Goran Senjanović. Predictions of supersymmetric grand unified theories. *Phys. Rev. D*, 25:3092–3095, Jun 1982.

[85] Michael Dine, Ann E Nelson, and Yuri Shirman. Low energy dynamical supersymmetry breaking simplified. *Physical Review D*, 51(3):1362, 1995.

[86] Stephen P. Martin. A Supersymmetry primer. *Adv.Ser.Direct.High Energy Phys.*, 21:1–153, 2010.

[87] G Jungman, M Kamionkowski, and K Griest. Supersymmetric dark matter. *arXiv preprint hep-ph/9506380*, 1995.

[88] Rudolf Haag, Jan T. opuszaski, and Martin Sohnius. All possible generators of supersymmetries of the s-matrix. *Nuclear Physics B*, 88(2):257 – 274, 1975.

[89] S. Dimopoulos and G.F. Giudice. Naturalness constraints in supersymmetric theories with nonuniversal soft terms. *Phys.Lett.*, B357:573–578, 1995.

[90] Vasiliki A. Mitsou. Highlights from SUSY searches with ATLAS. *EPJ Web Conf.*, 70:00072, 2014.

[91] A. Arbey, M. Battaglia, F. Mahmoudi, and D. Martnez Santos. Supersymmetry confronts $B_s{}^{+-}$: Present and future status. *Phys.Rev.*, D87(3):035026, 2013.

[92] CMS Collaboration. *CMS-PAS-HIG-12-020*, 2012.

[93] G. Aad et al. [ATLAS Collaboration]. *ATLAS-CONF-2012-093*, 2012.

[94] Sidney Coleman and Jeffrey Mandula. All possible symmetries of the s matrix. *Physical Review*, 159(5):1251, 1967.

[95] P. Ramond. Dual theory for free fermions. *Phys. Rev. D*, 3:2415–2418, May 1971.

[96] J.-L. Gervais and B. Sakita. Field theory interpretation of supergauges in dual models. *Nuclear Physics B*, 34(2):632 – 639, 1971.

[97] D.V. Volkov and V.P. Akulov. Is the neutrino a goldstone particle? *Physics Letters B*, 46(1):109 – 110, 1973.

[98] Yu A Gol'Fand and EP Likhtman. Extension of the algebra of poincaré group generators and violation of p invariance. In *Supergravities in diverse dimensions. Volume 1*. 1989.

[99] Gian Francesco Giudice and Riccardo Rattazzi. Theories with gauge-mediated supersymmetry breaking. *Physics Reports*, 322(6):419–499, 1999.

[100] Cyrus Faroughy and K. Grizzard. Raising the Higgs mass in supersymmetry with t-t mixing. *Phys.Rev.*, D90(3):035024, 2014.

[101] R. Barbieri and A. Strumia.

[102] G. F. Giudice and R. Rattazzi. Nucl. phys. b. 19(757), 2006.

[103] M. A. Luty.

[104] L.M. Carpenter, D. E. Kaplan and E. -J. Rhee. *Phys. Rev. Lett.*, 99(211801), 2007.

[105] L. M. Carpenter, D. E. Kaplan and E. J. Rhee.

[106] P. W. Graham, D. E. Kaplan, S. Rajendran and P. Saraswat.

[107] J. Fan, M. Reece, and J. T. Ruderman. *JHEP*, 1111(012), 2011.

[108] G. D. Kribs and A. Martin.

[109] M. Baryakhtar, N. Craig, and K. Van Tilburg.

[110] K. Choi, K. S. Jeong, T. Kobayashi and K. i. Okumura. *Phys. Lett. B*, 633(355), 2006.

[111] R. Kitano and Y. Nomura. *Phys. Lett. B*, 631(58), 2005.

[112] Z. Chacko, Y. Nomura, and D. Tucker-Smith. *Nucl. Phys. B*, 725(207), 2005.

[113] J. R. Ellis, J. F. Gunion, H. E. Haber, L. Roszkowski and F. Zwirner. *Phys. Rev. D*, 39(844), 1989.

[114] J. R. Espinosa and M. Quiros. *Phys. Rev. Lett.*, 81(516), 1998.

[115] P. Batra, A. Delgado, D. E. Kaplan and T. M. P. Tait. *JHEP*, 0402(043), 2004.

[116] A. Maloney, A. Pierce, and J. G. Wacker. *JHEP*, 0606(034), 2006.

[117] J. A. Casas, J. R. Espinosa and I. Hidalgo. *JHEP*, 0401(008), 2004.

[118] A. Brignole, J. A. Casas, J. R. Espinosa and I. Navarro. *Nucl. Phys. B*, 666(105), 2003.

[119] R. Harnik, G. D. Kribs, D. T. Larson and H. Murayama. *Phys. Rev. D*, 70(015002), 2004.

[120] S. Chang, C. Kilic, and R. Mahbubani. *Phys. Rev. D*, 71(015003), 2005.

[121] A. Delgado and T. M. P. Tait. *JHEP*, 0507(023), 2005.

[122] A. Birkedal, Z. Chacko, and Y. Nomura. *Phys. Rev. D*, 71(015006), 2005.

[123] K. S. Babu, I. Gogoladze, and C. Kolda.

[124] K. Choi, K. S. Jeong, T. Kobayashi and K. i. Okumura. *Phys. Rev. D*, 75(095012), 2007.

[125] B. Dutta and Y. Mimura. *Phys. Lett. B*, 648(357), 2007.

[126] H. Abe, Y. G. Kim, T. Kobayashi, and Y. Shimizu. *JHEP*, 0709(107), 2007.

[127] R. Dermisek and H. D. Kim. *Phys. Rev. D*, 96(211803), 2006.

[128] H. Abe, T. Kobayashi, and Y. Omura. *Phys. Rev. D*, 76(015002), 2007.

[129] B. Dutta, Y. Mimura, and D. V. Nanopoulos. *Phys. Lett. B*, 656(199), 2007.

[130] T. Kikuchi.

[131] S. G. Kim, N. Maekawa, A. Matsuzaki, K. Sakurai, A. I. Sanda and T. Yoshikawa. *Phys. Rev. D*, 74(115016), 2006.

[132] M. Dine, N. Seiberg, and S. Thomas. *Phys. Rev. D*, 76(095004), 2007.

[133] R. Dermisek and J. F. Gunion. *Phys. Rev. Lett.*, 95(041801), 2005.

[134] B. Bellazzini, C. Csaki, A. Delgado, and A. Weiler.

[135] I. Gogoladze, M. U. Rehman, and Q. Shafi.

[136] P. W. Graham, A. Ismail, S. Rajendran and P. Saraswat. *Phys. Rev. D*, 81(055016), 2010.

[137] S. P. Martin. *Phys. Rev. D*, 81(035004), 2010.

[138] G. Burdman, Z. Chacko, H. S. Goh, and R. Harnik. *JHEP*, 0702(009), 2007.

[139] Z. Chacko, H. S. Goh, and R. Harnik. *Phys. Rev. Lett.*, 96(231802), 2006.

[140] S. Chang, L. J. Hall, and N. Weiner. *Phys. Rev. D*, 75(035009), 2007.

[141] A. Falkowski, S. Pokorski, and M. Schmaltz. *Phys. Rev. D*, 74(035003), 2006.

[142] N. Arkani-Hamed, A. G. Cohen, E. Katz and A. E. Nelson. *JHEP*, 0207(034), 2002.

[143] N. Arkani-Hamed, A. G. Cohen and H. Georgi. *Phys. Lett. B*, 513(232), 2001.

[144] S. P. Martin and J. D. Wells.

[145] J. A. Aguilar-Saavedra, R. Benbrik, S. Heinemeyer, and M. Perez-Victoria.

[146] CMS Collaboration. *Phys. Lett. B*, 729:149, 2014.

[147] A. Ceccucci and Z. Ligeti and Y. Sakai [Particle Data Group]. *CKM quark-mixing matrix*. Particle Data Group, 2012.

[148] T. Aaltonen *et al.* [CDF Collaboration]. *Phys. Rev. Lett.*, 100(161803), 2008.

[149] CMS Collaboration. *JHEP*, 1205(123), 2012.

[150] G. Aad *et al.* [ATLAS Collaboration].

[151] CMS Collaboration.

[152] CMS Collaboration.

[153] G. Aad *et al.* [ATLAS Collaboration]. *Phys. Lett. B*, 712(22), 2012.

[154] M. Geller, S. Bar-Shalom, and G. Eilam.

[155] G. Aad et al [ATLAS Collaboration]. *ATLAS-CONF-2013-018*, 2013.

[156] J. Beringer et al. [Particle Data Group]. *Phys. Rev. D*, 86(010001), 2012.

[157] S Chatrchyan, G Hmayakyan, V Khachatryan, AM Sirunyan, W Adam, T Bauer, T Bergauer, H Bergauer, M Dragicevic, J Erö, et al. The cms experiment at the cern lhc. *Journal of Instrumentation*, 3(08):S08004, 2008.

[158] S. P. Martin and M. T. Vaughn. *Phys. Rev. D*, 50(2282), 1994.

[159] L. Lavoura and J. P. Silva. *Phys. Rev. D*, 47(2046), 1993.

[160] S. Eidelman et al. [Particle Data Group]. *Phys. Lett. B*, 592(1), 2004.

[161] S. P. Martin, K. Tobe and J. D. Wells. *Phys. Rev. D*, 71(073014), 2005.

[162] L. Lavoura and J. P. Silva. *Phys. Rev. D*, 47:1117, 1993.

[163] Julius Wess. *Supersymmetry and supergravity.* Princeton university press, 1992.

Vita

Kevin Grizzard received a Bachelor of Arts degree in Philosophy and the History of Math & Science from St. John's College in Annapolis, Maryland in 2006, and then a Bachelor of Science in Physics with a minor in Mathematics from Virginia Commonwealth University in his hometown of Richmond, Virginia in 2009. In between, he took classes at Stanford University and fell in love with the Bay Area. His first published paper was in astronomy and was the result of a National Science Foundation Research Experience for Undergraduates with David Cohen at Swarthmore University in 2005. He was fortunate enough to do another NSF-REU under Marc Sher at William & Mary College in 2008, this time in particle theory. Although this project did not result in a publication, it did produce results that were shown at a talk at CERN in the following year. In 2010 he began his Doctor of Philosophy program in Physics at Johns Hopkins University in Baltimore, Maryland. He enjoys reading, music, and experiencing the local arts community, as well as volunteering with the Baltimore mentoring program called Thread.

VITA